Magnetic properties of nanoparticles: from individual objects to cluster assemblies

Florent TOURNUS

“Magnetic nanostructures” group

Institut Lumière Matière, UMR 5306 CNRS & Univ. Lyon 1

Université de Lyon, France

florent.tournus@univ-lyon1.fr

Outline

Introduction

Part I: Magnetism, from the bulk to nanomagnets

Part II: Behaviour of a nanomagnet (macrospin)

Part III: Nanoparticle assemblies, from models to experiments

(Experimental results on diluted nanomagnet assemblies)

Motivation and potential applications

Fundamental questions

➡ Understand magnetism at the nanoscale

Nanoparticle = intermediate between molecule and bulk material

Potential applications

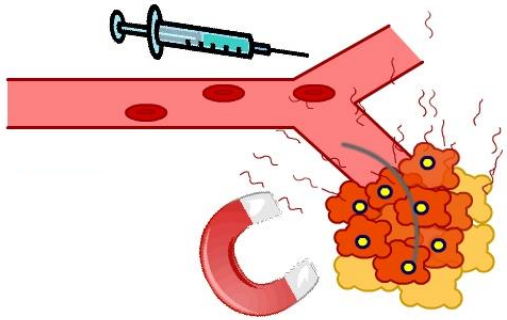

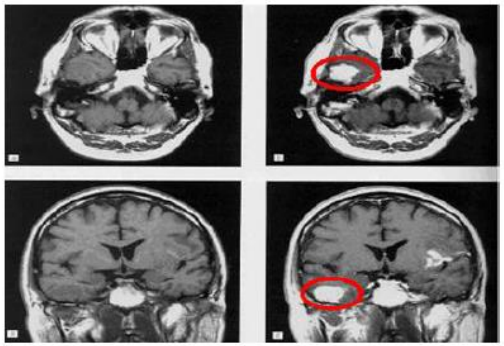

✓ Biology / health

- Target drug delivery
- Hyperthermia (cancer treatment)
- Contrast agent for MRI

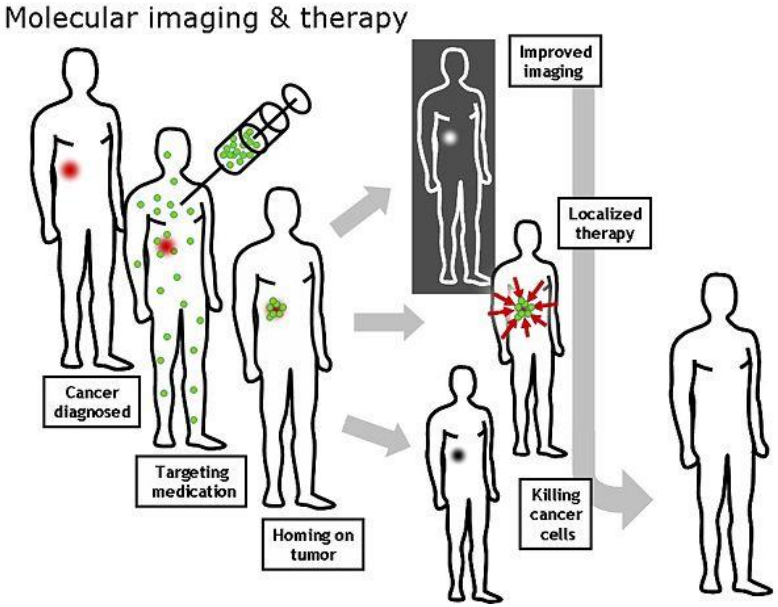

Motivation and potential applications

✓ Spintronics (memories, transistors, oscillators, sensors…)

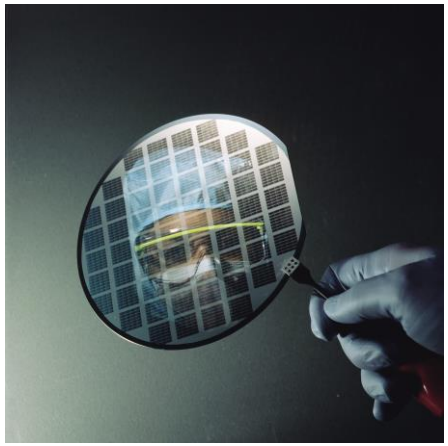

➡ electronics using the spin of electrons

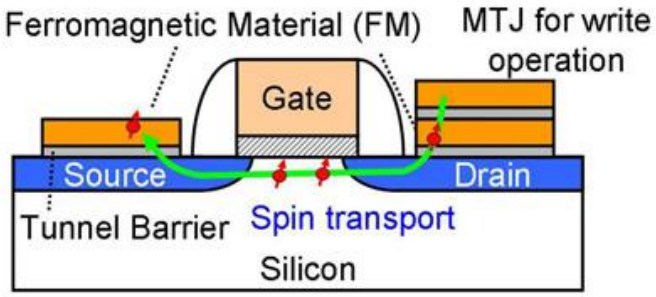

Diagram of Toshiba's spintronics-based MOS field-effect transistor

✓ Information storage

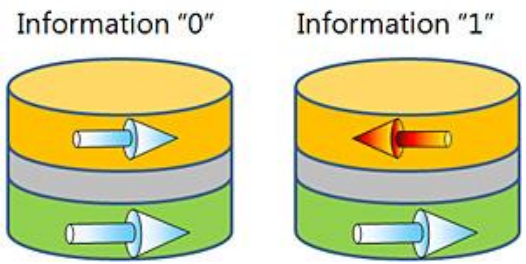

Hard drive

Motivation and potential applications

✓ Catalysis

➡ Catalytic activity of transition metals (and alloys)

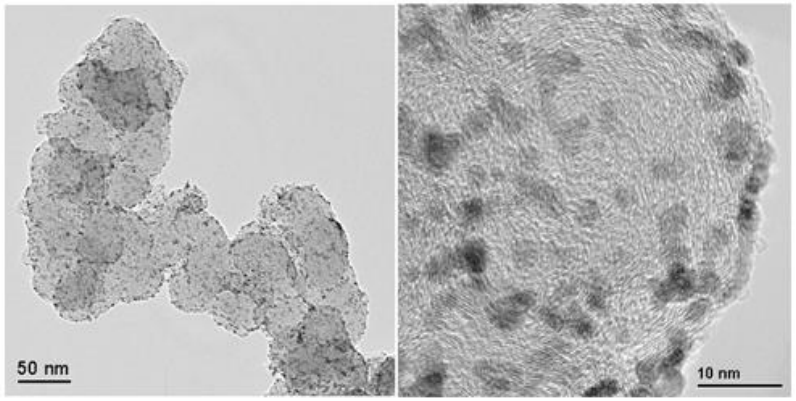

Co-Pt particles on carbon, for fuel-cell applications

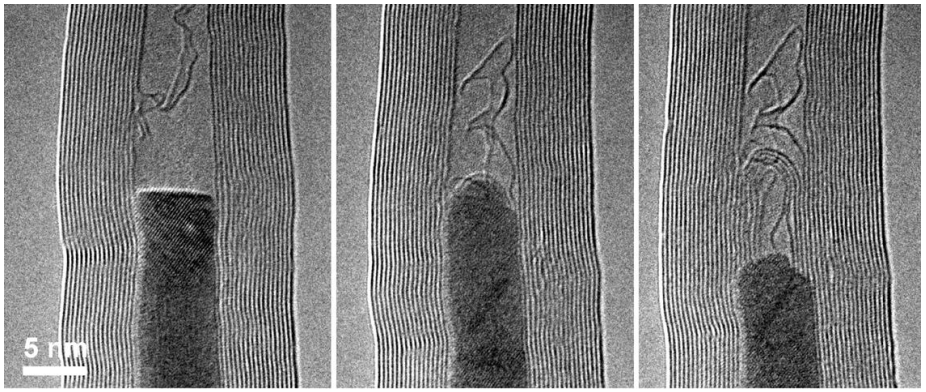

In-situ carbon nanotube growth, du to the metal particle. Fe, Co and FeCo are used as catalyst.

Why investigating the magnetic properties?

New information

- ✓ Can be useful for the determination of the particle size distribution in an assembly
- ✓ Indirect information on the particle structure (interface, shape, chemical arrangement…)

Magnetism is sensitive to the electronic structure: fine probe of atomic changes

➡ Monitor changes in the nanoparticle structure (with annealing, reaction…)

Part I: Magnetism, from the bulk to nanomagnets

- Basics on magnetism
  (magnetic field, magnetic moment, magnetic order…)

- Magnetic anisotropy, magnetic state
  (compromise between the different energy contributions)

- Going to small sizes, monodomain particles and other effects

Magnetism: basics

Magnet → North and south pole

Produces a magnetic field → Field lines (stray field)

Magnetic dipole → Magnet = ensemble of magnetic dipoles

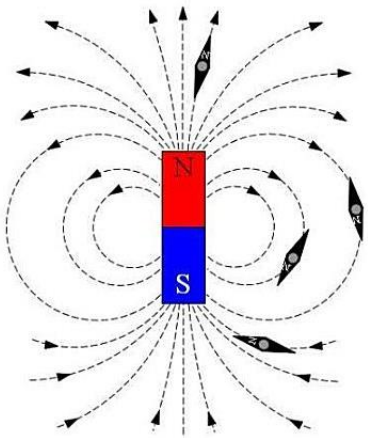

Stray field map of a magnet

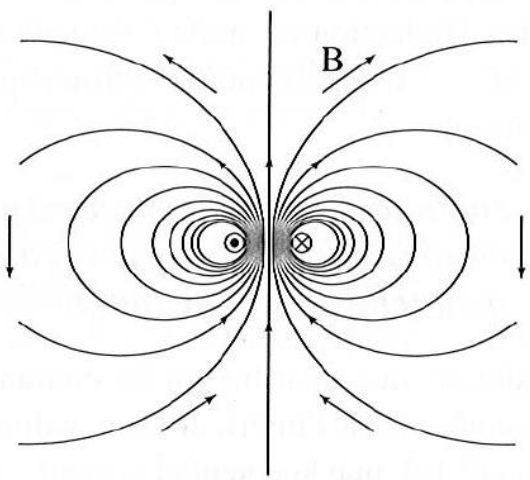

Current loop,
Magnetic moment : m = IS

Magnetic moment = elemental "piece" of a magnet

Energy (Zeeman) of a magnetic moment **m** in an external magnetic field **B** :

$$E = - \mathbf{m}.\mathbf{B}$$

→ The moment "wants" to be aligned along the field direction (like a compass!)

Magnetic matter, M and H

Vector fields **H**, **B**, **M**

- **H**: Magnetic field
- **B**: Magnetic induction
- **M**: Magnetization (magnetic moment per volume unit = 0 outside a magnet)

Maxwell equations for magnetism (statics)

$$\begin{cases} \text{div } \mathbf{B} = 0 \\ \mathbf{rot\ H} = \mathbf{j} \end{cases}$$

$\mathbf{j}$ → Charge currents

with the definition: $\mathbf{B} = \mu_0 (\mathbf{H}+\mathbf{M})$

At rest (no current), we have:
rot H = 0 and div **H** = –div **M**

→ Different approaches to calculate **H** at a certain point, created by a given **M** field.

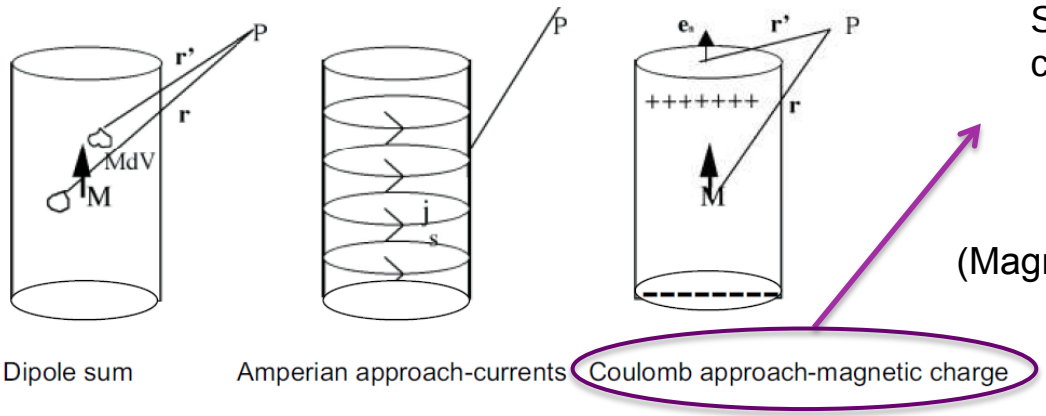

Same expression as the electric field created by a charge distribution

- Volume density of "charge": $\rho_m = -\text{div } \mathbf{M}$
- Surface density of "charge": $\sigma_m = \mathbf{M.e_n}$

(Magnetic "potential" solution of a Poisson equation)

For a magnetic piece of matter, the magnetization **M** creates a magnetic field **H**, *outside* and *inside* the material

Magnetic field and magnetization

$\mathbf{B} = \mu_0 (\mathbf{H}+\mathbf{M})$ Rk: B is expressed in Tesla, while H and M are in A/m.

Difficulty: the magnetization **M** of a material depends on the total field **H**

…and **H** depends on the magnetization → **M**(**H**)

$\mathbf{H} = \mathbf{H_0} + \mathbf{H_d}(\mathbf{M})$

Externally fixed by the experimenter

"Demagnetizing" or "dipolar" field, created by the magnetization

Self-consistent problem, difficult to solve!

Exact calculations can only be performed for a few specific cases

[and it is necessary to know the relation M(H) between M and H]

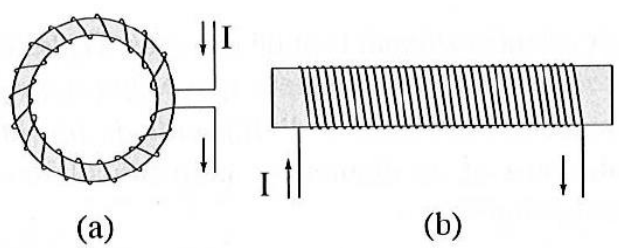

The value of **H** inside a material can be fixed experimentally (with particular geometries)

Demagnetizing field

For a uniformly magnetized ellipsoid $\mathbf{H_d} = -\mathbf{N}\,\mathbf{M}$

Tensor (*demagnetizing factor*)

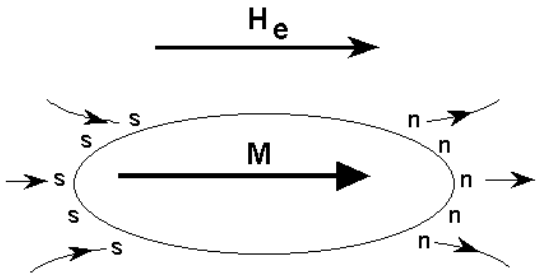

Magnetization Produces Apparent Suface Pole Distribution

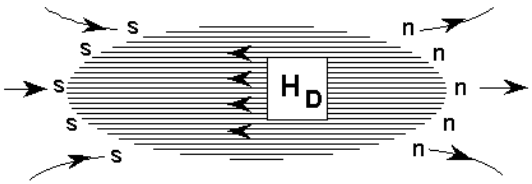

Demagnetizing Field Due to Apparent Surface Pole Distribution

Particular case of a sphere with a uniform **M**

$\mathbf{H_d} = -\,1/3\,\mathbf{M}$ inside the sphere

H and **B** are also uniform in the sphere

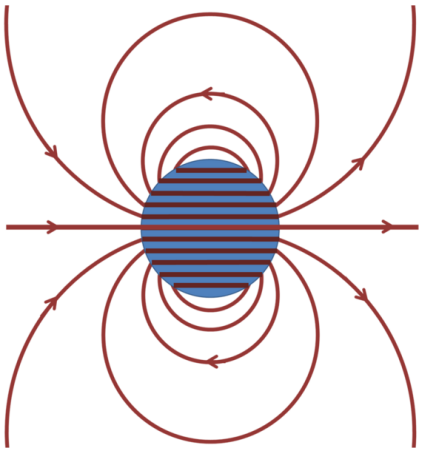

✓ There exist geometries of particular interest, where $H_d \rightarrow 0$

The true H inside the material is the one imposed

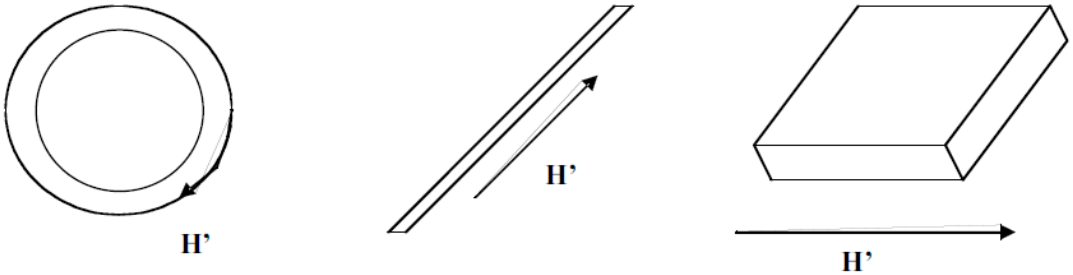

Ways of measuring magnetization with no need for a demag correction

toroid long rod thin film

Magnetic response

M(H) characterizes the magnetic response of a material

➡ Different behaviors for M(H)

Ferromagnet = permanent magnet (like iron)

➡ Remanent magnetization (M_R), without any external applied field

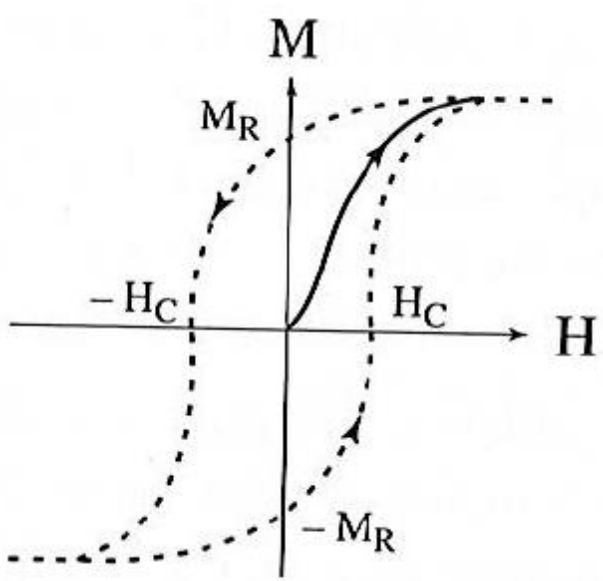

Hysteresis loop: “memory” effect

Coercive field H_C to suppress the magnetization

Remark: for a given H field, there are many possible states…

Note: the susceptibility χ is defined by $M = \chi H$ (particular case: linear response)

Ferromagnetism

While most isolated atoms have a magnetic moment, only a few solid compounds are ferromagnetic

Transition metals
(3d electrons)

H																	He dia
Li para	Be dia											B dia	C dia	N dia	O AF	F dia	Ne dia
Na para	Mg para											Al para	Si dia	P dia	S dia	Cl dia	Ar dia
K para	Ca para	Sc para	Ti para	V para	Cr AF	Mn AF	Fe Ferro	Co Ferro	Ni Ferro	Cu dia	Zn dia	Ga dia	Ge dia	As dia	Se dia	Br dia	Kr dia
Rb para	Sr para	Y para	Zr para	Nb para	Mo para	*Tc*	Ru para	Rh para	Pd para	Ag dia	Cd dia	In dia	Sn *	Sb dia	Te dia	I dia	Xe dia
Cs para	Ba	La	Hf	Ta para	W para	Re para	Os para	Ir para	Pt para	Au dia	Hg dia	Tl dia	Pb dia	Bi dia	*Po*	*At*	Rn dia
Fr	*Ra*	*Ac*															
				Ce *	Pr para	Nd AF	*Pm*	Sm AF	Eu Ferri	Gd Ferro	Tb Ferro	Dy Ferro	Ho Ferri	Er Ferri	Tm Ferri	Yb para	Lu para
				Th para	*Pa*	U para	*Np*	*Pu*	*Am*	*Cm*	*Bk*	*Cf*	*Es*	*Fm*	*Md*	*No*	*Lw*

Rare earth elements
(4f electrons)

Origin of the magnetic moment

Linked to the orbital momentum and spin momentum of **electrons** (negligible contribution of the nucleus)

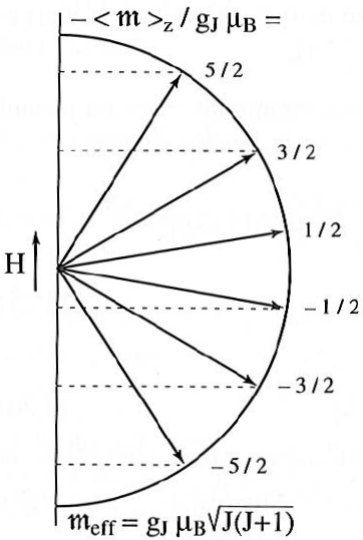

For isolated atoms, it depends on the quantum numbers L and S

The m_z projection is quantized

Ion 4f	$^{2S+1}L_J$	L	S	J	gJ	m_0 (μ_B)
Ce^{3+} ($4f^1$)	$^2F_{5/2}$	3	1/2	5/2	6/7	2,14
Pr^{3+} ($4f^2$)	$^3H_4$	5	1	4	4/5	3,20
Nd^{3+} ($4f^3$)	$^4I_{9/2}$	6	3/2	9/2	8/11	3,27
Pm^{3+} ($4f^4$)	$^5I_4$	6	2	4	3/5	2,40
Sm^{3+} ($4f^5$)	$^6H_{5/2}$	5	5/2	5/2	2/7	0,71
Eu^{3+} ($4f^6$)	$^7F_0$	3	3	0	–	0
Gd^{3+} ($4f^7$)	$^8S_{7/2}$	0	7/2	7/2	2	7,00
Tb^{3+} ($4f^8$)	$^7F_6$	3	3	6	3/2	9,00
Dy^{3+} ($4f^9$)	$^6H_{15/2}$	5	5/2	15/2	4/3	10,00
Ho^{3+} ($4f^{10}$)	$^5I_8$	6	2	8	5/4	10,00
Er^{3+} ($4f^{11}$)	$^4I_{15/2}$	6	3/2	15/2	6/5	9,00
Tm^{3+} ($4f^{12}$)	$^3H_6$	5	1	6	7/6	7,00
Yb^{3+} ($4f^{13}$)	$^2F_{7/2}$	3	1/2	7/2	8/7	4,00

An electron has a spin equal to 1/2

→ 2 possibilities
- m_S = +1/2 : spin "up" ↑
- m_S = -1/2 : spin "down" ↓

Rk.: in a solid, the orbital (and spin) momentum is often quenched

With many electrons → Short range **exchange** interaction: $E_{exchange} = -\sum_{ij} J_{ij}\, \vec{S_i} . \vec{S_j}$

Origin of exchange: Coulomb interaction + anti-symmetry Pauli principle

Ferromagnetism in metals

The case of transition metals (Fe, Co, Ni)

- Band structure, with a different density of states (DOS) for spin up and spin down electrons.

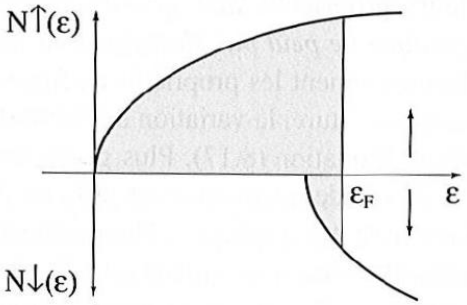

Resulting spin polarization (magnetic moment)

- Itinerant (delocalized) magnetism, as opposed to the highly localized 4f orbitals of rare earth elements.

bulk Co

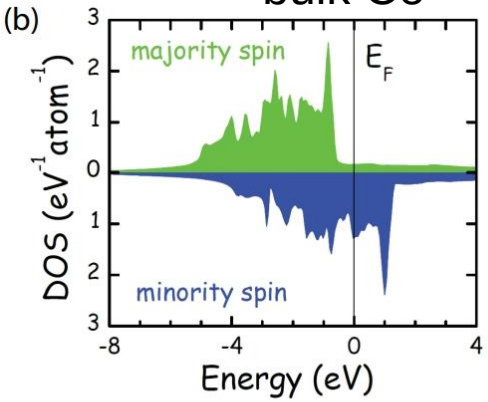

$3d^7 4s^2$ $n = 9$ $n_\uparrow = 5.3$ $n_\downarrow = 3.7$

$m = (n_\uparrow - n_\downarrow) m_s = 1.6 \mu_B$

Delocalized spin density, but a schematic view with localized “arrows” is still convenient…

Keep in mind: magnetism has a **quantum origin**, it is sensitive to the **electronic configuration**

Magnetic order

Different **magnetic orders**: ferro, para, antiferro…

✓ Ferromagnetism:

Exchange favors ⇑⇑

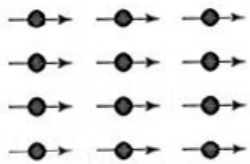

Spontaneous orientation of the moments, up to Curie temperature T_C

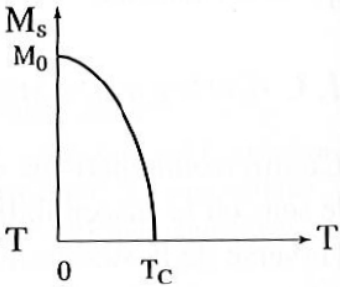

✓ Antiferromagnetism:

Exchange favors ⇑⇓

Compensation ⇒ No net magnetization

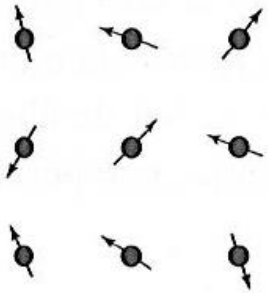

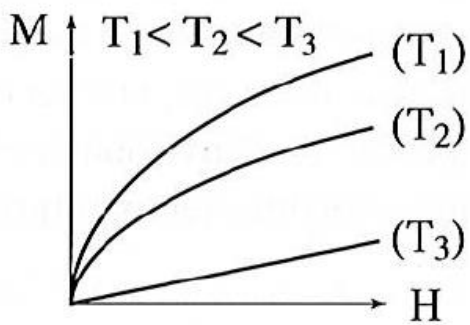

✓ Paramagnetism:
No exchange (or negligible)

Orientation of the magnetic moments, only with the application of an external field

Rk.: a ferromagnet becomes a paramagnet above T_C

Another parameter: the magnetic anisotropy

Important parameters for a material

- Magnetization (moment per atom)
- Exchange coupling (magnetic order)
- Anisotropy (magneto-crystalline)

Anisotropy:
- the magnetic behaviour depends on the direction of the applied field
- the energy depends on the magnetization orientation

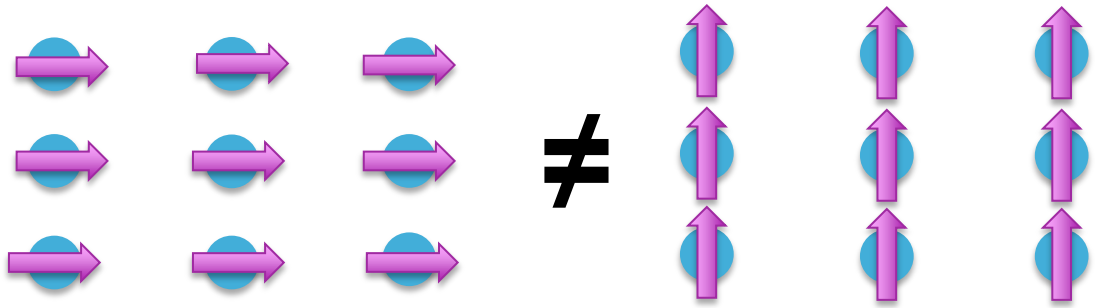

Small energy difference (related to spin-orbit coupling), which reflects the lattice symmetry

The two orientations are not equivalent

Preferential directions (easy axis) for the magnetization, tilting away from these directions has an energetic cost…

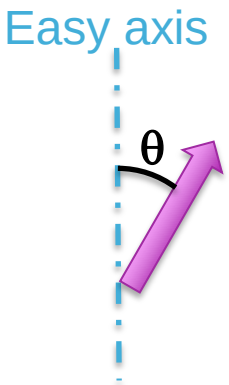

Example: uniaxial anisotropy → $E_{ani}/V = K_u \sin^2\theta$

(minimum for $\theta=0$ and $\theta=\pi$)

Magnetic state of a bulk sample: a compromise

Energetic compromise:
Dipolar field + exchange + anisotropy + Zeeman

➡ **Magnetic domains**

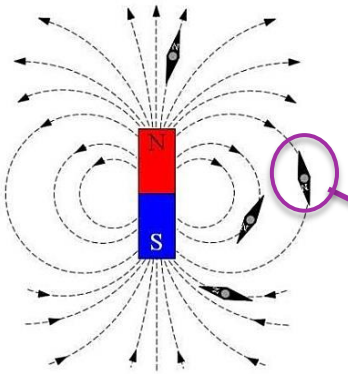

Near a dipole, the created field is in opposite direction

Demagnetizing field ("dipolar" field) H_d

➡ A uniform magnetization (large H_d) has an energetic cost

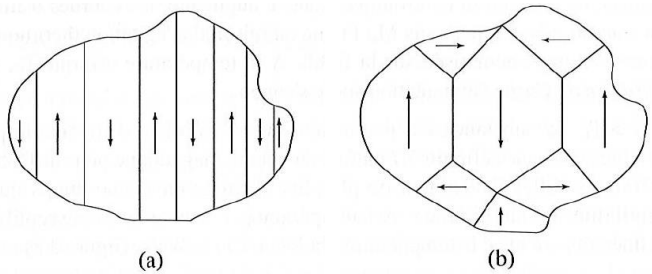

A configuration with domains in different directions can be more favorable (depends on the material, the shape, the applied field)

Domain walls

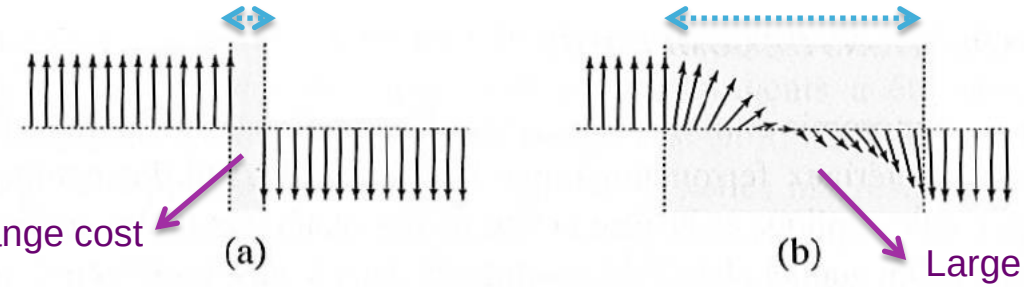

Large exchange cost

Large anisotropy cost

➡ Domain walls width: $\delta_0 = \sqrt{A/K_1}$

exchange

anisotropy

Going to nano-size

Length scales

→ Comparison of the different energies

Exchange versus anisotropy: $\delta_0 = \sqrt{A/K_1}$

(typically, tens of nm)

Exchange versus demagnetizing field:

$L_{exch} = \sqrt{A/\mu_0 M_S^2}$ (a few nm)

Existence of critical sizes

$R_{mono} = 36\ L_{exch}^2 / \delta_0$ → Single domain (monodomain), no domain wall

$R_{coh} = 5\ L_{exch}$ → Coherent reversal (the atomic moments are always parallel)

→ Small ferromagnetic particle ($R < R_{mono}$ and R_{coh}) = a single vector!

"Giant" magnetic moment (**macrospin**) with a classical behavior: $\mu = M_S V$

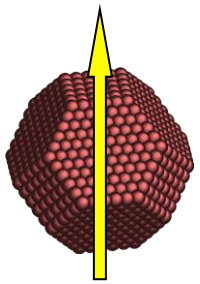

Macrospin

The situation gets simpler with the size reduction!

Specific effects at nano-sizes

Things are not so simple…

- ✓ Modification of the atomic magnetic moments due to the surface (lower coordination)

➡ Increase of the moment

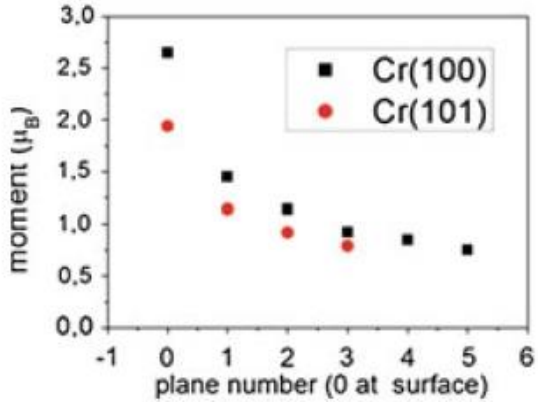

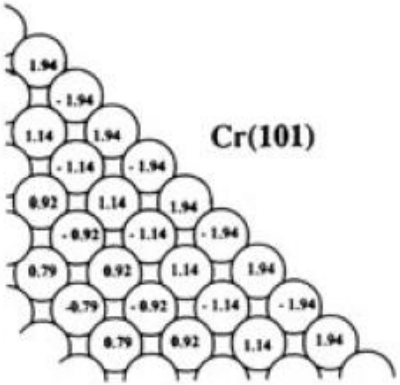

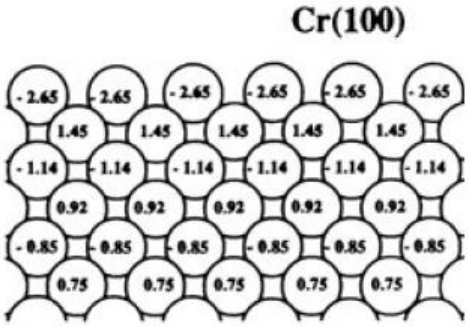

Calculations for a Cr surface (Cr is antiferro)

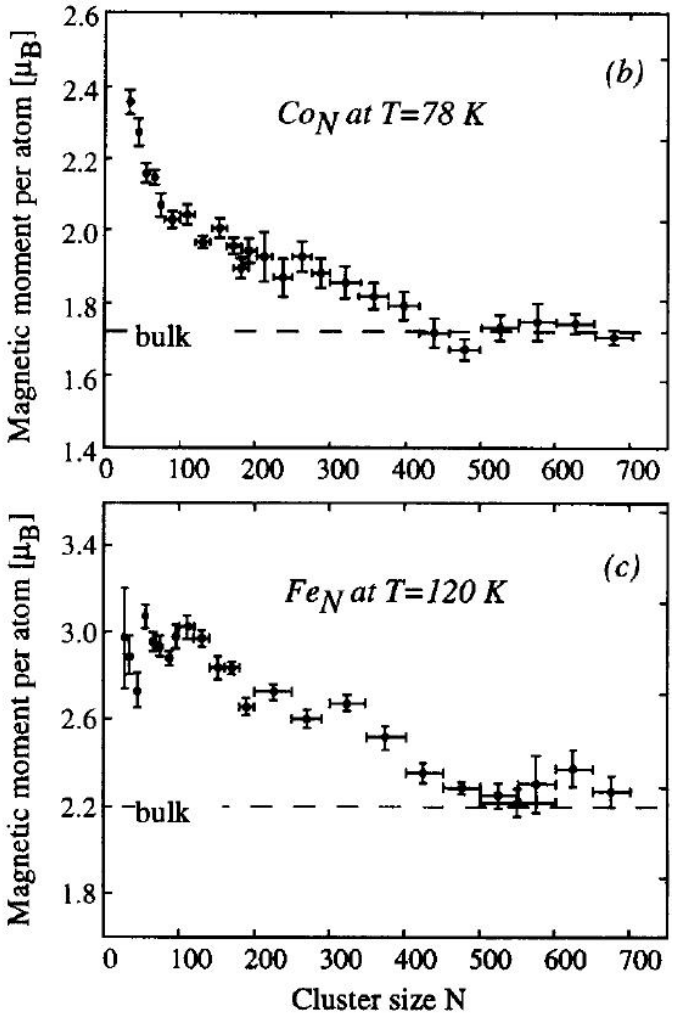

Experimental measurements on free clusters

Specific effects at nano-sizes

✓ Modification of the magnetic anisotropy due to the surface/interface

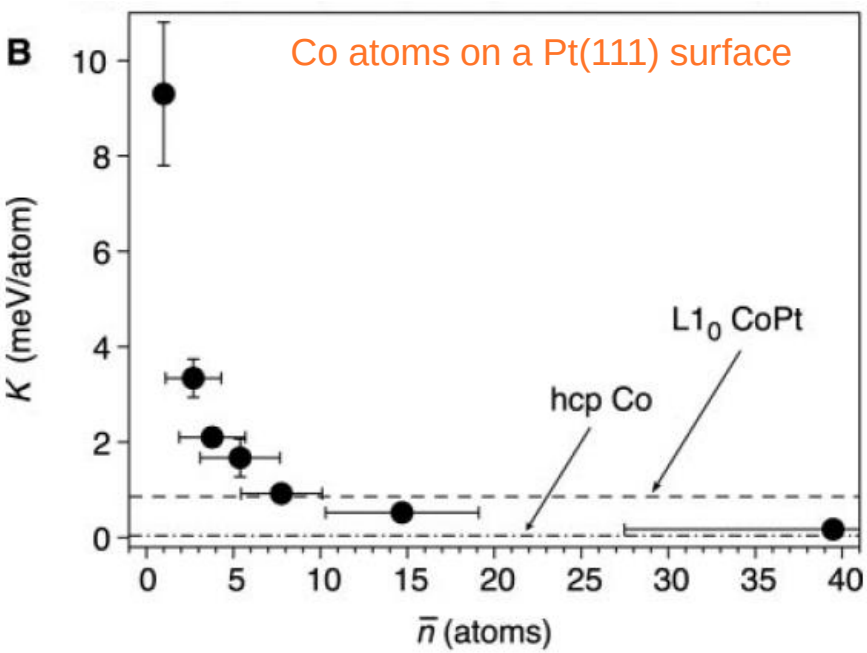

XMCD measurements (Co L edge)

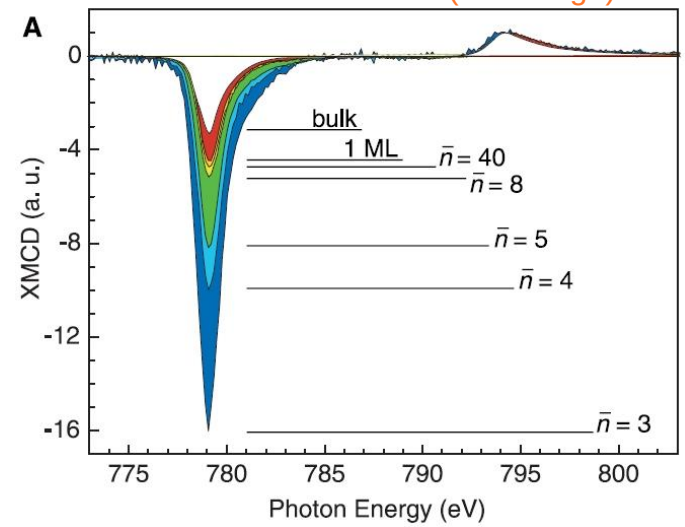

Evolution of the orbital moment / spin moment ratio

Co/Pd multilayers

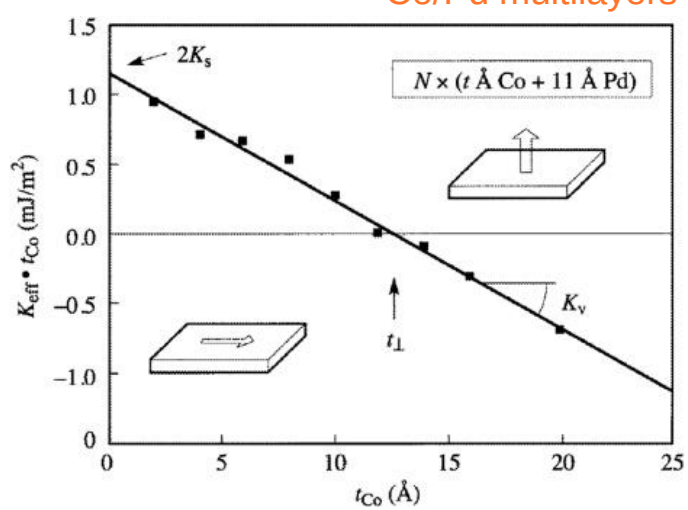

Interface anisotropy

➡ Transition between in plane and perpendicular orientation of the magnetization, depending on the Co layer thickness

Specific effects at nano-sizes

✓ Effects linked to structural modifications (distortions, geometries specific to small particles…)

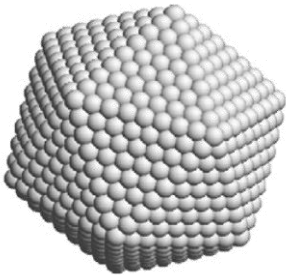

Icosahedron

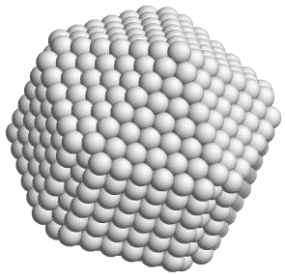

Decahedron

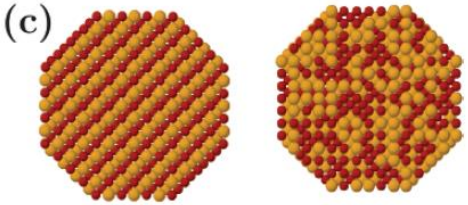

Bimetallic particles, alloys

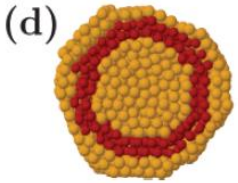

+ other subtle effects (modification of the magnetic coupling/order, dynamical behavior…)

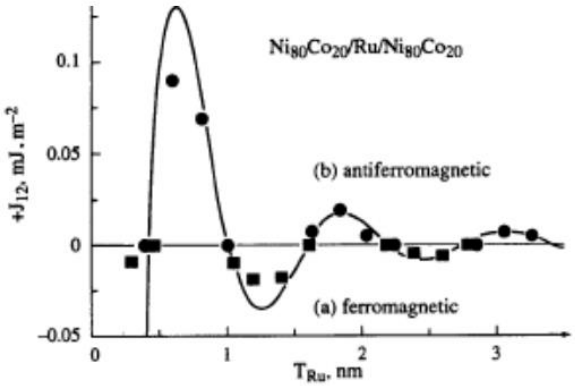

Trilayer $Ni_{80}Cu_{20}/Ru/Ni_{80}Cu_{20}$

Part II: Behaviour of a nanomagnet (macrospin)

- Magnetic anisotropy of a particle
- Stoner-Wohlfarth model (T=0), macrospin switching
- Relaxation (non-zero temperature), superparamagnetism
- Equilibrium vs. Blocked regime

Key parameters for a nanomagnet

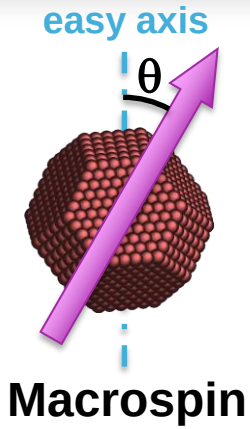

Parameters characterizing a monodomain nanomagnet

- Volume V
- Magnetic moment $\mu = M_S V$ (Vector $\mathbf{\mu} = \mu\, \mathbf{m}$)
- Magnetic anisotropy energy $K = K_{eff} V$

➡ Type of anisotropy : simplest case = uniaxial

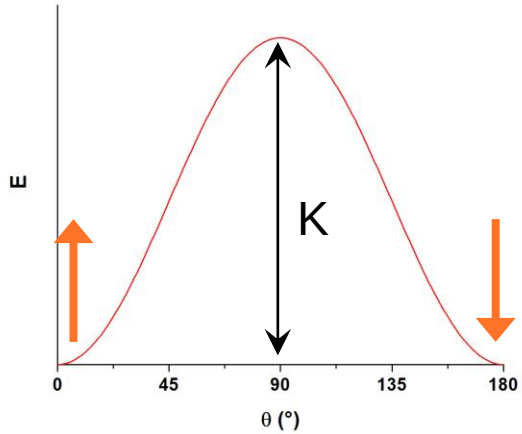

Magnetic anisotropy energy (MAE) = energy barrier to switch the magnetization direction, along the easy axis

Rk.: Because of the size reduction, M_S and K_{eff} may be different from the bulk value

Magnetic anisotropy of a particle

Several sources of anisotropy

Shape anisotropy: The dipolar (demagnetizing) field depends on the magnetization orientation

Easy axis along the longest dimension:

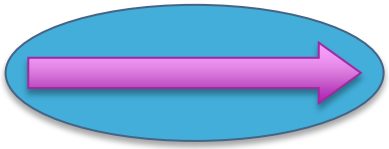

More favorable than

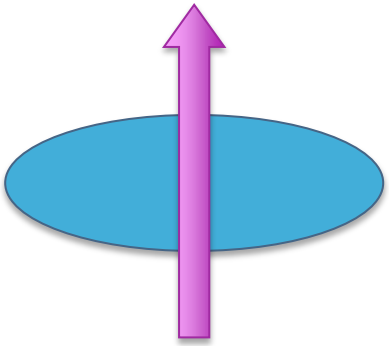

Rk.: For an ellipsoid, with one long axis (c/a ratio > 1), uniaxial anisotropy

Magneto-crystalline anisotropy: Linked to the underlying crystal lattice (as for the bulk)

+ **Surface contribution** (broken bonds)

Additional facets make different orientations non-equivalent

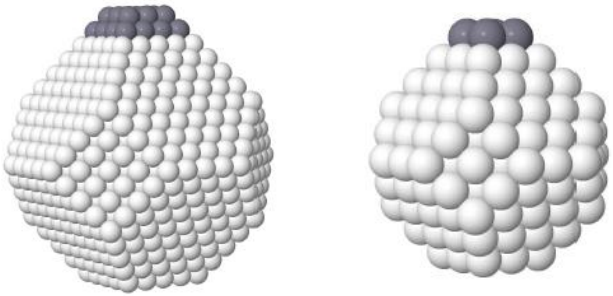

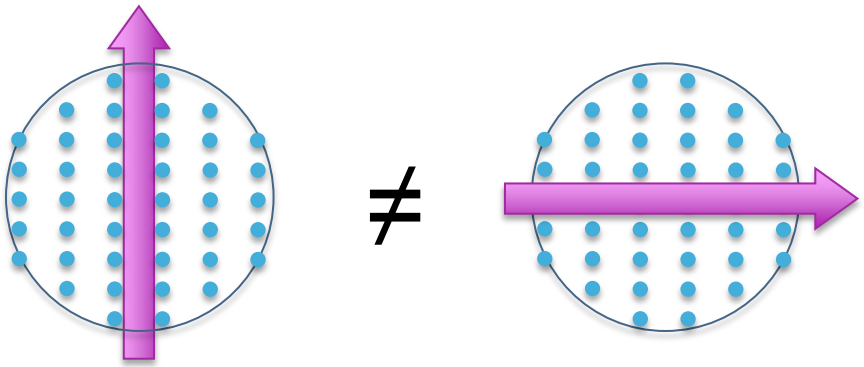

In any case, the magnetic anisotropy **reflects the symmetry** of the particle

Magnetic anisotropy of a particle

A uniaxial anisotropy is a good approximation (but we may go beyond…)

Expression of the anisotropy energy: $E_{ani} = K \sin^2\theta$

Equivalent to $\boxed{E_{ani}/V = -K_{eff}\, m_z^2}$ (minimum for $m_z = \pm 1$)

- Angle θ between the easy axis (z direction) and the magnetic moment
- Unit vector $\mathbf{m} = \boldsymbol{\mu}/\mu$ of coordinate (m_x, m_y, m_z)
- K_{eff} effective anisotropy "constant", anisotropy energy per volume unit

Bi-axial anisotropy: $\boxed{E_{ani}/V = K_1\, m_z^2 + K_2\, m_y^2}$

With $K_1 < 0 < K_2$ ⇒ In the hard plane (x,y), the direction x is more favorable

The smallest energy barrier to switch the magnetization (from +z to –z) is simply K_1V, and corresponds to keeping $m_y=0$

Stoner Wohlfarth model

Uniaxial macrospin, under an applied field **H**

Total energy:

$$E = K_{eff} V \sin^2\theta - \mu_0 H M_S V \cos(\theta - \varphi)$$

Anisotropy

Zeeman

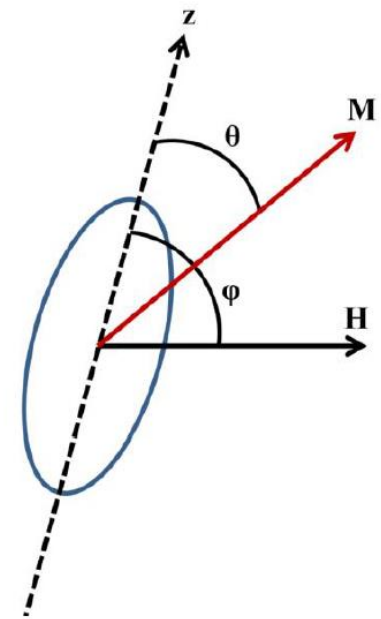

Expression with reduced units: $E/K = \sin^2\theta - 2h\cos(\theta - \varphi)$

With $h = H/H_A$ and $H_A = 2K_{eff}/(\mu_0 M_S)$ → "Anisotropy field"

➡ Function of several variables $E(h,\theta,\varphi)$

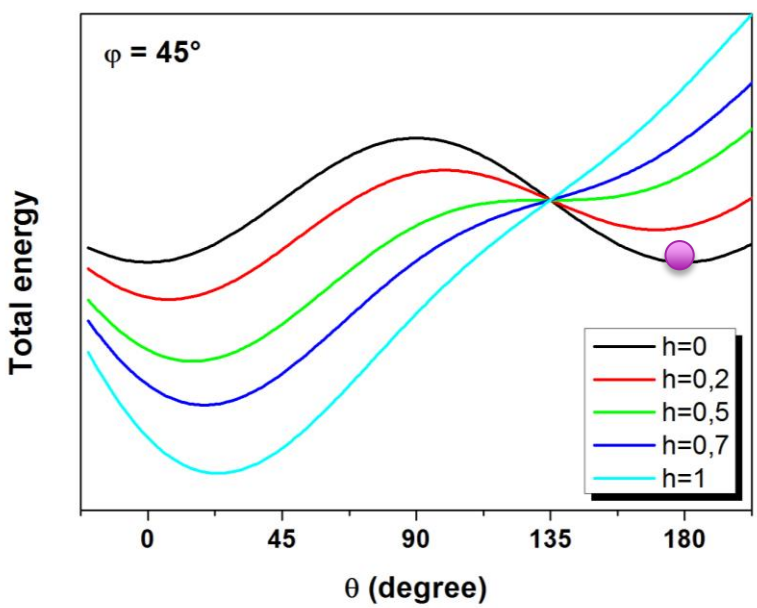

With an applied field, there is one stable minimum and a metastable one, as long as $H < H_{sw}$

For $H=H_{sw}$ the metastable minimum disappears

➡ Only one stable orientation

The magnetization can stay in the metastable minimum, until it **switches** (at H_{sw})

In this example (φ=45°), this happens for $H=H_A/2$

Stoner Wohlfarth model

Other example, with φ=0°

- The macrospin is initially pointing in the –z direction
- The field is applied in the +z direction
- Nothing happens, until $H=H_A$ where it switches along the +z direction

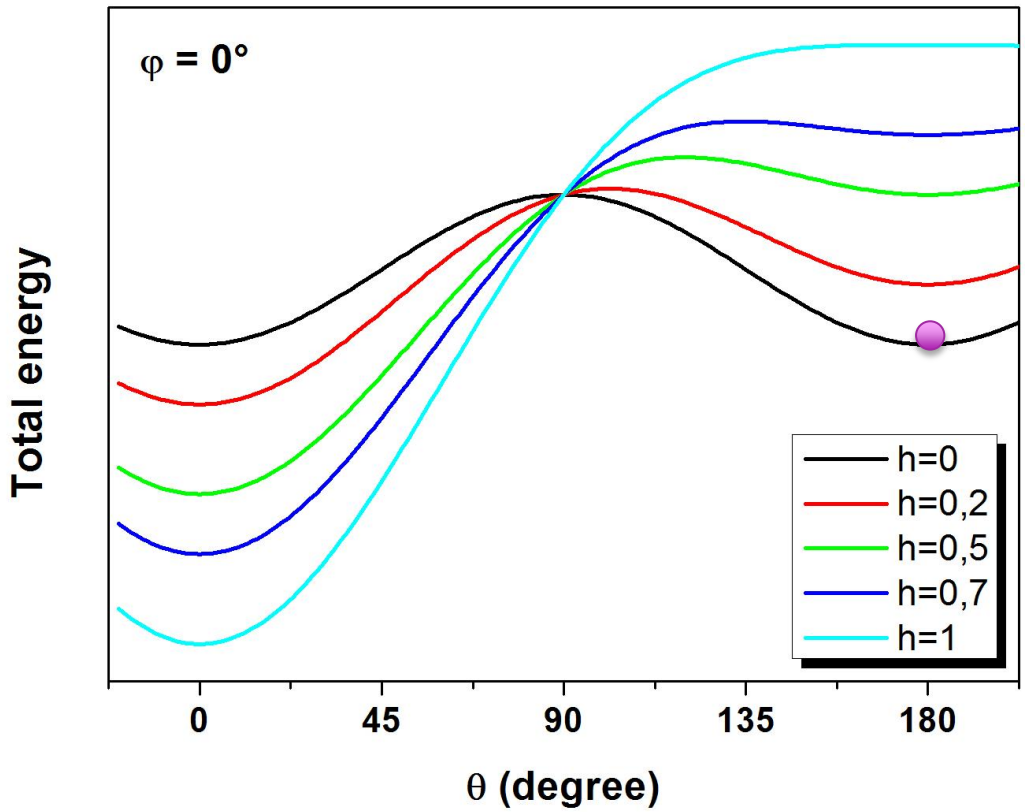

With no applied field, the switching energy barrier is $\Delta E = K_{eff}V$

ΔE decreases when H increases, and vanishes for $H=H_{sw}$

In this model, we suppose that T=0 ⇒

- ✓ Only the minima are populated (no statistical occupation)
- ✓ Switching only if $\Delta E=0$ (no thermal activation, static theory)

Stoner Wohlfarth model

For a given field, we can find the values of θ minimizing E

The minima satisfy $\frac{\partial E}{\partial \theta} = 0$ (and $\frac{\partial^2 E}{\partial \theta^2} > 0$)

The **switching field** corresponds to having simultaneously $\frac{\partial E}{\partial \theta} = 0$ and $\frac{\partial^2 E}{\partial \theta^2} = 0$

From the expression of the energy, this allows us to derive the analytical expression

$$H_{sw}^0 = H_A(\sin^{2/3}\varphi + \cos^{2/3}\varphi)^{-3/2}$$

It may be plotted as an *astroid* (polar plot)

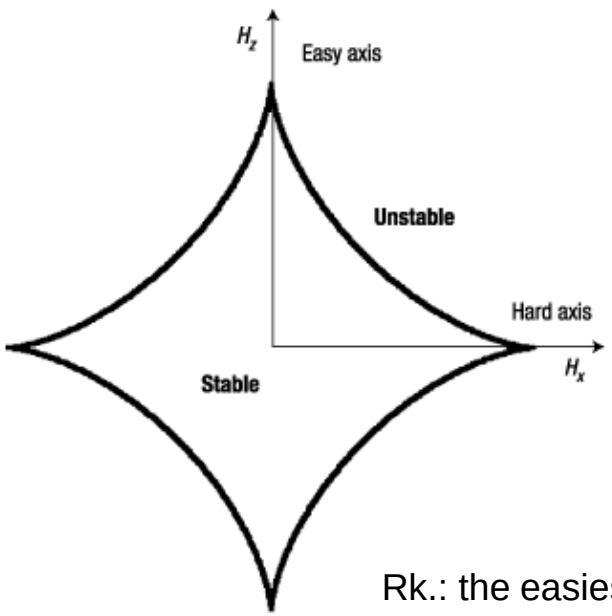

The switching field depends on the angle φ, and is controlled by the **anisotropy field** $H_A = 2 K_{eff} / \mu_0 M_S$

No size dependence

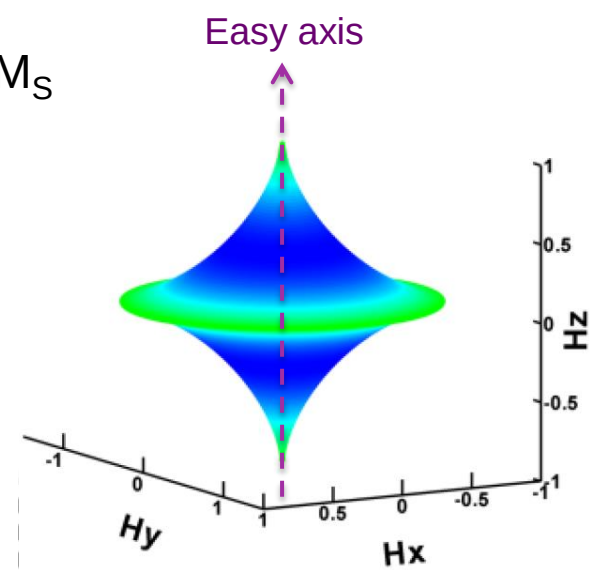

Rk.: the easiest switching is for a 45° angle between the applied field and the easy magnetization axis

Stoner Wohlfarth model

Experimental measurements of astroids for an **individual** nanoparticle

➡ Main contribution = uniaxial anisotropy

Due to the surface (additional facets)

(μ-SQUID technique, with a 3 nm diameter fcc Co nanoparticle)

Experimental

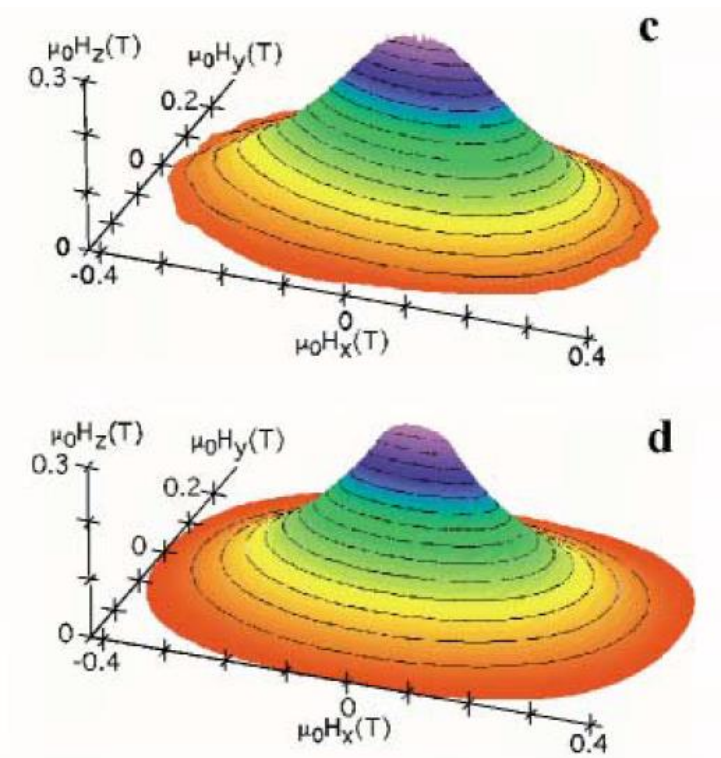

Simulated

Jamet et al. Phys. Rev. Lett. **86**, 4676 (2001)

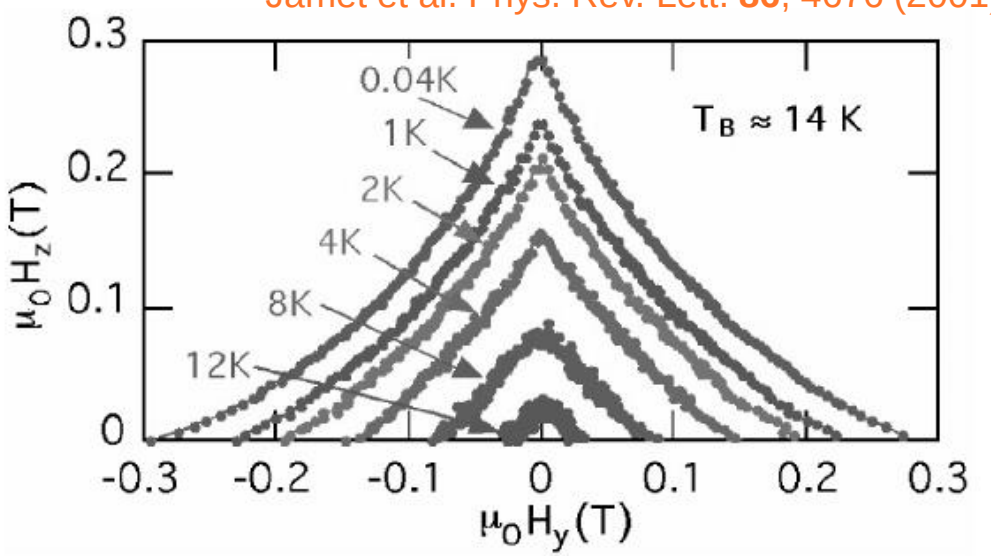

Relevance of the Stoner-Wohlfarth macrospin model for small nanomagnets!

Stoner Wohlfarth model

One can also compute hysteresis loops

- ✓ For each orientation of the field with respect to the easy axis
  - ➡ Coercive field between 0 and H_A
    Remanence between 0 and M_S

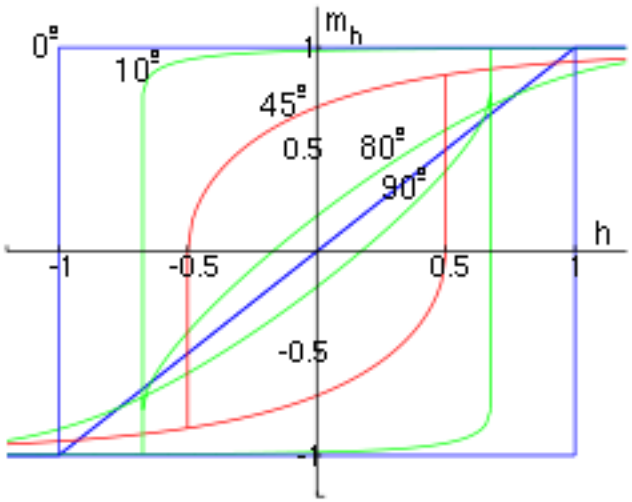

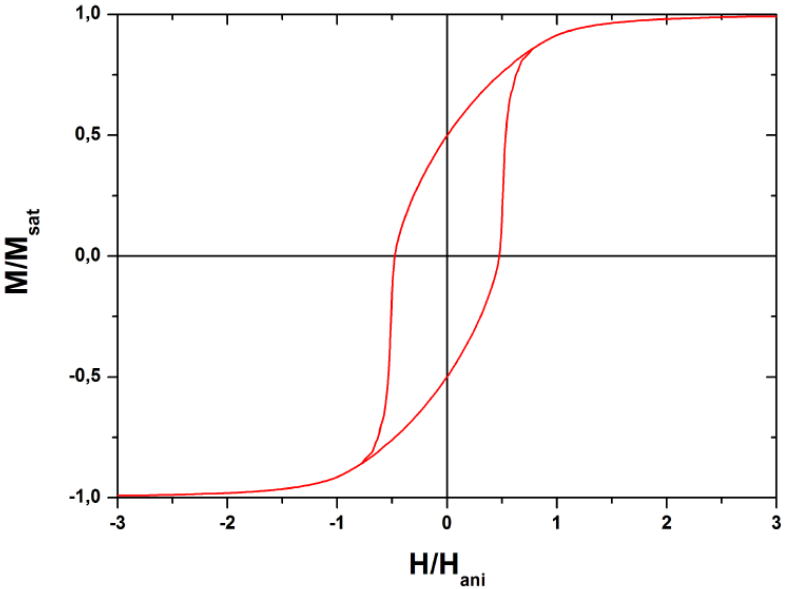

- ✓ For the case of an assembly with randomly oriented easy axes
  - ➡ Coercivity: $H_C/H_A \sim 0.48$
    Remanence: $M_R/M_S = 0.5$

Rk.: H_C scales linearly with the anisotropy constant K_{eff}

No size dependence (model at T=0)

Non-zero temperature: relaxation

Probability to overcome the energy barrier, due to thermal energy

➡ Spontaneous macrospin switching

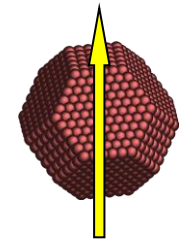

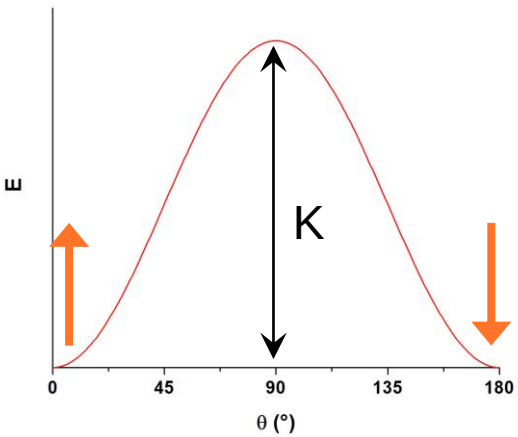

Switching frequency (Néel relaxation):

$$\nu = \nu_0 \exp(-\Delta E / k_B T)$$

➡ Stability time of a given orientation: $\tau = 1/\nu$

Without external field, the barrier is $\Delta E = K$

➡ $\tau = \tau_0 \exp(K / k_B T)$ with a typical $\tau_0 \sim 10^{-9}$ s

If the measurement time τ_m is smaller than the switching time

➡ "**blocked**" regime: the macrospin keeps its orientation and can be detected

If the measurement time τ_m is larger than the switching time

➡ "**superparamagnetic**" regime: occupation of the two minima, the average magnetic moment is zero (like a paramagnet)

Superparamagnetism

The frontier between the blocked and superparamagnetic regime is a question of <u>measurement time</u>

Experimental technique	Measurement time
magnetization	1–100 s
ac susceptibility	10^{-6}–100 s
Mössbauer spectroscopy	10^{-9}–10^{-7} s
Ferromagnetic resonance	10^{-9} s
Neutron scattering	10^{-12}–10^{-8} s

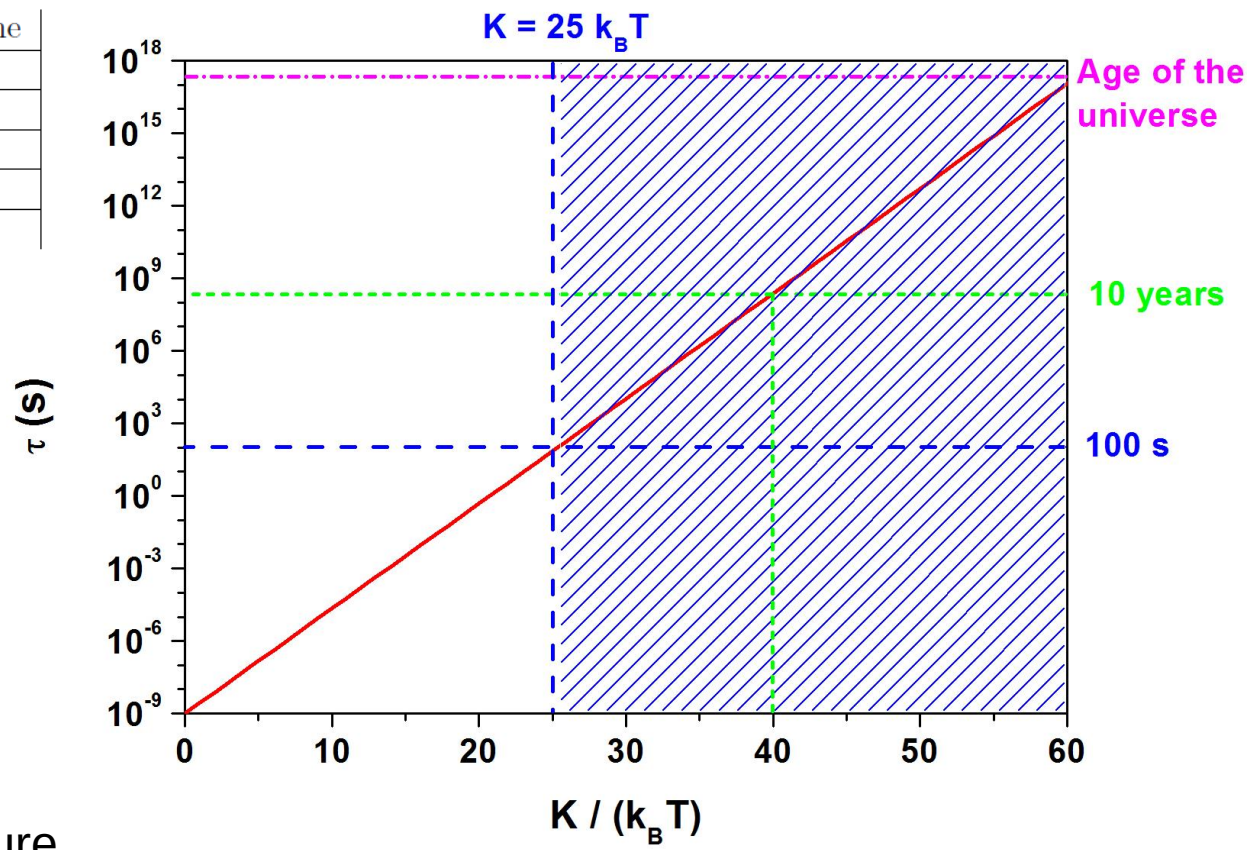

For a quasi-static characterization, typically τ_m ~100 s

⇩

Blocked regime for $K > 25\ k_B T$

✓ Blocking at low temperature

Concept of **blocking temperature**

⇨ T_B such that $\tau = \tau_m$

- Under T_B = blocked regime
- Over T_B = superparamagnetic regime (equilibrium)

Superparamagnetic limit

$\tau = \tau_0 \exp(K / k_B T)$
with $\tau = \tau_m$

$$T_B = K / [k_B \ln(\tau_m/\tau_0)]$$

The blocking temperature is proportional to the **magnetic anisotropy energy**

Since $K = K_{eff} V$, it means that T_B scales with the particle volume

Small particles becomes superparamagnetic, except at low enough temperature

Ex.: for a 3 nm diameter Co particle, magnetization switching on the ns scale (at room temperature).

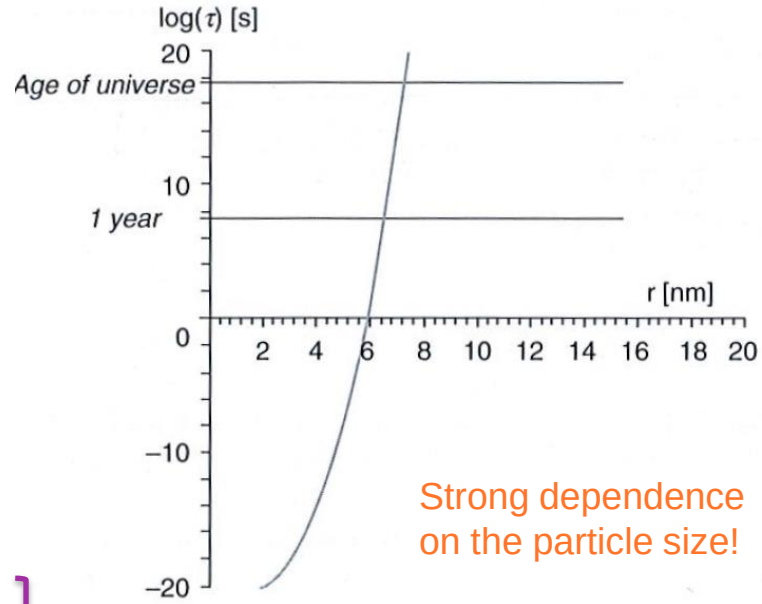

Strong dependence on the particle size!

This can be a problem (or not), depending on the targeted applications

- Magnetic data storage: needs stability
- Hyperthermia therapy: needs dissipation
- MRI contrast agent: needs fluctuation

Avoid the super-paramagnetic regime!

Equilibrium regime

Equilibrium regime = superparamagnetic regime

Statistical population of the energy landscape

➡ Properties governed by the partition function (thermodynamics, Boltzmann distribution)

When **T much larger than T_B**, no more influence of the anisotropy ($K << k_B T$)

➡ Exactly the same situation as a paramagnet: $E = -\mu_0 \mathbf{H}.\boldsymbol{\mu}$

Reduced parameter: $\xi = \dfrac{\mu_0 M_S V H}{k_B T}$

$$\mathcal{Z}_{\mathrm{Lan}} = \frac{2}{\xi}\sinh\xi\,, \qquad \mathcal{F}_{\mathrm{Lan}} = k_{\mathrm{B}}T[\ln(\xi) - \ln(2\sinh\xi)]$$

Analytical solution for $m_{eq}(H)$

⬇

Langevin function:

$$L(x) = \coth(x) - \frac{1}{x}$$

⬇

$$m_{\mathrm{eq}} = \mu\left[\coth\left(\frac{\mu_0\mu H}{k_B T}\right) - \frac{k_B T}{\mu_0\mu H}\right]$$

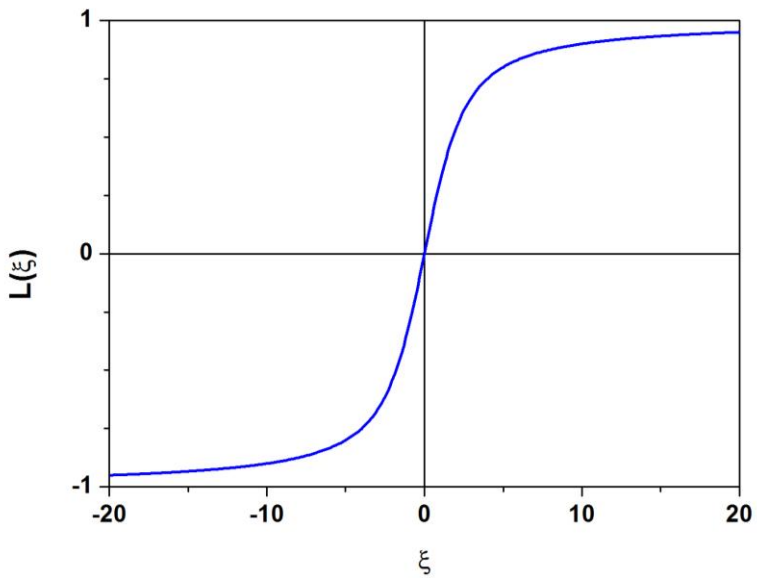

Equilibrium regime, m(H) curves

- Influence of temperature
  - ➡ Lower slope when T increases
- Influence of particle size
  - ➡ Higher slope when the particle size increases

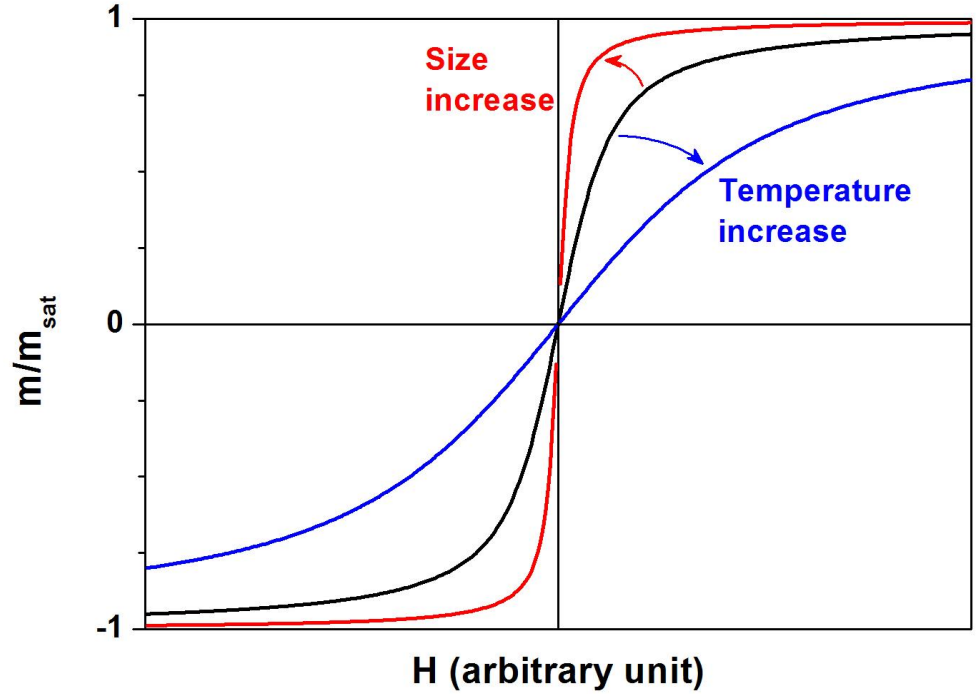

Scaling property:

In the *superparamagnetic regime* (negligible effect of anisotropy), the m(H) curves display a H/T scaling

When T is close to T_B ➡ Equilibrium response (no remanent magnetization), but with an influence of the anisotropy

More complicated situation! ➡ No analytical expression for m(H,T)

Magnetic susceptibility

$M = \chi H$ Small perturbation ($H \to 0$), <u>linear response</u>

Susceptibility

Equilibrium susceptibility:

- High enough above T_B

  ➡ Curie Law:
  χ is proportional to 1/T

$$m_{eq} = \frac{\mu_0 \mu^2 H}{3 k_B T}$$

Series expansion of the Langevin function:

$$L(x) = \frac{1}{3}x - \frac{1}{45}x^3 + \frac{2}{945}x^5 - \frac{1}{4725}x^7 + \frac{2}{93555}x^9 + \cdots$$

- General case (anisotropy taken into account)

  ➡ The parallel and perpendicular susceptibility depend on the dimensionless parameter $\sigma = K/(k_B T)$

Taylor expansion as a function of σ or $1/\sigma$ for $\chi_\parallel$ and $\chi_\perp$

$$\chi_\parallel = \chi_0(1+2S) \quad \text{and} \quad \chi_\perp = \chi_0(1-S)$$

$$\text{with} \quad S \simeq 1 - \frac{3}{2\sigma} \quad (\sigma \gg 1)$$

M.I. Shliomis, V.I. Stepanov, J. Magn. Magn. Mater. **122**, 176 (1993)

For a **randomly oriented assembly**:

$$\tilde{\chi} = \frac{1}{3}\chi_\parallel + \frac{2}{3}\chi_\perp \quad \Rightarrow \quad \tilde{\chi} = \chi_0 = \frac{\mu_0 \mu^2 / V}{3 k_B T}$$

Simplification: Curie law still valid!
(no effect of anisotropy)

Blocked susceptibility and transition

In the **blocked regime** (extreme case: T=0)

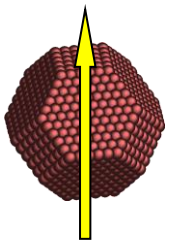

- If H parallel to the easy axis: nothing changes ($H << H_{sw}$)
- If H perpendicular to the easy axis: tilt of the macrospin (no switching)

$$\chi_{\parallel} = 0$$
$$\chi_{\perp} = \frac{\mu_0 \mu^2 / V}{2K}$$

For a **randomly oriented assembly**:

"Blocked" susceptibility:

$$\chi_b = 2\chi_{\perp}/3$$

and

$$m_b = \frac{\mu_0 \mu^2 H}{3K}$$

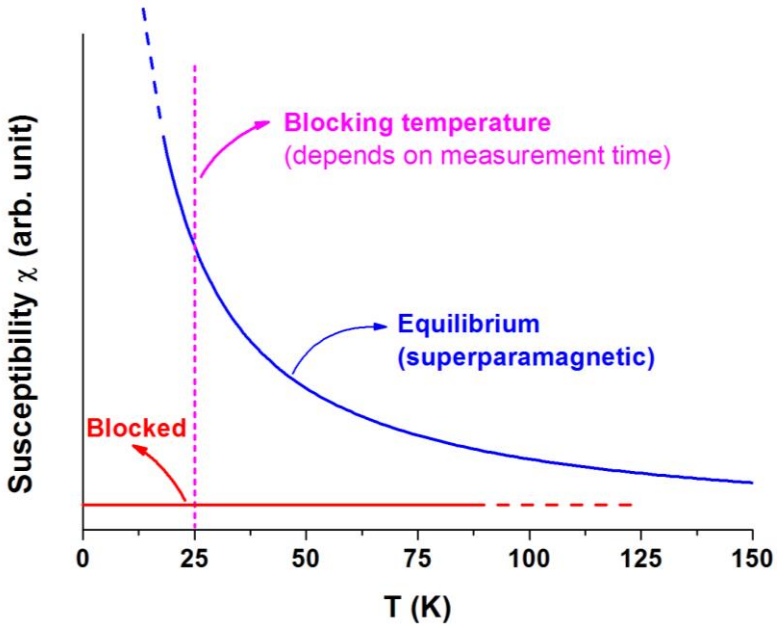

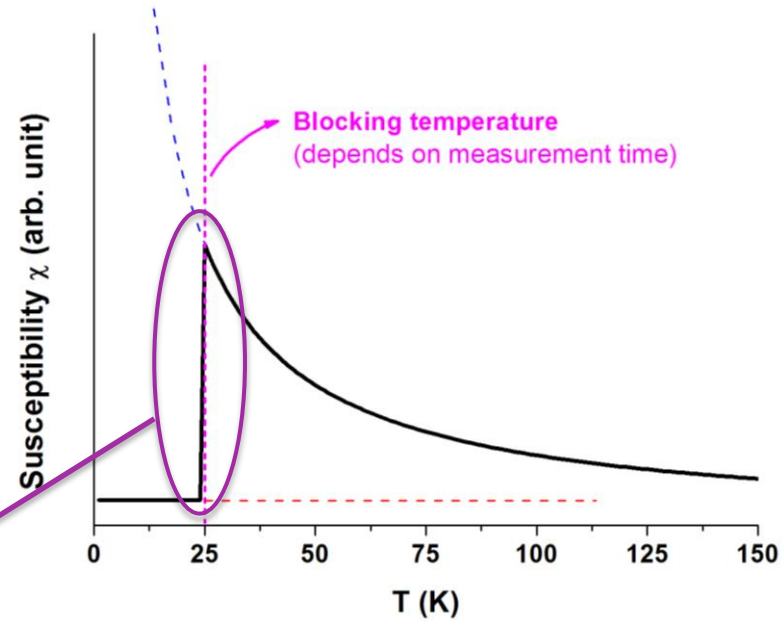

Abrupt change of the susceptibility, when reaching the <u>blocking temperature</u>

Signature of the magnetic anisotropy

Part III: Nanoparticle assemblies, from models to experiments

- Theoretical framework
- Magnetic anisotropy and particle size distribution (zero-field cooled/field cooled curves)
- Experimental results (Co, CoPt, FePt and FeRh nanoparticles)
- Advanced magnetic characterization (Interactions, bi-axial anisotropy…)

  ➡ Modeling of remanence curves

From model to real samples

Our goal: determination of the **intrinsic properties** of magnetic nanoparticles

➡ Beyond a simple descriptive analysis (susceptibility peak, coercive field…)

Keep in mind that they can differ from the bulk ones (size and interface effects)

➡ Link between the magnetic properties and the structure, chemistry etc.

For a real sample, we have a size distribution, the temperature is T≠0…

➡ A realistic description requires a cautious modeling

Our experimental approach: preformed particles deposited under vacuum, diluted in a non-magnetic matrix

Theoretical framework

Non-interacting macrospins, with a randomly oriented uniaxial (or bi-axial) anisotropy, Néel relaxation

For each particle
- Moment: $\mu = M_S V$
- Anisotropy: $K = K_{eff} V$

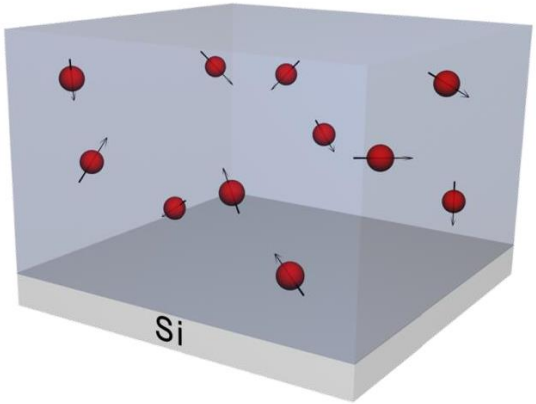

Cluster deposition

Deposition of preformed clusters (physical route)

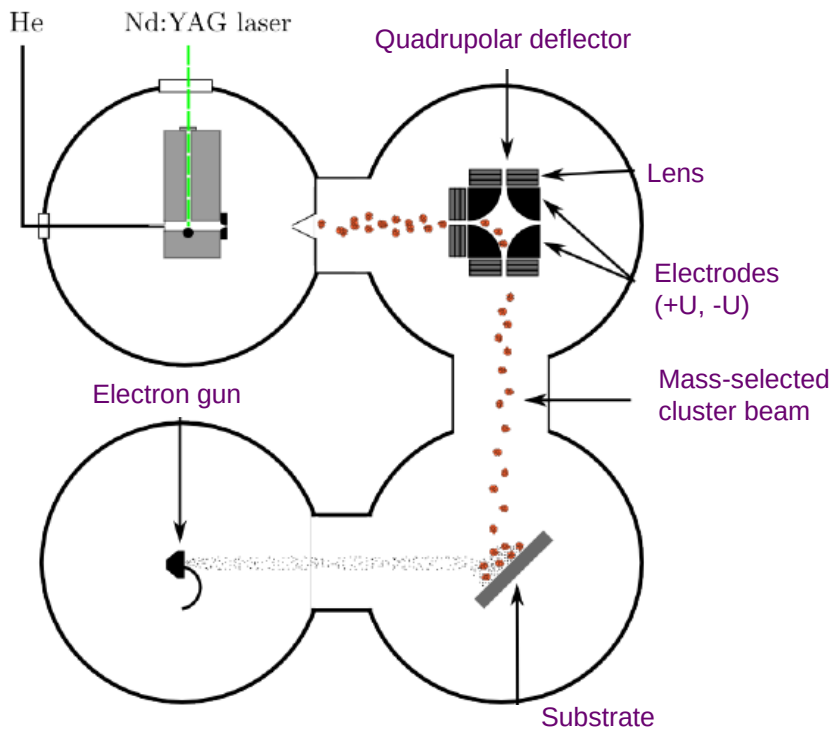

A. Perez *et al.*, Int. J. Nanotechnol. **7**, 523 (2010)

R. Alayan *et al.*, Rev. Sci. Instrum. **75**, 2461 (2004)

Low energy cluster beam deposition, based on a laser vaporization source

✓ Deposition under ultra-high vacuum

✓ Adjustable composition (target)

✓ Capping or co-deposition in a matrix

→ • Protect the particles
• Avoid coalescence

✓ Possibility of size selection (quadrupolar electrostatic deflector)

All the particles have the same velocity

→ Selection of kinetic energy = mass selection

Typical particle size ~ 3 nm diameter

Random deposition → Diluted assemblies of particles, which are then far enough from each other to **avoid magnetic interactions**

Nanoparticle assemblies

- Adjustable particle size, independently from the surface density.

Diluted assemblies (avoid interactions)

✓ Typical concentration for 3D samples ~1% in volume

- Relative diameter dispersion lower than 10 % with size selection.

Examples of 2D assemblies (TEM grids)

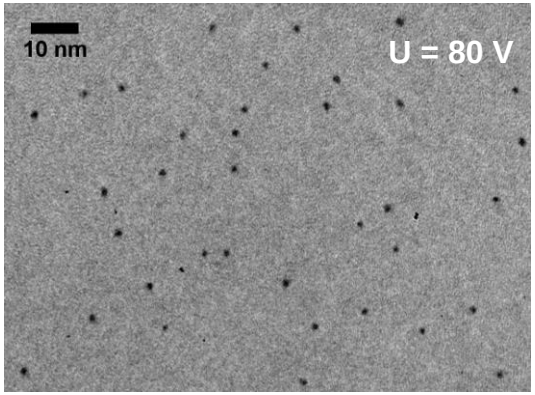

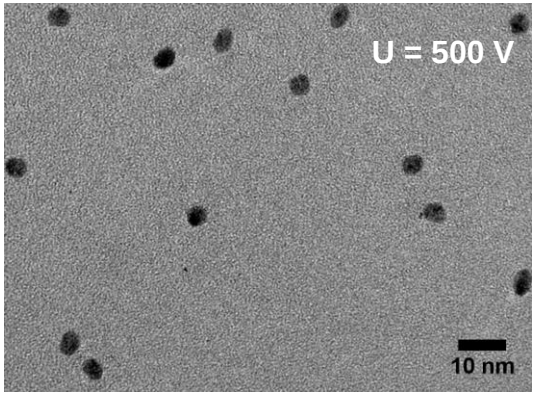

CoPt nanoparticles

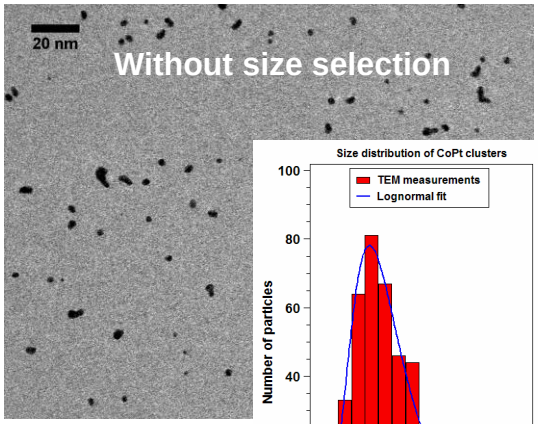

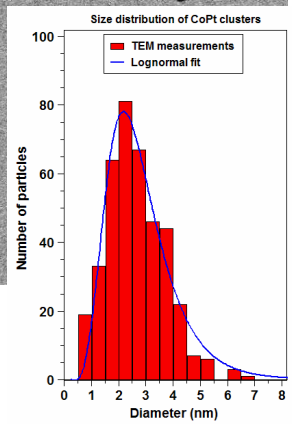

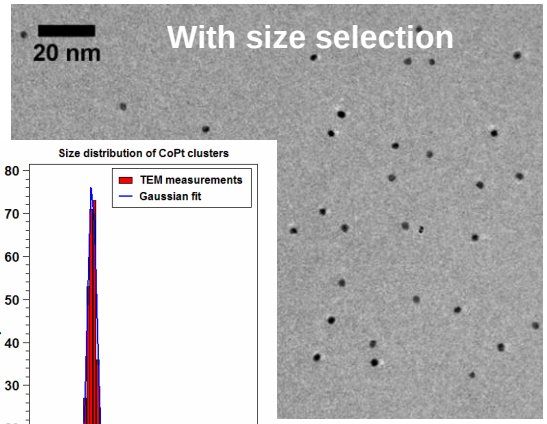

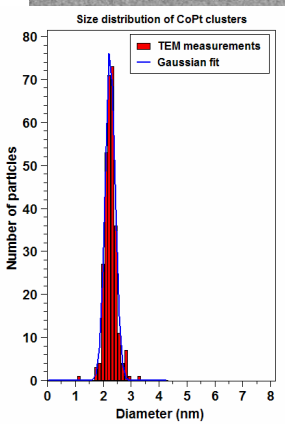

$\Delta D/D_m$ ~ 7-8 %

Magnetic anisotropy: ZFC/FC measurements

Zero-Field Cooled / Field Cooled (ZFC/FC) protocol

Low field susceptibility curves, as a function of temperature

➡ blocked → superparamagnetic crossover

Requirement: the sample has no remanent magnetization at 300 K

➡ Superparamagnetic sample

- We start from a zero applied field (H = 0), at room temperature: M = 0
- The sample is cooled down (2 K), with no applied field (zero-field cooled): M = 0
- Once at low T, a small field is applied (H ~ 50 Oe, B ~ 5 mT)

The measurement starts

- Slow increase of T, with applied field H: for each T the magnetic moment is measured ➡ $M_{ZFC}(T)$
- Once room temperature is reached, slow decrease of T, with the same applied field H (field cooled): for each T the magnetic moment is measured ➡ $M_{FC}(T)$

ZFC/FC = “round trip” (2K → 300 K → 2 K), with applied field H

ZFC/FC measurements

Sample made of ferromagnetic nanoparticles: ZFC ≠ FC

➡ Signature of the **magnetic anisotropy**

Dynamical process

⬇

Temperature sweep at a rate

$v_T = dT/dt$

What we would like to know:

- Influence of the different parameters (size distribution, anisotropy…)
- Analytical expression of the curves?

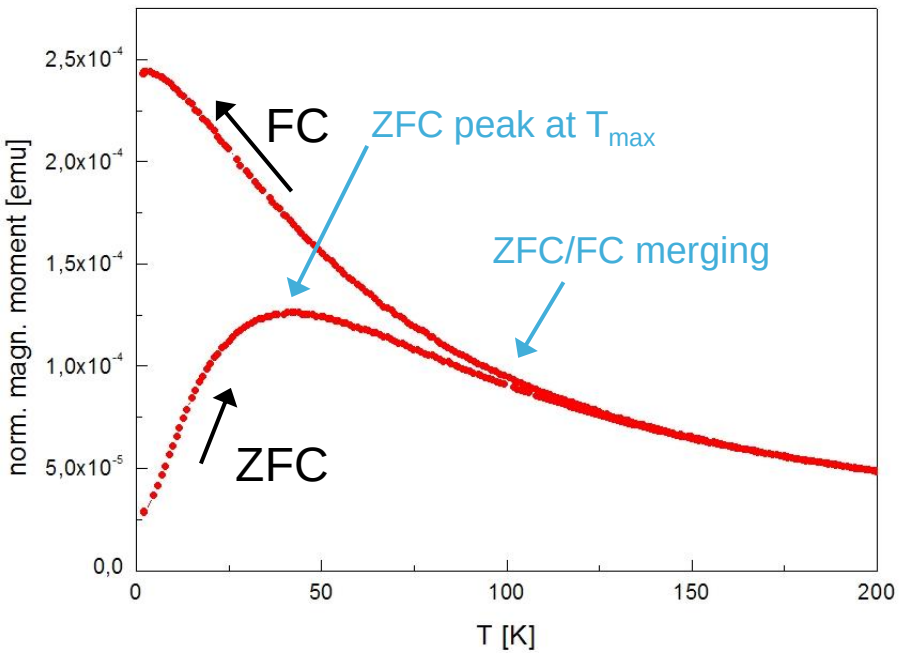

When T increases, it becomes possible to overcome the anisotropy energy barrier

➡ The magnetic anisotropy energy distribution controls the entire curve.

The curves are often only *qualitatively* analyzed (with a focus on the peak temperature)

✓ **Quantitative** analysis of experimental curves ➡ **Best fit procedure**

ZFC/FC modeling

F. Tournus, E. Bonet, J. Magn. Magn. Mater. **323**, 1109 (2011).

Assembly of randomly oriented uniaxial identical macrospins

Dynamical linear susceptilibilty: $\tilde{\chi}(\omega) = \dfrac{\chi_{eq} + i\omega\tau\chi_b}{1 + i\omega\tau}$ with $\tau = 1/\nu \simeq \tau_0 \exp\left(\dfrac{\mathrm{K}}{k_\mathrm{B}\mathrm{T}}\right)$ Néel relaxation

➡ Differential equation for the ZFC/FC protocol:

$$\frac{1}{\nu}\frac{\mathrm{d}M}{\mathrm{d}t} + M = \frac{\mu_0 \mu^2 H}{3 k_B T}$$

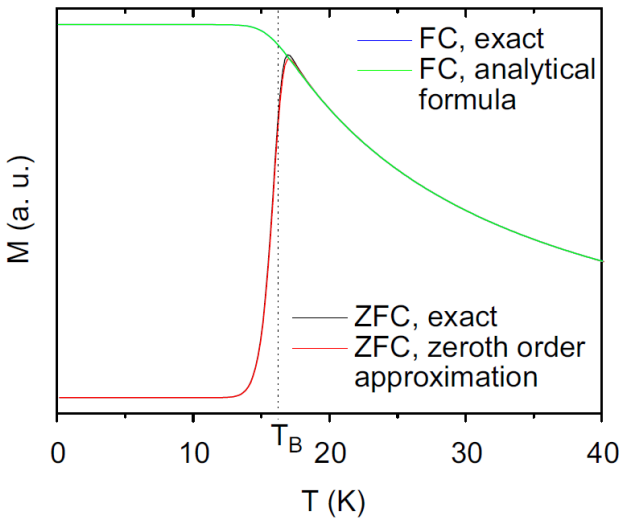

Solution for a temperature sweep:

Remarkably simple approximate expression (very close to the exact one)

$$M^0_{ZFC}(T) = M_b e^{-\nu\delta t} + M_{eq}(1 - e^{-\nu\delta t})$$

with $\delta t(T)$ effective waiting time

$$\delta t(\mathrm{T}) \simeq 0.6727 \frac{\mathrm{T}}{\nu_\mathrm{T}} \left(\frac{\mathrm{K}}{k_\mathrm{B}\mathrm{T}}\right)^{-0.9}$$

➡ **Progressive crossover** from blocked to superparamagnetic (equilibrium) regime

• Improved description compared to the *abrupt transition model* where the macrospins are either fully blocked or superparamagnetic, with a transition at $T_B = \dfrac{K}{k_B \ln(\nu_0 \tau_{\mathrm{meas}})}$

ZFC/FC simulation

- Extension of the blocking temperature concept, taking into account the temperature sweeping rate: *crossover temperature* T_X (depends on several parameters).

- Similar expression for the FC curve, with $M_b^{FC} = M_{eq}(T_X)$

➡ Semi-analytical expression, *progressive crossover model*

Efficient simulation of the entire ZFC/FC curves for an assembly with a particle size distribution

For a single size (volume V known), T_{max} can directly provide the value of the anisotropy constant K_{eff}:

$$K_{eff}V \sim 25\ k_B T_{max}$$

The same "rule of thumb" procedure **cannot be used** with a size dispersion (by using the mean or median volume)

The size distribution has a strong impact on the curves

➡ Modifies the ZFC peak width and position

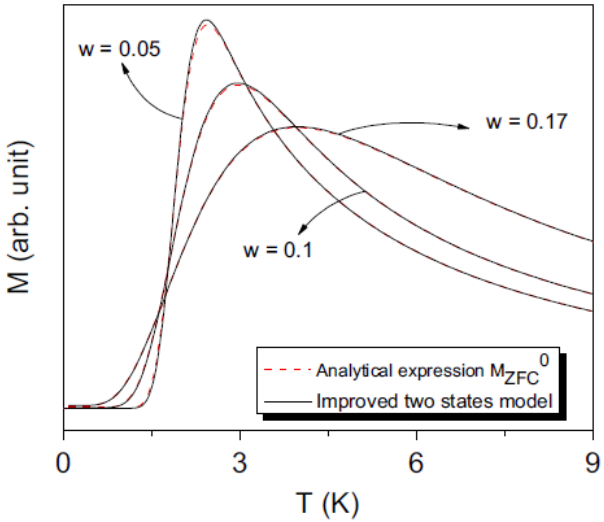

Uncertainties on the size-distribution ➡ Significant potential errors on the anisotropy

ZFC/FC simulation

Rk.: The blocking temperature is only relevant for a single size!

Effect of the size dispersion

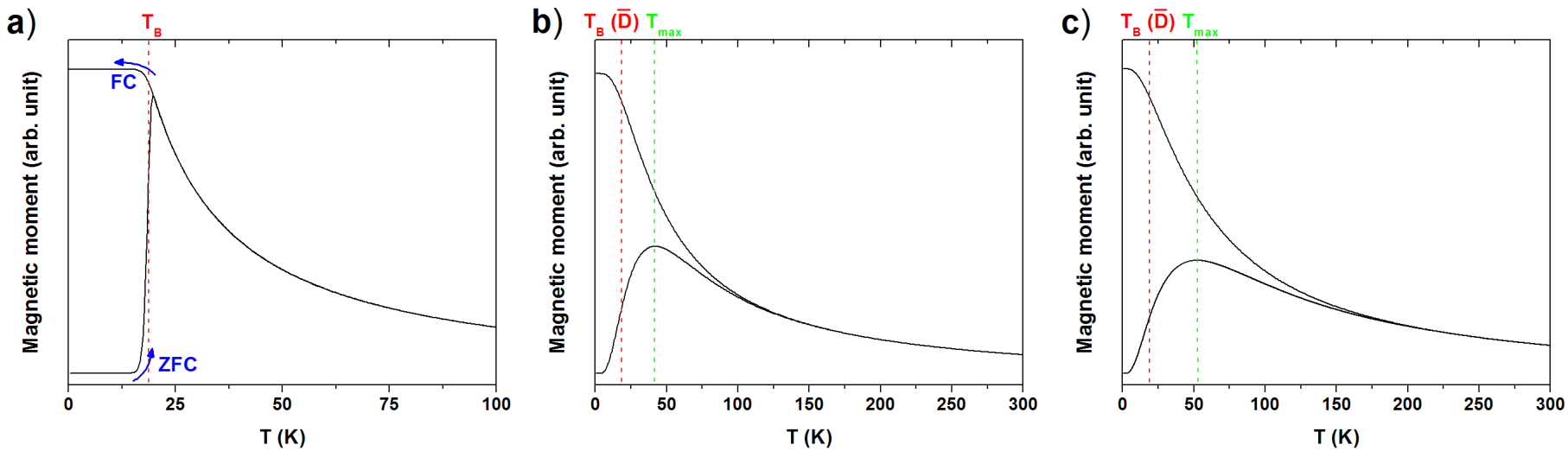

Single size

Lognormal distribution (dispersion w=0.2)

Lognormal distribution (dispersion w=0.25)

Keep in mind: The ZFC peak temperature T_{max} is <u>not</u> the blocking temperature of the mean particle size!

Quantitative analysis using a “triple fit”

“triple fit” of experimental curves

Simultaneous fit of ZFC/FC curves and M(H) loop at 300 K (superparamagnetic)

The fit (Langevin functions) of a super-paramagnetic magnetization loop is not very discriminating

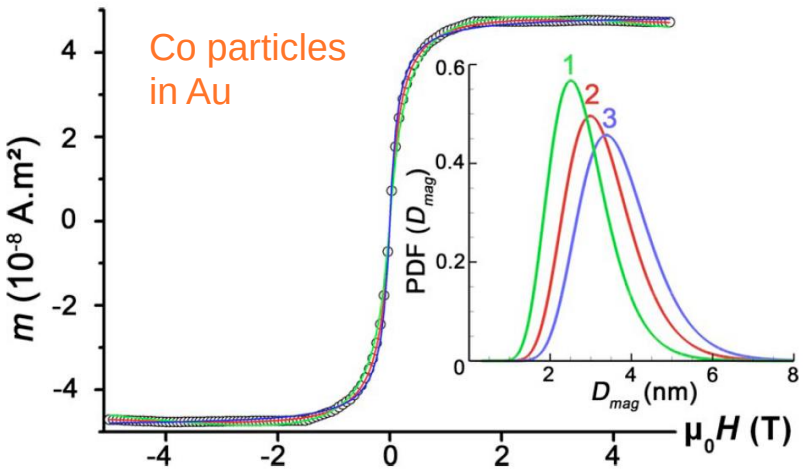

Different size distributions can fit the M(H) curves

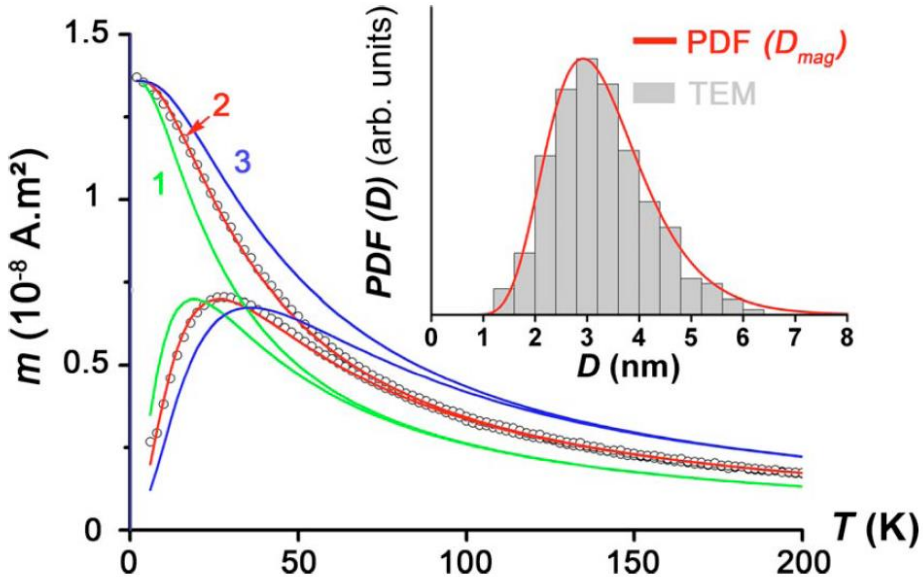

Co particles in Au

Use of the “progressive crossover model” for ZFC/FC curves

Adjustable parameters:

- Size distribution
- Number of particles
- Anisotropy constant

→ Increased reliability and accuracy

A. Tamion et al., Appl. Phys. Lett. **95**, 062503 (2009)

“triple fit”

Accurate and efficient **fitting procedure** (triple fit)

➡ Reliable determination of the magnetic size distribution and anisotropy for nanomagnet assemblies

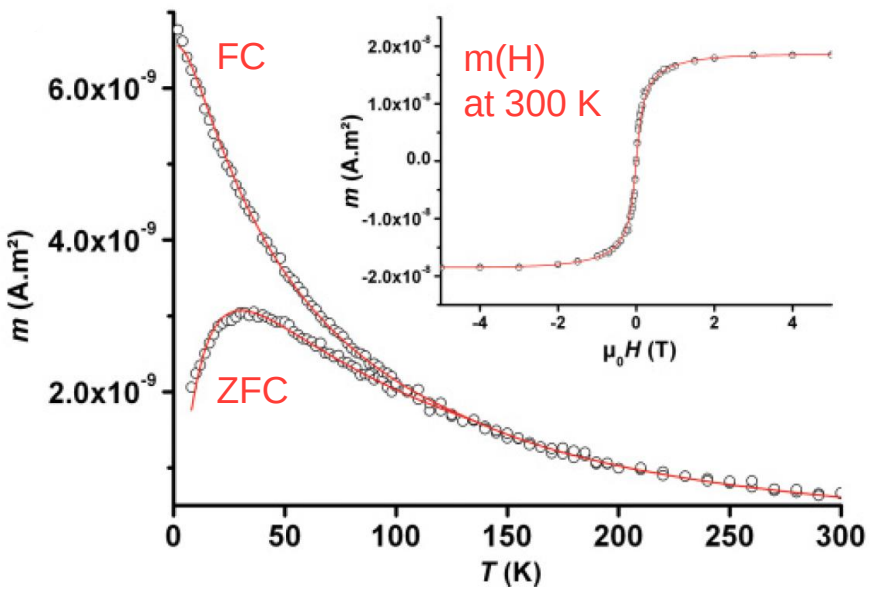

Example of fit for 3 nm Co nanoparticles in germanium

A. Tamion *et al*., Phys. Rev. B **85**, 134430 (2012).

$$m(H) = N_{tot} M_S \int_0^{\infty} \left[\coth\left(\frac{\mu_0 M_S V H}{k_B T} \right) - \frac{k_B T}{\mu_0 M_S V H} \right] V f(V) dV$$

✓ A failure of the “triple fit” can be the signature of non-negligible interactions between the particles

Coercive field and anisotropy

Stoner-Wohlfarth model, at 0 K

➡ Coercive field H_C linked to the anisotropy

$H_C(T)$ is always lower than $H_C(0)$

➡ Extrapolation to T=0 would give ~$H_A/2$

CoPt nanoparticles (3.8 nm diameter)

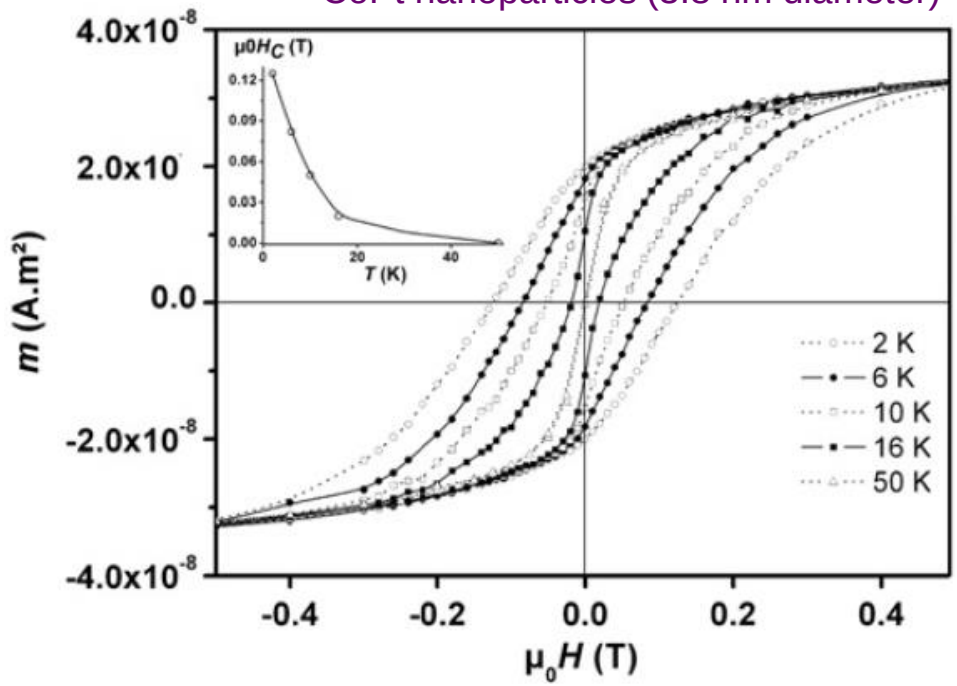

F. Tournus *et al.*, J. Magn. Magn. Mater. **323**, 1868 (2011).

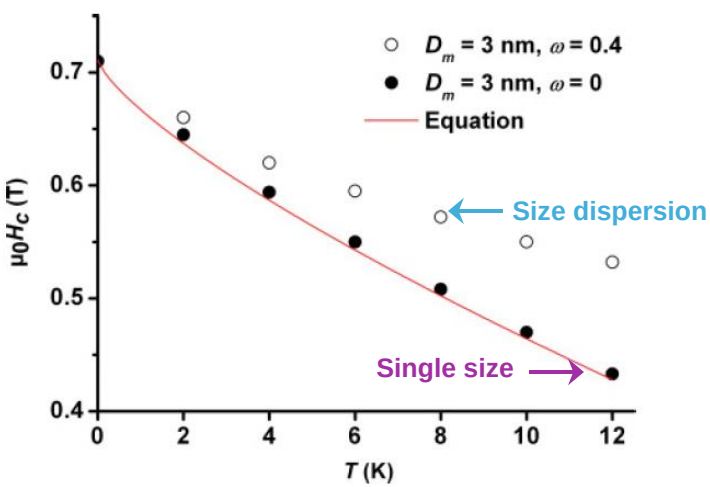

A. Tamion *et al.*, Phys. Rev. B **85**, 134430 (2012).

Sharrock formula for the evolution of $H_C(T)$

$$H_c(T,V) = H_c(T=0K)[1-(25k_BT/|K_1|V)^{3/4}]$$

➡ Not valid for a <u>size dispersion</u>! Hazardous method…

Rk.: Beware of a direct comparison of H_C values…

Scaling properties, experimental examples

F. Tournus *et al.*, J. Magn. Magn. Mater. **323**, 1868 (2011)

CoPt nanoparticles (3.1 nm diameter)

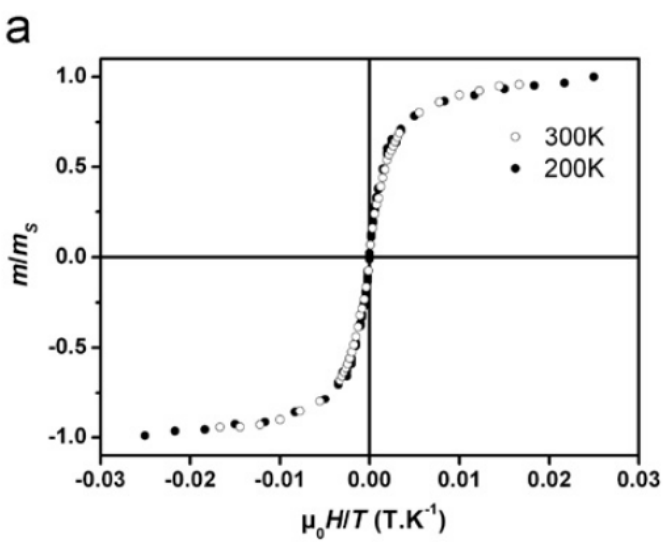

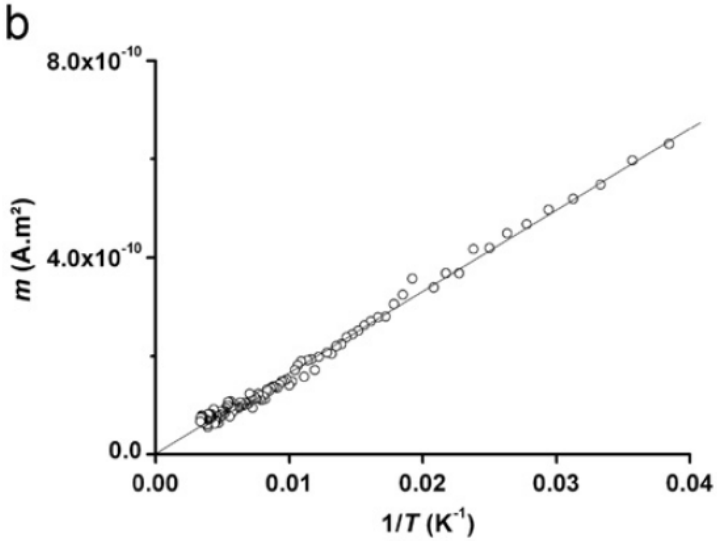

1/T evolution of the susceptibility (m at low field)

Verification of the H/T scaling in the superparamagnetic regime

Rk.: interactions can induce a scaling failure

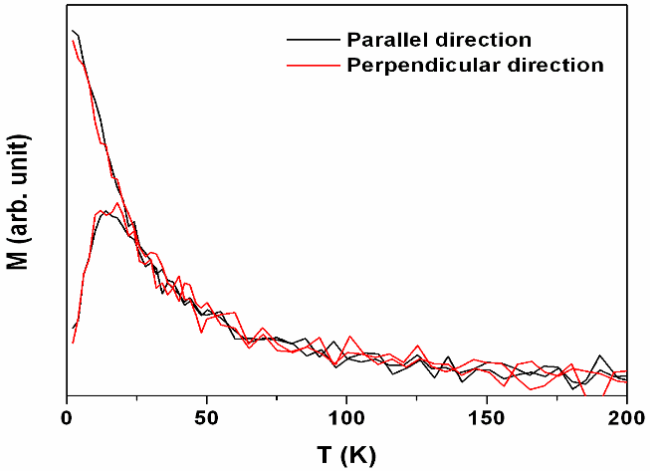

No signature of interactions: no “sample shape” effect

Magnetic size and apparent size

JOURNAL OF APPLIED PHYSICS **110**, 063904 (2011)

Demixing in cobalt clusters embedded in a carbon matrix evidenced by magnetic measurements

Alexandre Tamion,[1] Matthias Hillenkamp,[1,2,a)] Arnaud Hillion,[1] Florent Tournus,[1] Juliette Tuaillon-Combes,[1] Olivier Boisron,[1] Spiros Zafeiratos,[3] and Véronique Dupuis[1]

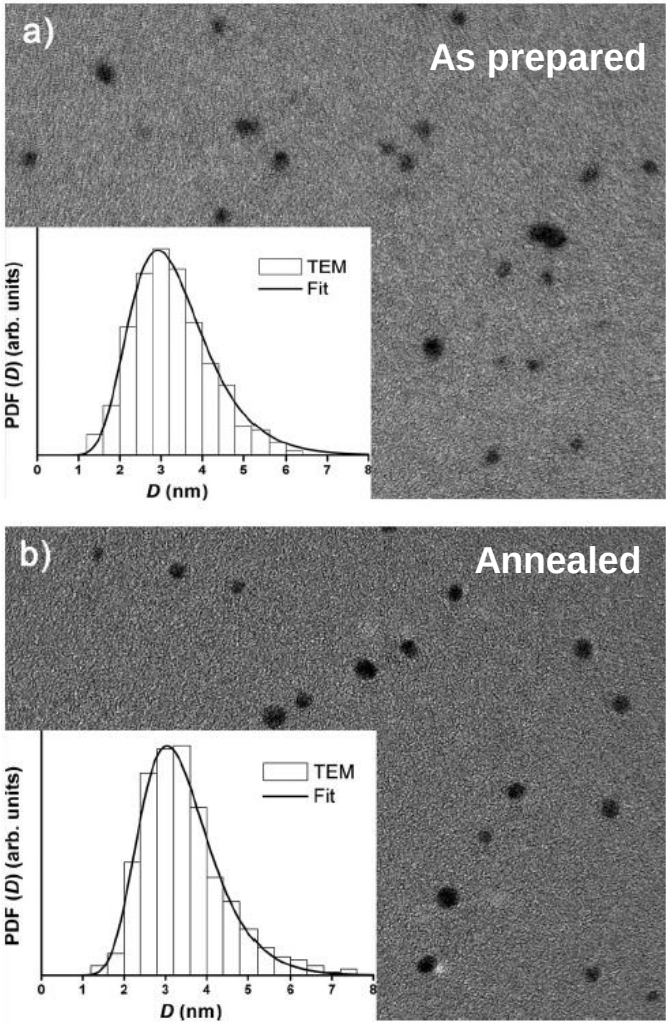

FIG. 1. Transmission electron microscopy (TEM) images of as prepared (a) and annealed (b) samples with Co clusters embedded in amorphous carbon. The inset displays the deduced size histograms, together with the best fits corresponding to a lognormal distribution.

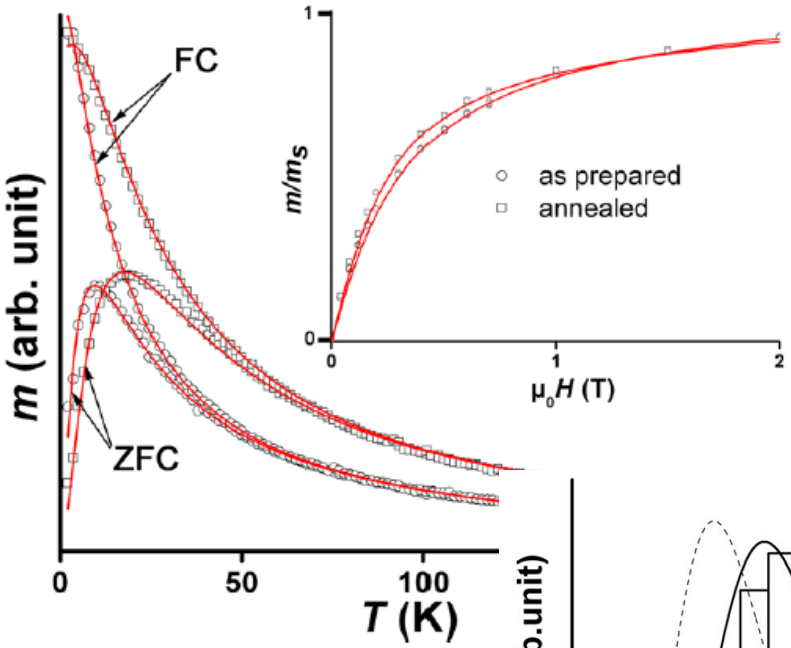

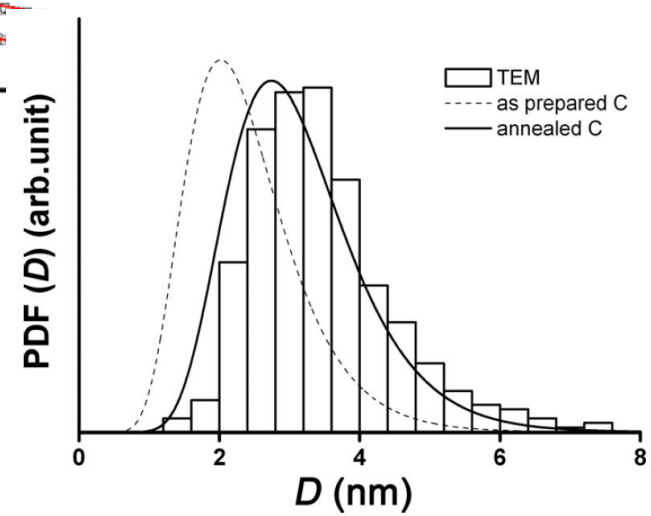

A recent study on bimetallic nanoparticles: CoPt (and FePt) cluster films

- Magnetic properties, in relation with their atomic structure

CoPt (and FePt) alloys

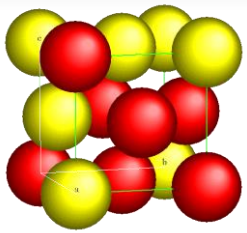

A1 phase

- Chemically disordered
- fcc cell

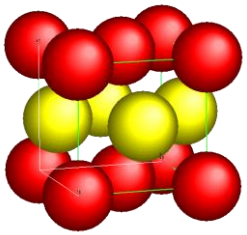

$L1_0$ phase

- Chemically ordered
- tetragonal cell (c/a < 1)

The $L1_0$ phase has a huge magnetic anisotropy constant (K_{eff}~ 5 MJ/m^3)

➡ Interesting for magnetic storage applications

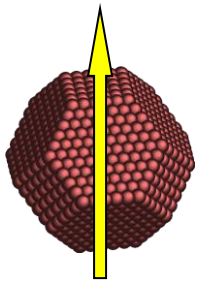

The $L1_0$ phase is stable at room temperature, but A1 is metastable

➡ Chemical ordering obtained by annealing

$L1_0$: S = 1
A1: S = 0

With size reduction, chemical order phase transition shifted and smoothed

➡ Threshold size for $L1_0$ stability?

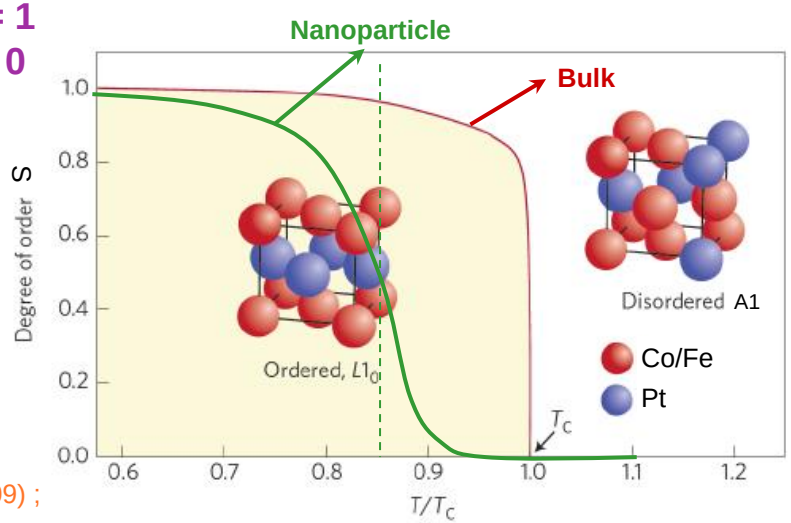

D. Alloyeau *et al.*, Nature. Mater. **8**, 940 (2009) ;
K. Sato, Nature Mater. **8**, 924 (2009).

CoPt/FePt: Structure and size reduction

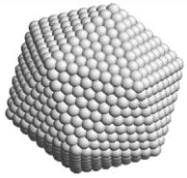

Icosahedron

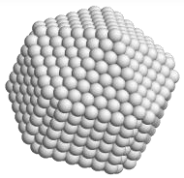

Decahedron

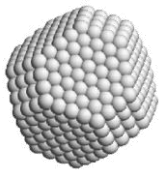

Truncated-octahedron

- As a function of particle size, competition between different geometries

→ Multiply-twinned particles

- Various theoretical predictions

→ $L1_0$ ordered decahedron should be favorable

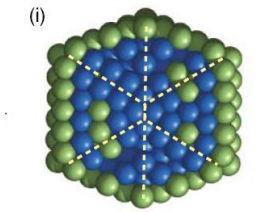

Core–shell icosahedron with depleted subsurface shell

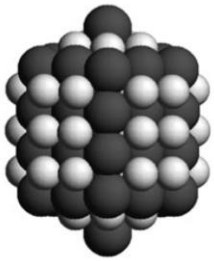

M. Grüner *et al.*, *Phys. Rev. Lett.* **100**, 087203 (2008)

G. Rossi *et al.* *Faraday Discuss.* **138**, 193 (2008)

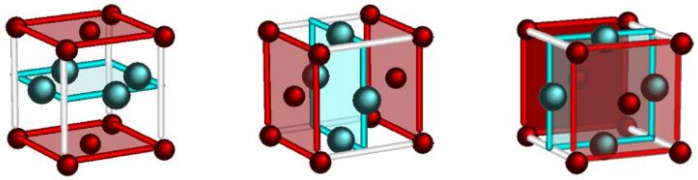

From cubic to tetragonal: 3 equivalent directions for the chemical order (variants)

- Antiphase, c-phase or twin boundaries between different $L1_0$ domains

→ Observed in films and large particles
Are they met in small particles?

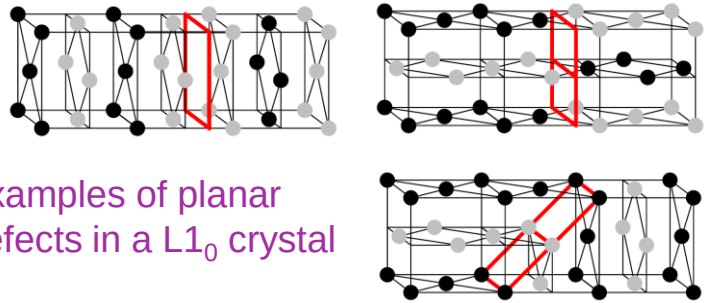

Examples of planar defects in a $L1_0$ crystal

A. Alam *et al.*, Phys. Rev. B **82**, 024435 (2010)

Intrinsic properties of ordered particles?

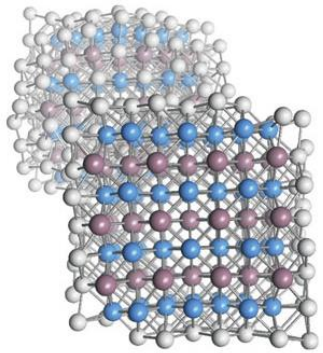

$Fe_{80}Pt_{67}Al_{162}$

C. Antoniak *et al*., Nat. Commun. **2**, 528 (2011).

• Influence of the environment (interface, magnetically dead layer, inter-particle interactions…)

Intrinsic properties of the nanoparticles?

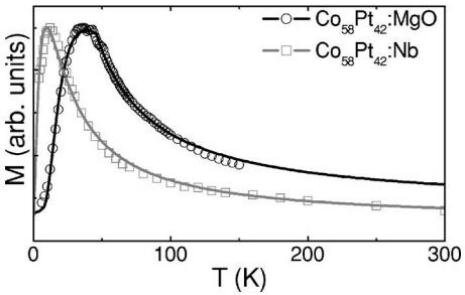

S. Rohart *et al*., Phys. Rev. B **74**, 104408 (2006).

Synthesis itself is a challenge (well defined size, no coalescence, no pollution…)

→ Our approach: diluted assemblies of nanoparticles, prepared by ***low energy cluster beam deposition***, and embedded in a carbon matrix

The intrinsic magnetic properties of nano-sized chemically ordered CoPt particles are difficult to determine reliably

→ Combine **structural** and **magnetic** characterizations of CoPt nanoparticles

Size selection of CoPt particles

Magnetometry measurements

➡ **Size selected CoPt nanoparticles (3 nm diameter), as prepared**

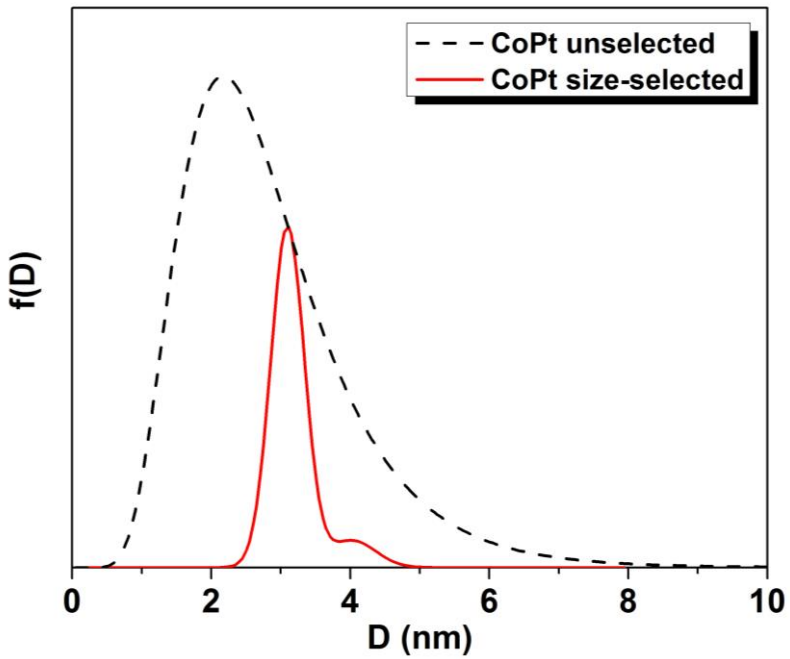

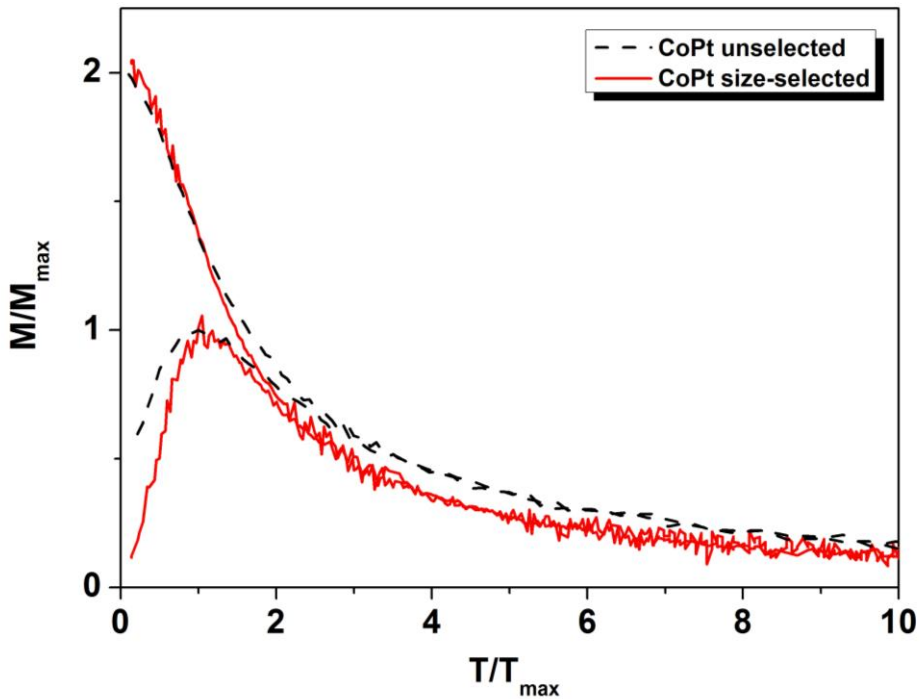

Although the size dispersion is greatly reduced with size selection, the ZFC peak is not much narrower…

Anisotropy constant dispersion

The usual $E_{ani} = K_{eff}V$ model is no more valid → Anisotropy constant **dispersion**

Gaussian distribution of K_{eff} :

- ✓ Relative dispersion ~ 40%
- ✓ $\langle K_{eff} \rangle$ ~ 200 kJ/m^3

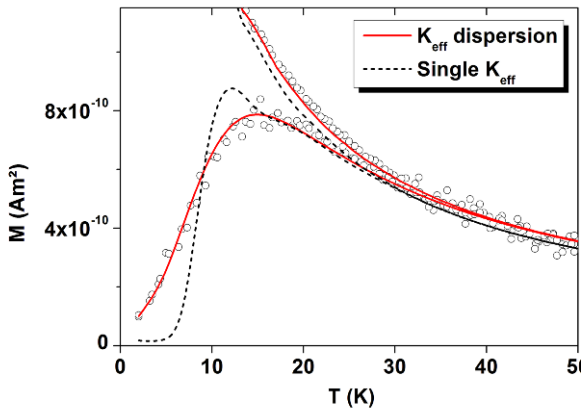

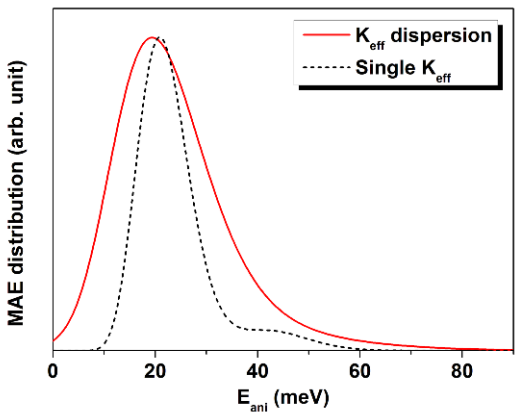

Such a K_{eff} dispersion was not detectable for particles without size selection

→ A narrow size distribution is necessary

Physical origin?

Nanoalloy effect

- ✓ Composition
- ✓ Chemical order
- ✓ **Atomic configuration** (chemical arrangement)

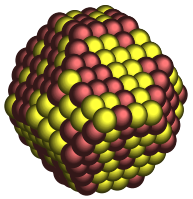

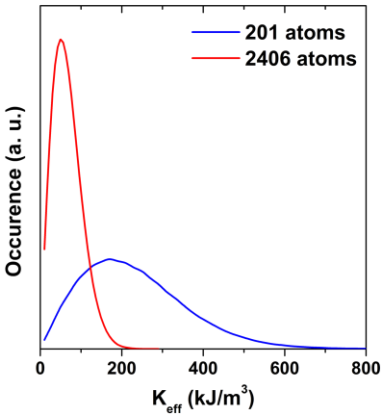

K_{eff} distribution calculated for chemically disordered CoPt particles

F. Tournus *et al.*, Phys. Rev. B **81**, 220405(R) (2010)

F. Tournus *et al.*, IEEE Trans. Magn. **44**, 3201 (2008)

Magnetic anisotropy evolution upon annealing

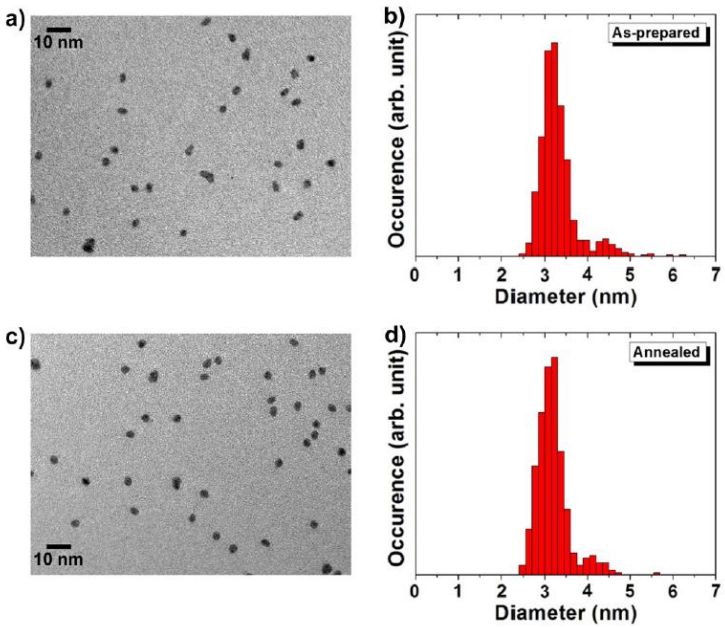

No modification of the particle size upon annealing

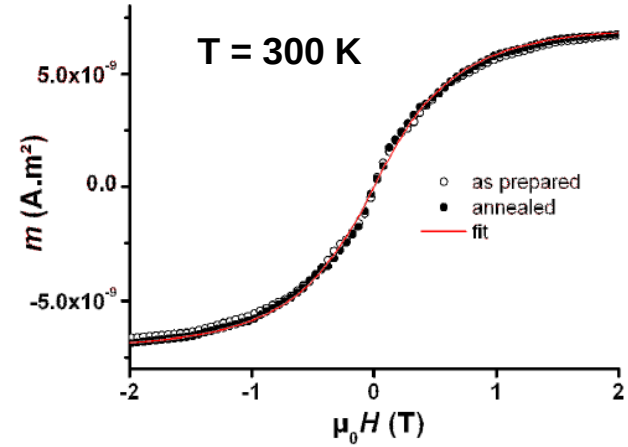

V. Dupuis *et al.*, IEEE Trans. Magn. **47**, 3358 (2011).

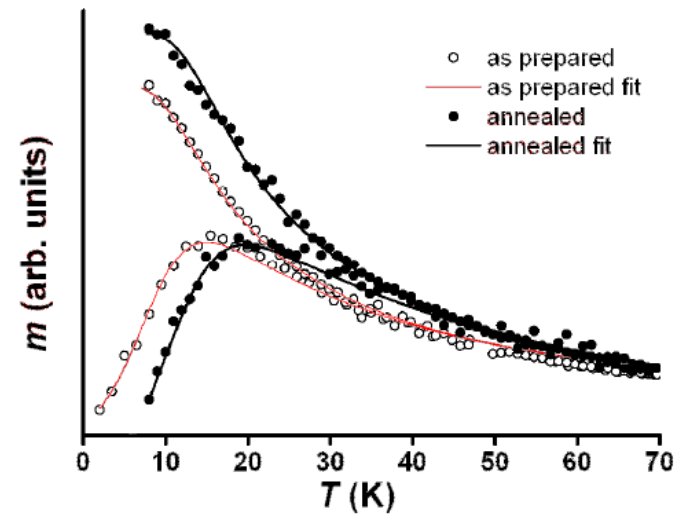

Evolution of the magnetic anisotropy

	As prepared	Annealed
D_m (nm)	3.12 ± 0.1	3.12± 0.1
ω (nm)	0.22 ± 0.05	0.22± 0.05
K_{eff}(kJ.m^{-3})	218 ± 20	293 ± 30
ω_K(kJ.m^{-3})	37% ± 5%	28% ± 5%

This increase is **much smaller** than what is observed in the bulk

To fix the ideas: with K_{eff} = 5 MJ/m^3 and D = 3 nm → T_B = 200 K

X-ray magnetic circular dichroism (XMCD)

F. Tournus *et al.*, Phys. Rev. B 77, 144411 (2008).
V. Dupuis *et al.*, J. Magn. Magn. Mater. **383**, 73 (2015).

Dichroism at the L absorption edges

→ magnetic moments (spin and orbital) of each element

XMCD at various $L_{2,3}$ edges	Co-edge μ_S (μ_B/at.) μ_L (μ_B/at.) μ_L/μ_S	Pt-edge μ_S (μ_B/at.) μ_L (μ_B/at.) μ_L/μ_S
CoPt as-prepared	**1.67** 0.13 0.077	**0.47** 0.07 0.150
CoPt annealed	**1.98** 0.20 0.101	**0.52** 0.10 0.192

- ✓ No Co oxidation, no "dead layer"
- ✓ Very high m_S value (Co bulk = 1.6 μ_B/at)
- ✓ Increase of m_S, m_L and m_L/m_S upon annealing

Annealing induces a change of the magnetic moments

→ **A1 → $L1_0$ chemical ordering?**

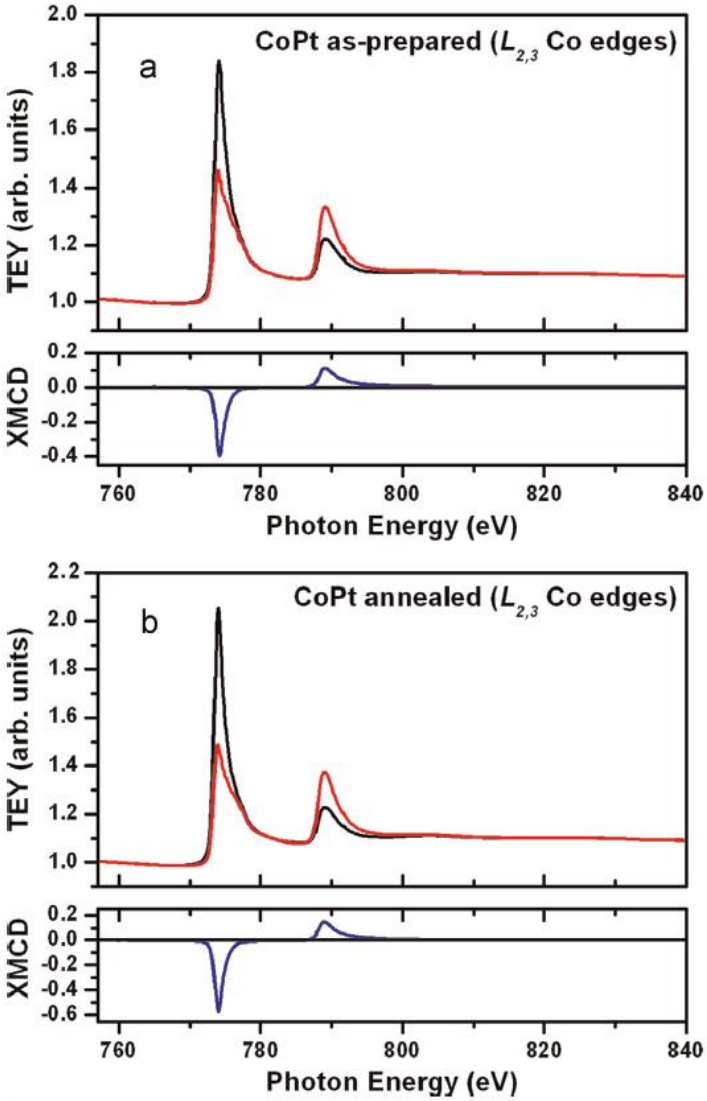

Fig. 2. Comparison between the XMCD spectra at the $L_{2,3}$ Co edges measured in TEY in a 5 T applied field and 4.2 K temperature at DEIMOS on 3 nm CoPt samples before (a) and after annealing (b).

✓ Structural characterization of CoPt particles in C

- EXAFS measurements (Extended X-ray Absorption Fine Structure)
- HRTEM observations

Chemical order and relaxation

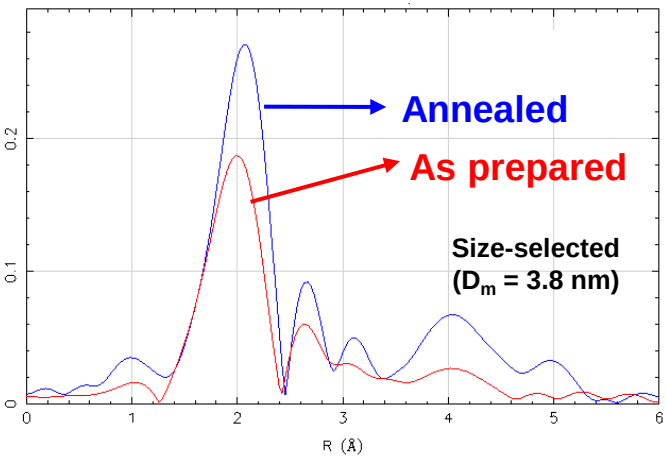

N. Blanc *et al.*, Phys. Rev. B **87**, 155412 (2013)
V. Dupuis *et al.*, Eur. Phys. J. B **86**, 1 (2013)

EXAFS measurements: probe the local environment of one type of atoms

- Drastic change upon annealing
- Evolution of N_{Co}/N_{Pt}

A1 → $L1_0$ transition

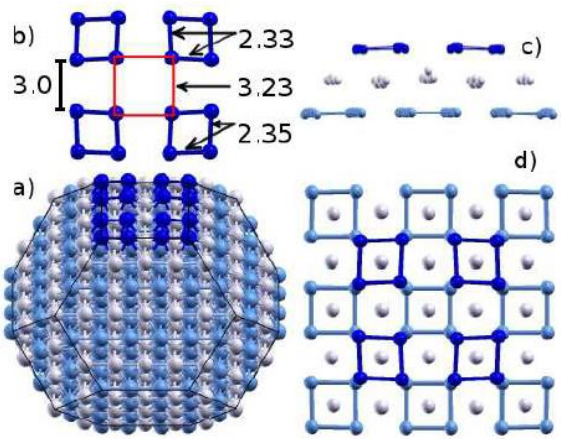

Apparent c/a ratio

→ Different around Co and Pt atoms: $d_{Pt\text{-}Pt} \neq d_{Co\text{-}Co}$

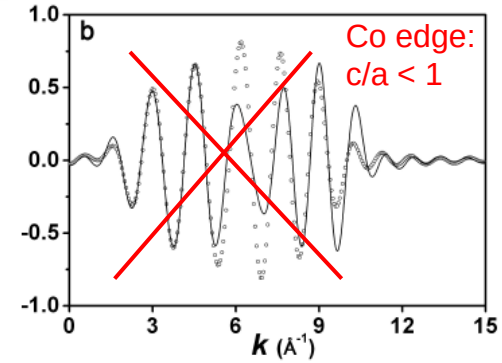

Tetragonalization different from the bulk

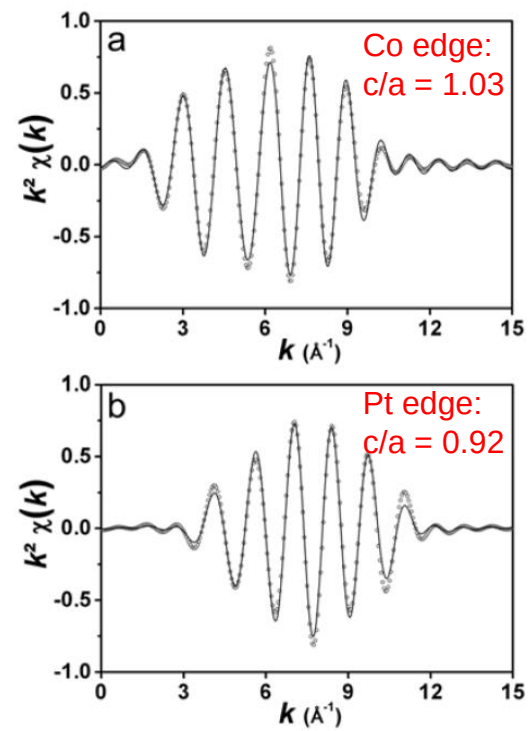

DFT calculations: "$L1_0$ like" structure

→ Strong relaxation of the Co-Co distances

Transmission electron microscopy

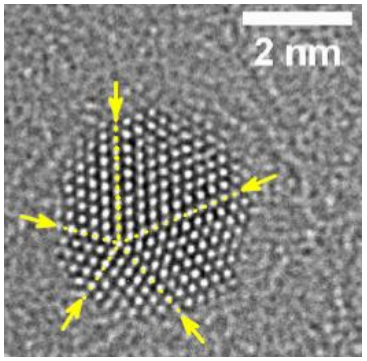

- ✓ Coexistence of fcc and multiply-twinned particles
- ✓ No chemical order before annealing
- ✓ $L1_0$ contrast ([001] peak) after annealing, even for the smallest particles

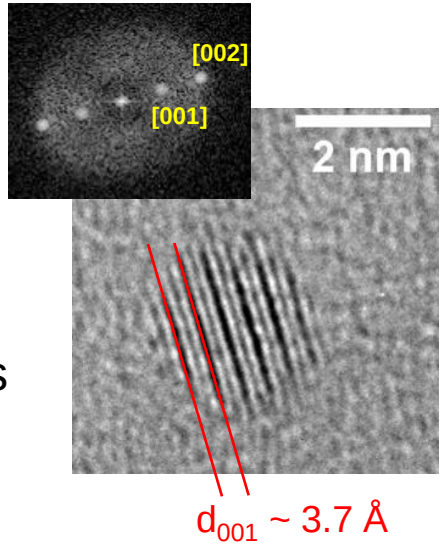

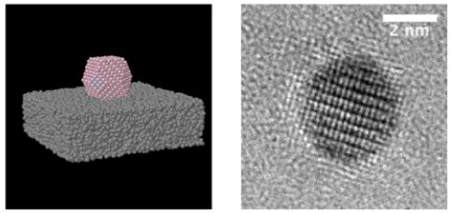

Quantification of the chemical order parameter for a single nanoparticle (S ~ 1)

N. Blanc *et al*., Phys. Rev. B **83**, 092403 (2011)

F. Tournus *et al*., Phys. Rev. Lett. **110**, 055501 (2013)

Particles with several $L1_0$ domains

Coexistence of several $L1_0$ variants (with antiphase boundaries)

In a single-crystal particle of 2 nm diameter!

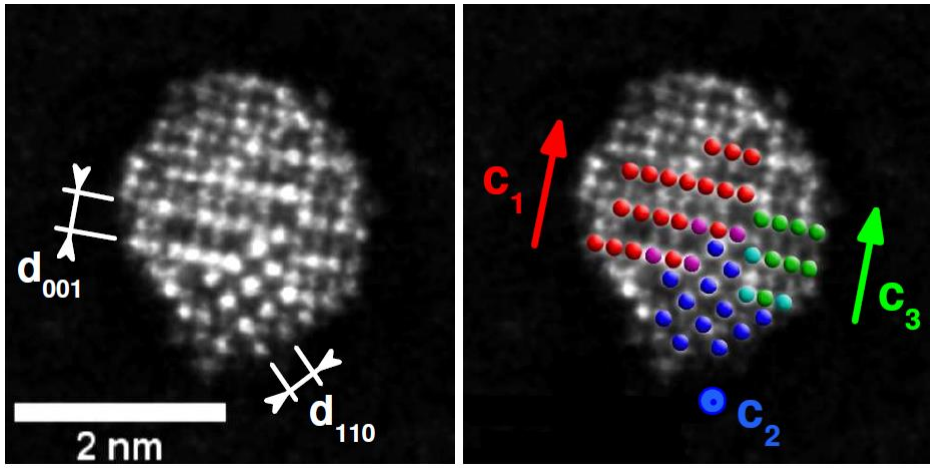

STEM HAADF (Z contrast) image of a CoPt particle

Chemically ordered decahedra

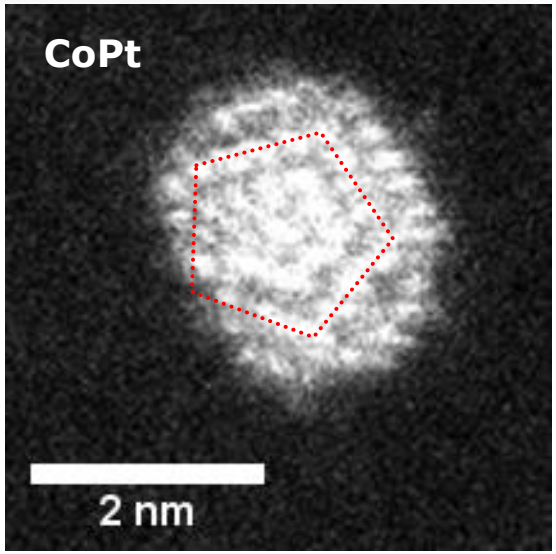

STEM-HAADF image

Decahedral particles with a chemical order

→ Five $L1_0$ domains with c axes in different directions

✓ Theoretically predicted structure

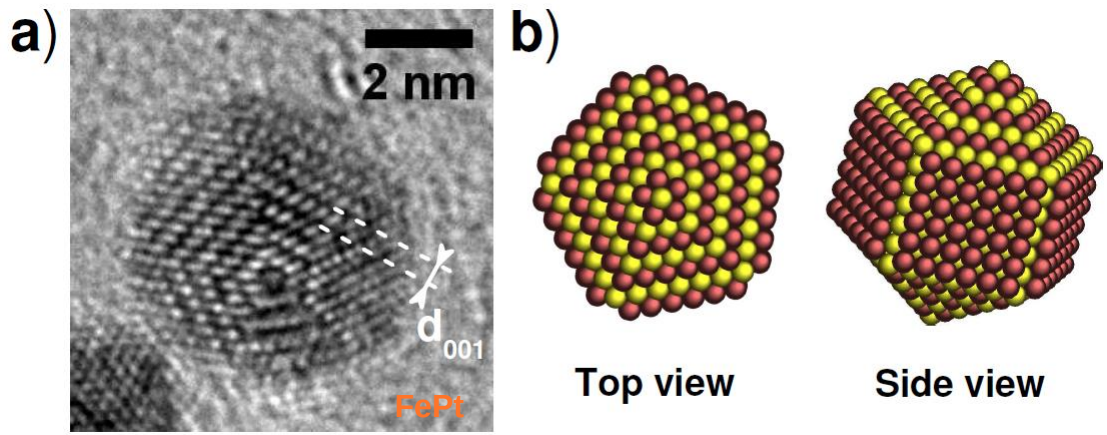

Particles with several $L1_0$ domains → **Lowering of the anisotropy!** (+ relaxation, $L1_0$ like)

Coexistence of various structures → Anisotropy constant dispersion

Similar observations for FePt nanoparticles…

F. Tournus *et al.*, Phys. Rev. Lett. **110**, 055501 (2013).

Chemically ordered FePt particles

F. Tournus *et al*., Phys. Rev. Lett. **110**, 055501 (2013).

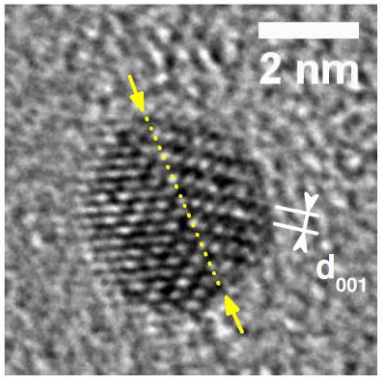

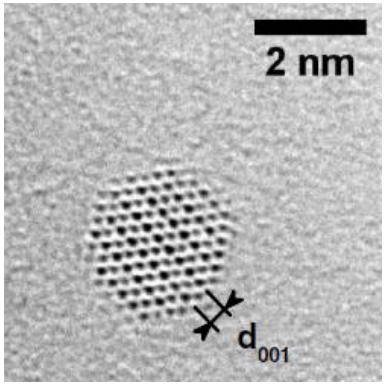

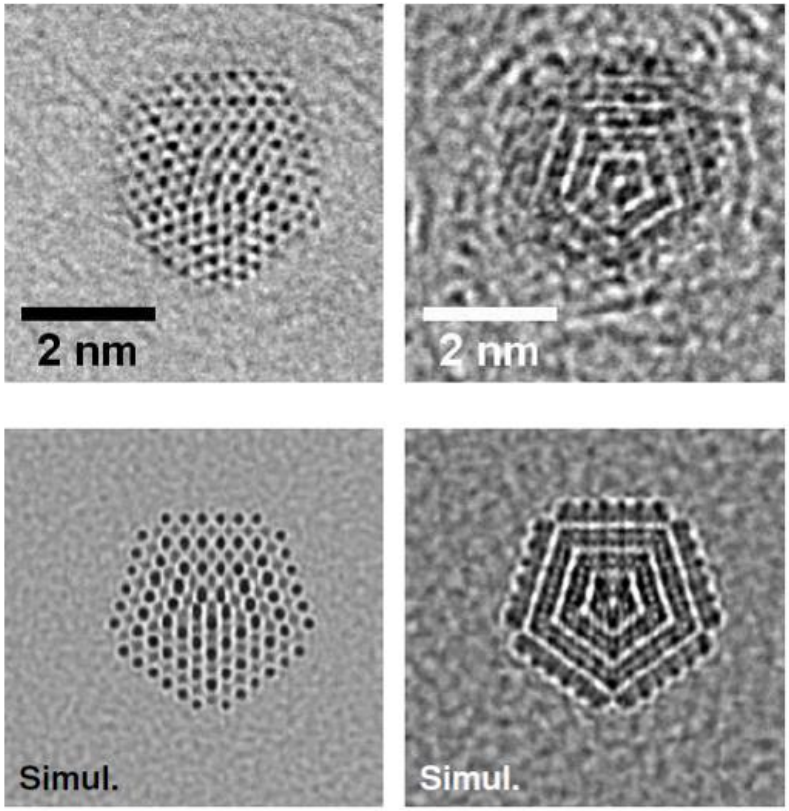

- Twinned particles with two $L1_0$ domains
- $L1_0$ order for small particles, down to 2 nm diameter
- Chemically ordered decahedra
- No surface segregation

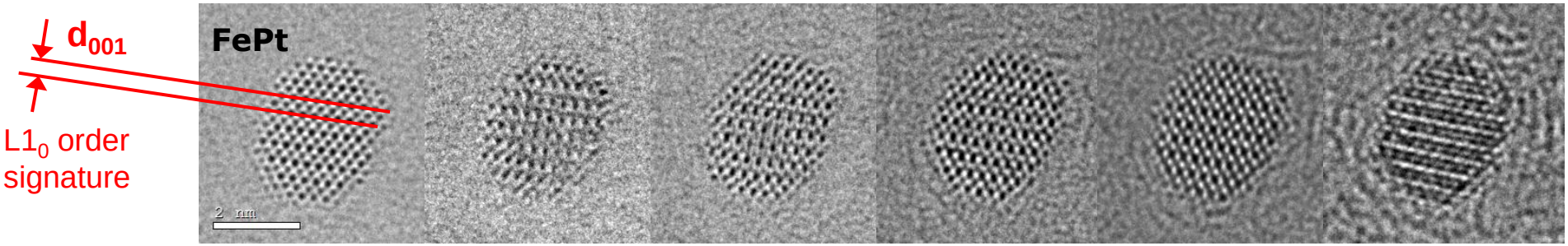

Through-focus HRTEM series of a FePt nanoparticle in the $L1_0$ phase

Difference between FePt and CoPt

Similar results of synchrotron measurements (XMCD, EXAFS)

After annealing
- Magnetic moments increase
- Fit with a $L1_0$ chemical order
- Relaxation ($d_{Fe-Fe} \neq d_{Pt-Pt}$)

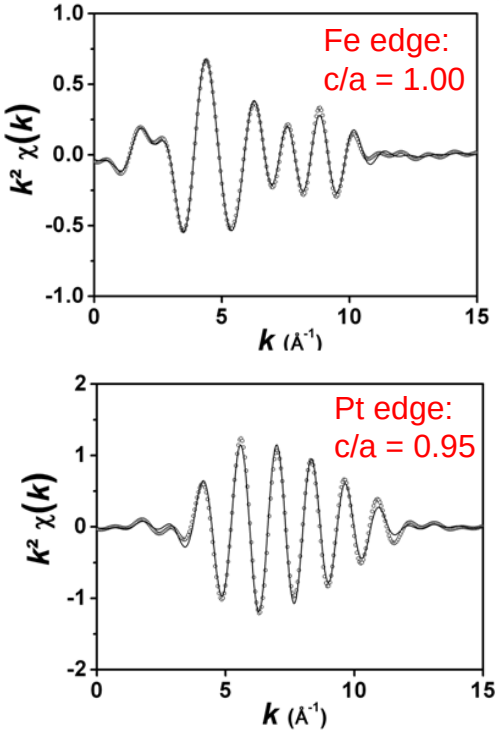

Magnetometry → Evolution upon annealing very different from CoPt nanoparticles

✓ Very large increase of the anisotropy (H_C and ZFC peak)

✓ Very large dispersion of the magnetic anisotropy energy

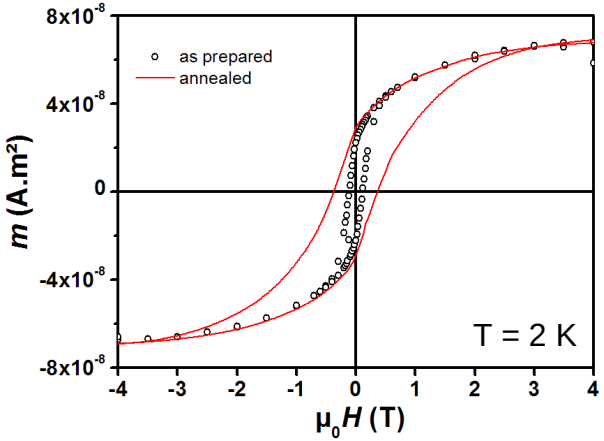

Huge magnetic anisotropy (> MJ/m³) for some particles

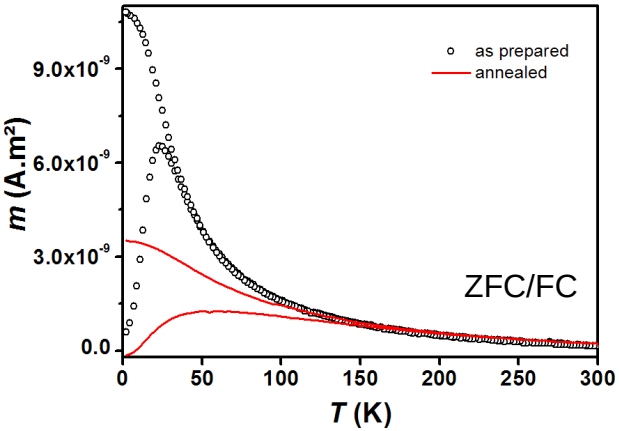

Conclusion on CoPt nanomagnets

✓ Effort for the determination of the intrinsic properties of CoPt nanoparticles

➡ Model systems, complementary characterizations

✓ Original properties of CoPt nanoparticles

- Magnetic anisotropy dispersion, evolution of the atomic magnetic moments
- For chemically ordered CoPt particles, the anisotropy remains much smaller than for the bulk $L1_0$ phase
- Existence of structures with several $L1_0$ domains, “exotic” geometries
- Relaxation of the inter-atomic distances because of finite size

✓ Similarities between CoPt and FePt nanoparticles

➡ But very different magnetic behavior!

Magnetic order: one example

The magnetic order can be influenced by the size reduction

➡ Example: FeRh nanoparticles

Chemically ordered particles (B2 phase), after annealing

The particles are ferromagnetic, down to 2 K, instead of anti-ferromagnetic

Chemically ordered FeRh particle

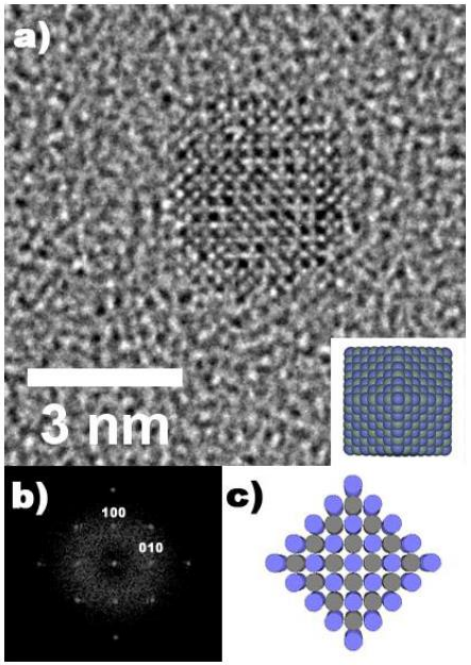

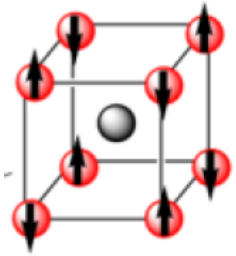

AF order

FM order

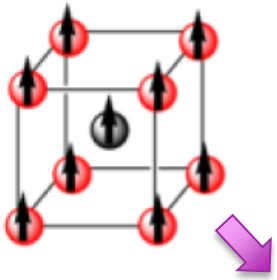

Chemically ordered FeRh particle

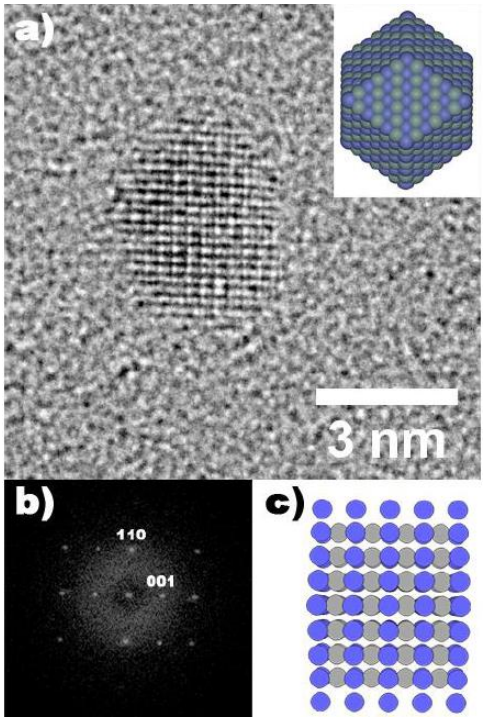

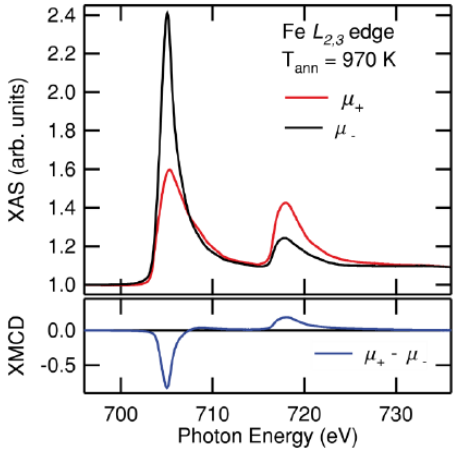

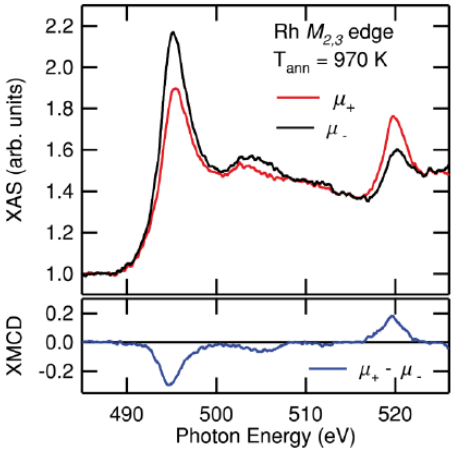

A. Hillion et al., Phys. Rev. Lett. **110**, 087207 (2013)

XMCD measurements at Fe and Rh edges

FeRh: Magnetometry measurements

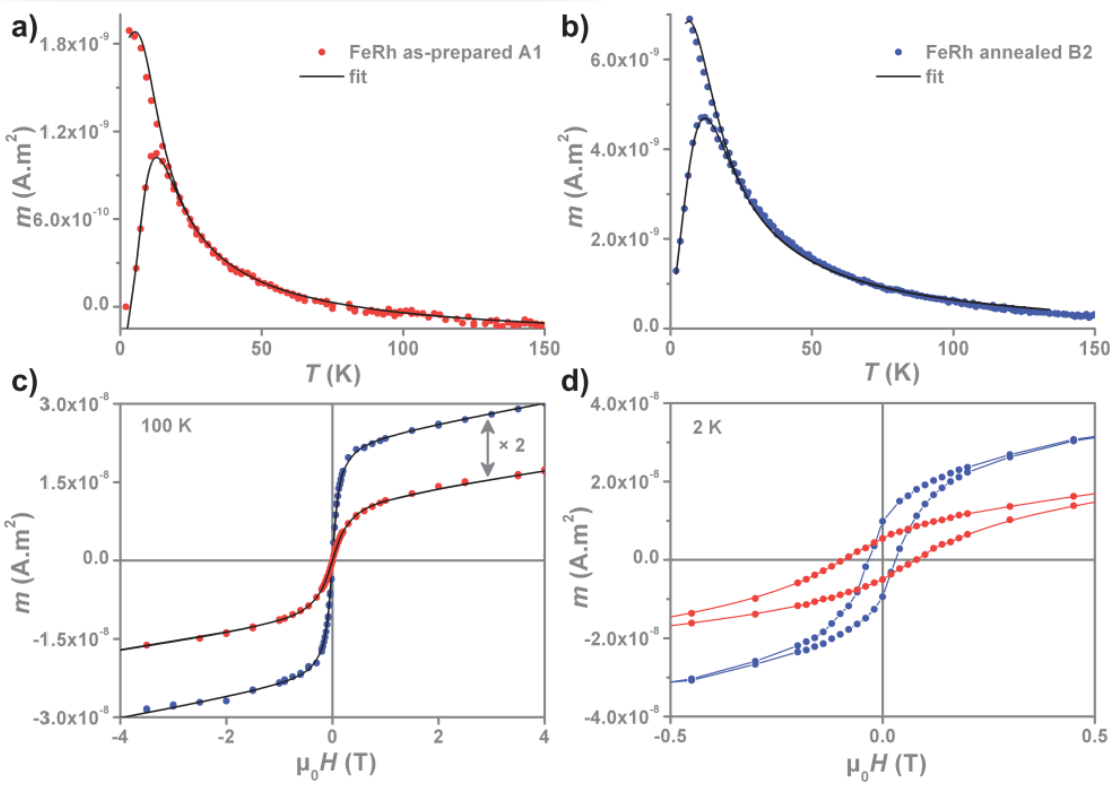

- ✓ **Strong increase of the total magnetic moment ($m = Ms.V$)**
- ✓ **Magnetic size distribution in agreement with TEM**
- ✓ **No modification of the anisotropy constant**
- ✓ **Decrease of the coercivity: $\mu_0 H_C \propto K_{eff}/M_S$**

	T_{max} (K)	$\mu_0 H_c$ (mT)	$D_{m\,m}$ (nm)	ω_{mag}	K_{eff} (kJ.m^{-3})
As prepared	12	80	3.3 ± 0.2	0.15 ± 0.05	127 ± 15
Annealed	12	35	3.3 ± 0.2	0.15 ± 0.05	133 ± 15

Results deduced from the "triple fit"

Ferromagnetic behavior down to 2 K.
No meta-magnetic phase transition!

Further modelling of magnetometry curves

A. Hillion et al., J. Appl. Phys. **112**, 123902 (2012)

The same ingredients can be used to simulate (and fit) various experimental curves

- AC susceptibility curves
  (magnetic anisotropy and relaxation time)
- Thermo-remanence curves $m_R(T)$
- ZFC/FC beyond the linear response approx.
  (influence of the applied field on ZFC/FC curves)
- Low T hysteresis loops, with a biaxial anisotropy

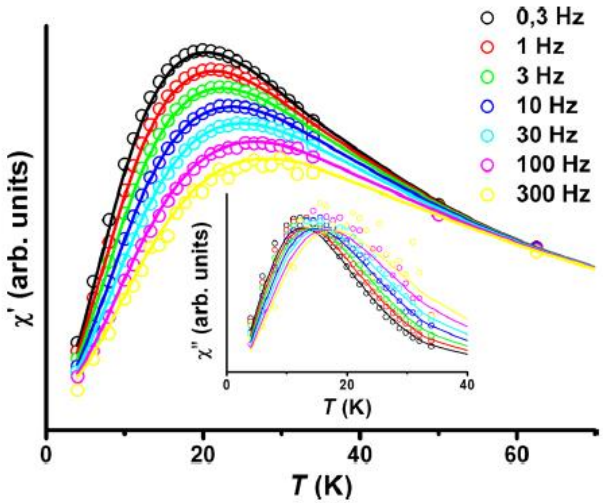

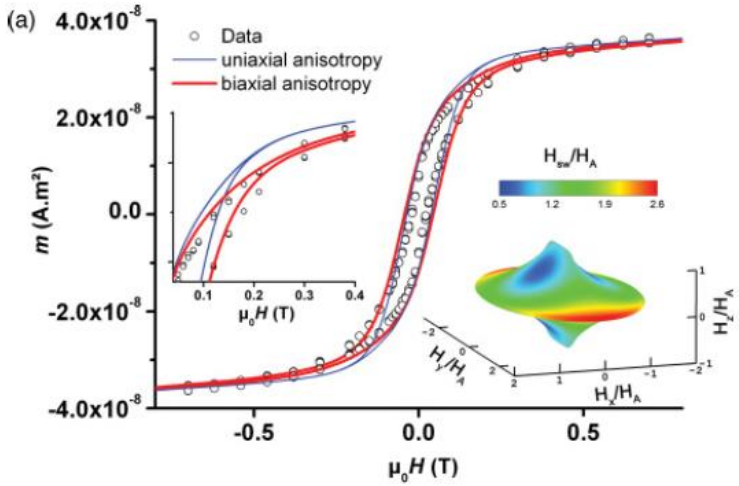

A. Tamion et al., Phys. Rev. B **85**, 134430 (2012)

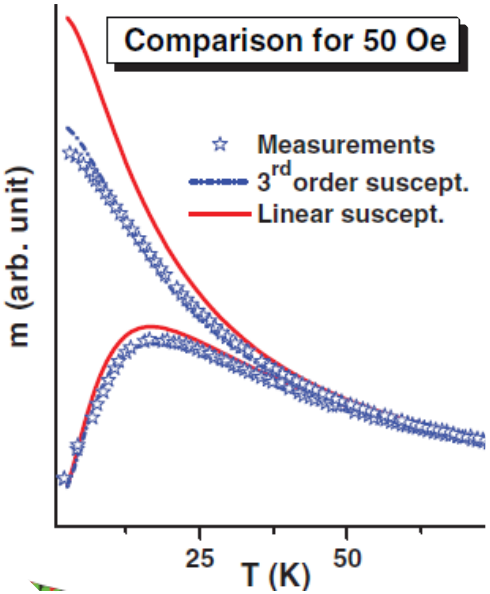

F. Tournus et al., Phys. Rev. B **87**, 174404 (2013)

CoPt magnetic properties from a global fit

Global fit, including a low T hysteresis loop.

→ Significant biaxial contribution to the anisotropy.

	As prepared	Annealed (750 K)
D_m (nm)	3.12 ± 0.1	3.12 ± 0.1
σ (nm)	0.22 ± 0.05	0.22 ± 0.05
K_{1m} (kJ m^{-3})	200 ± 25	260 ± 25
σ_{K1}/K_{1m}	$37\% \pm 5\%$	$31\% \pm 5\%$
K_2 (kJ m^{-3})	100 ± 25	150 ± 25

Size-selected CoPt nanoparticles (D = 3 nm) embedded in amorphous C

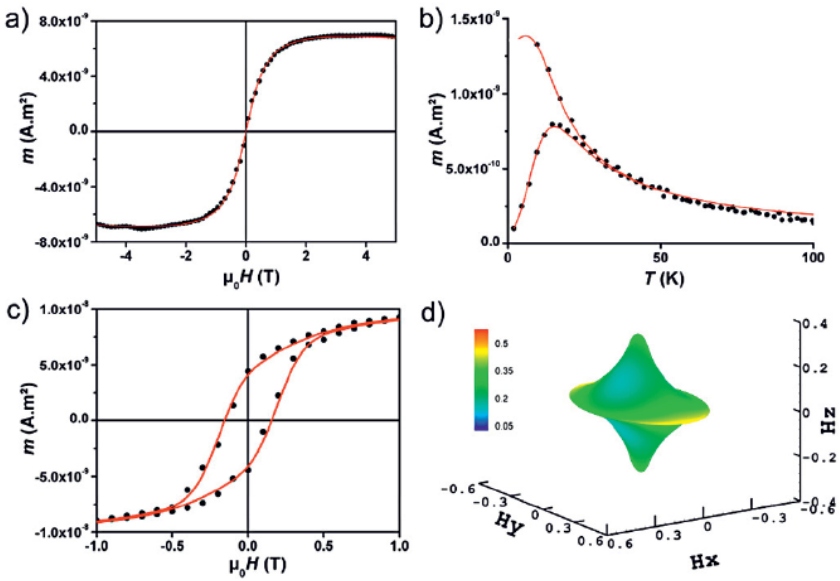

Fig. 3. (Color online) Hysteresis loops at 300 K (a), at 2 K (c) and ZFC/FC (b) for as-prepared CoPt nanoparticles embedded in C matrix. The solid lines correspond to the fit. Mean astroids associated to the biaxial fit (d).

As prepared

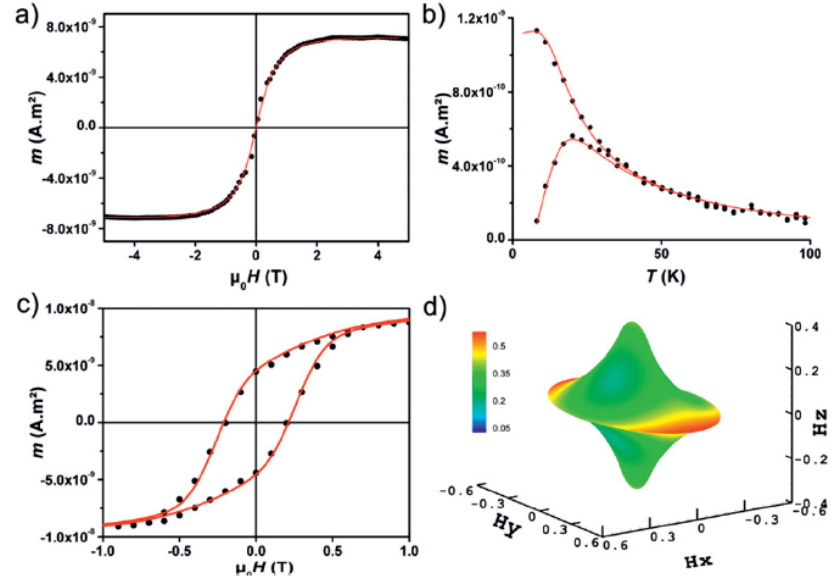

Fig. 4. (Color online) Hysteresis loops at 300 K (a), at 2 K (c) and ZFC/FC (b) for annealed CoPt nanoparticles embedded in C matrix. The solid lines correspond to the fit. Mean astroids associated to the biaxial fit (d).

Annealed

Further complementary measurements…

The **"triple fit"** is a powerful approach but one still would like to go further…

- ✓ Biaxial contribution to the anisotropy?

  ➡ $E_{\mathrm{ani}}/V = K_1 m_z^2 + K_2 m_y^2$ (hard axis in the hard magnetization plane)

- ✓ Verification that inter-particle interactions are negligible?

- ✓ Complementary measurement involving field-assisted switching

For ZFC/FC curves, we have a *thermal switching*:
what matters is the **anisotropy energy** K_{eff} V

➡ Strong dependence on the detailed particle size distribution

Remark: hysteresis loops are not straightforward to interpret ➡ Demanding simulations and the signal is the result of many contributions…

<u>Interesing complementary measurements:</u>

Isothermal remanence magnetization (IRM) curves

What is this? Why can they be useful?

Isothermal remanent magnetization (IRM)

Assembly of nanomagnets
(superparamagnetic at high T)

• First, the sample is <u>demagnetized</u>
(cooling to low T, with zero field)

Measurement of the remanent magnetization
after having applied a given field

• The applied field is increased, step by step

IRM(H) curve → **Signature of irreversible magnetization switching**

No spurious contribution:

- Superparamagnetic particles
- Diamagnetic substrate, paramagnetic impurities

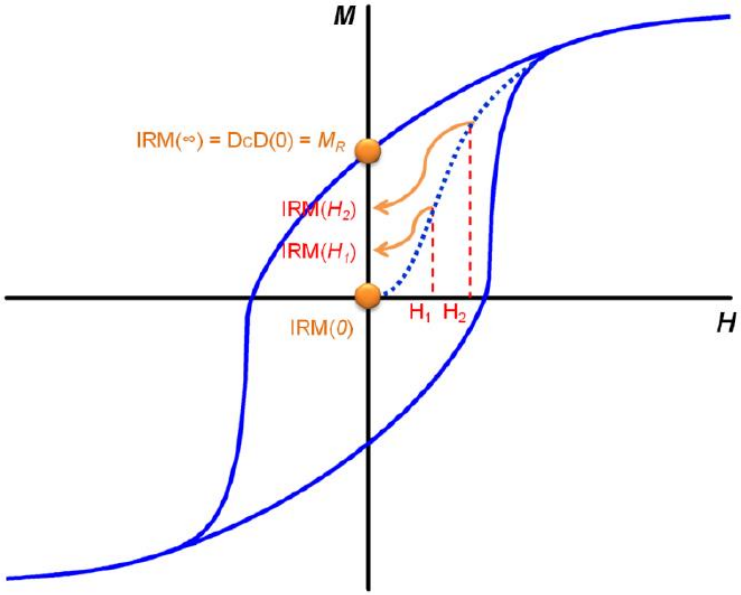

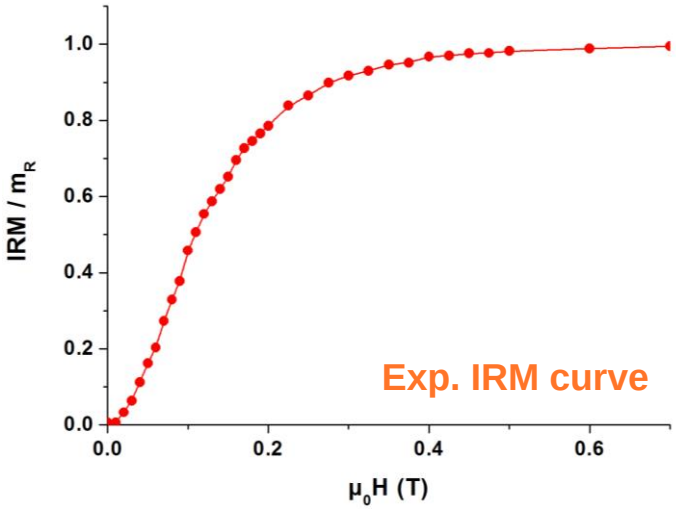

Measurements very easy to implement!

IRM, DcD and Δm curves

Direct current demagnetization (DcD)

➡ Measurement at remanence, but after having saturated the sample.

Schematic representation of the macrospins orientations in the sample

Initial config.

Final config.

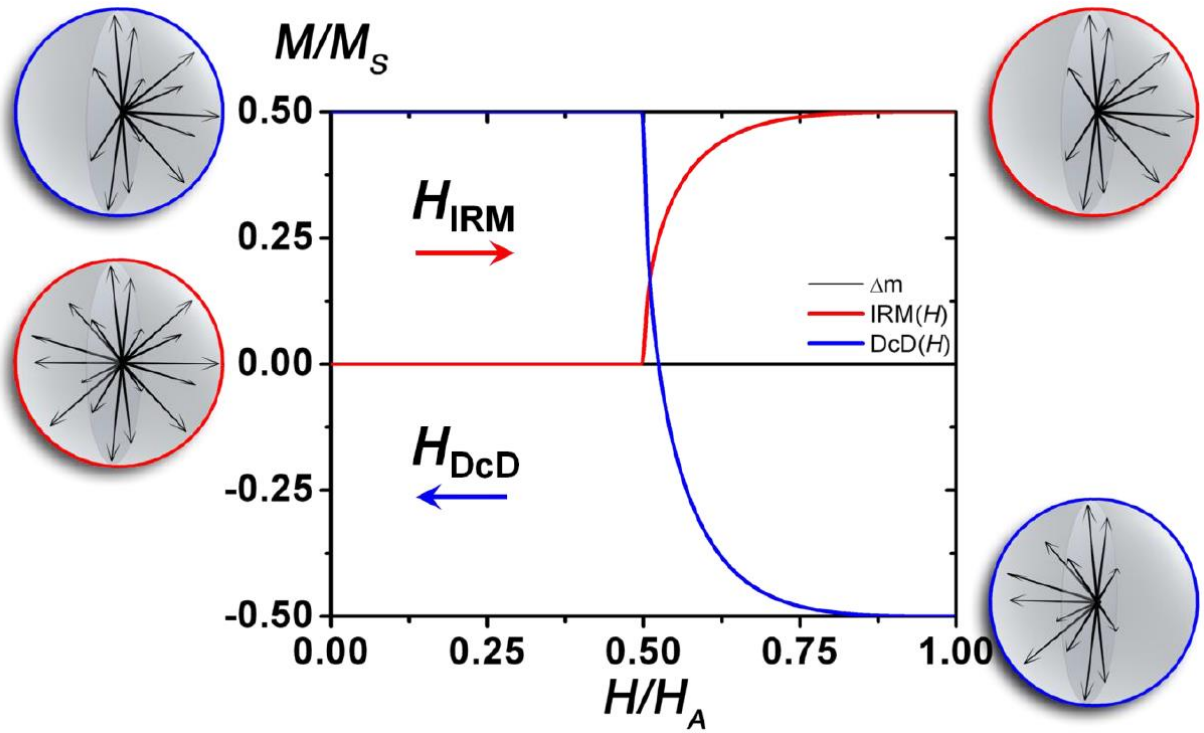

Different initial state:

- IRM: demagnetized
- DcD: saturated in the opposite direction, then M_R

If there is **no interaction**
(each particle switches independently)

➡ Factor 2 in the number of switching particles: m_R – DcD = 2 IRM

Δm and interactions

V. Dupuis *et al.*, PCCP (in press)

Δm parameter:

$\Delta m = DcD/m_R - (1 - 2\ IRM/m_R)$

If no interaction

➡ **Δm = 0 verified**

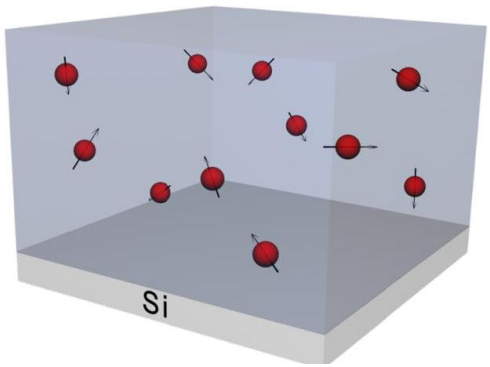

Clusters embedded in a non-magnetic matrix

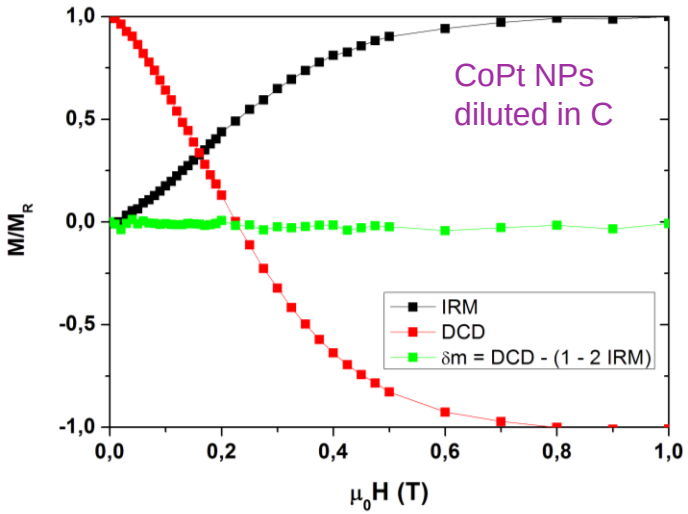

With our approach (Low Energy Cluster Beam Deposition), the dilution can be controlled

➡ Low concentration of magnetic nanoparticles

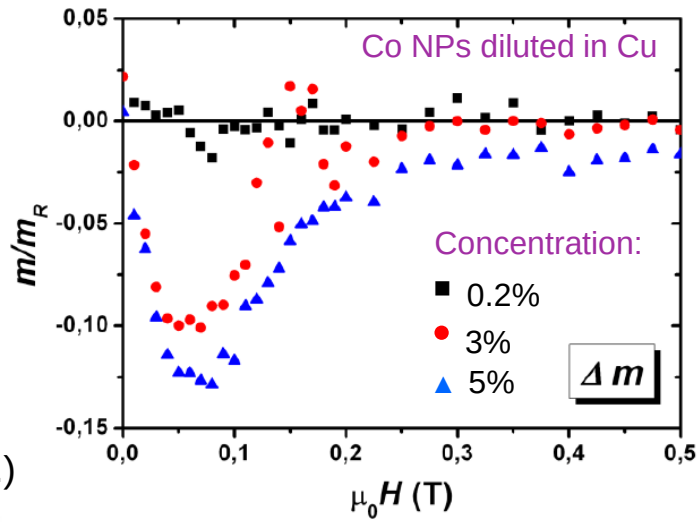

Δm is very sensitive to interactions!

Qualitatively
- Δm > 0 implies magnetizing interactions
- Δm < 0 implies demagnetizing interactions (dipolar inter.)

IRM curves simulation

How can we model these curves for a nanomagnet assembly?

Framework:

- Negligible interactions
- Macrospin approximation (uniaxial anisotropy, extended to bi-axial…)
- Random orientation of the anisotropy axes

Combined Stoner-Wohlfarth and Néel relaxation (switching) model

IRM modelling, analytical expression

A certain range of orientations (symmetric around 45°) will switch for a given applied field

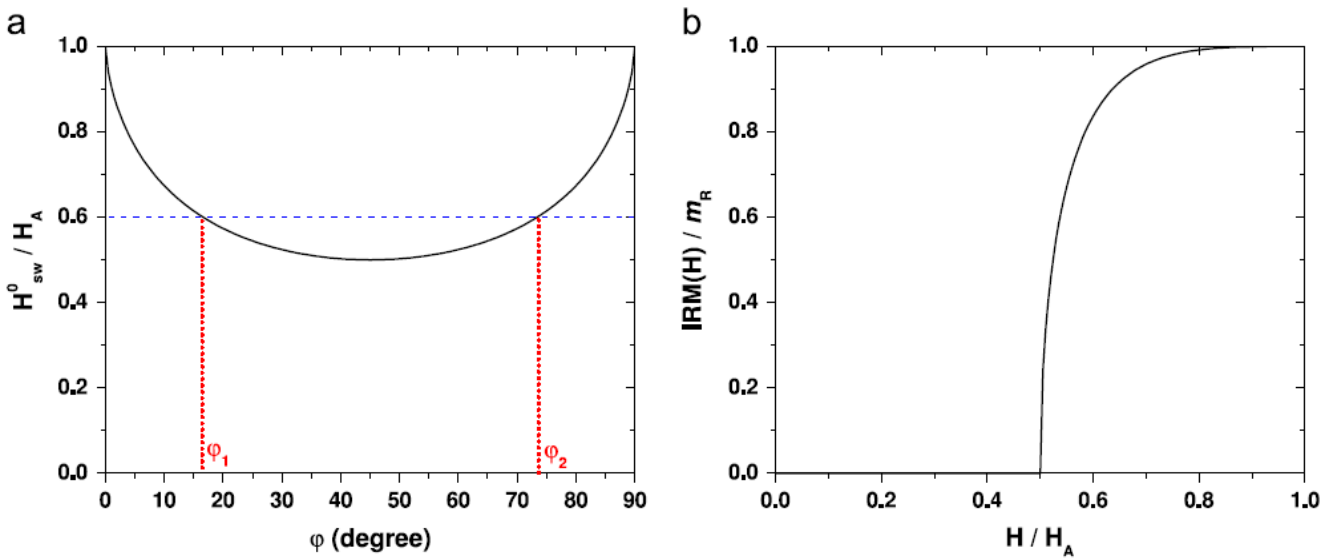

- ✓ For $H = H_A/2$
  - ➡ some macrospins begin to switch
- ✓ For $H = H_A$
  - ➡ all the macrospins have switched

The expression $H_{sw}(\varphi)$ can be **inverted** to determine which φ corresponds to a given switching field

Then, for randomly oriented uniaxial macrospins, one can establish a simple and compact **analytical expression** (independent of the particle size)

➡ $$\boxed{\mathrm{IRM}(H) = m_R \frac{1 - x_1^3}{1 + x_1^3}} \quad \text{for } H \in [H_A/2, H_A]$$

where $$\begin{cases} x_1 = \dfrac{1 + 2h^2 - \sqrt{12h^2 - 3}}{2(1 - h^2)} \\ \text{with } h = H/H_A \end{cases}$$

F. Tournus, J. Magn. Magn. Mater. **375**, 194 (2015).

IRM modelling, effect of temperature

Let us consider the case T≠0

Experimental parameter
$\epsilon_{sw} = \ln(\tau_m/\tau_0) \sim 25$

- **Néel** switching time: $\tau_{sw} = \tau_0 \exp\left(\frac{\Delta E}{k_B T}\right)$

  ➡ Switching if $\tau_{sw} < \tau_m$ (measure), which means $\frac{\Delta E(H_{sw})}{k_B T} = \ln(\tau_m/\tau_0)$

- Evolution of the **energy barrier** with the applied field: $\Delta E(H,\varphi) = K\left[1 - \frac{H}{H^0_{sw}(\varphi)}\right]^{\alpha(\varphi)}$

  ➡ $\Delta E(H,\varphi) = K\left[1 - \frac{H}{H^0_{sw}(\varphi)}\right]^{3/2}$ is a good approximation (for most orientations, α ~ 3/2)

The switching field decreases with the temperature: $H_{sw}(T) = H^0_{sw}\left\{1 - \left[\frac{k_B T}{K}\ln\left(\frac{\tau_m}{\tau_0}\right)\right]^{1/\alpha}\right\}$

➡ Shrinking of the astroid without deformation, so that the calculations are the same as for T=0

$$\boxed{\mathrm{IRM}(H,T) = m_R \frac{1 - x_1^3}{1 + x_1^3}} \quad \text{for } h \in \left[\frac{1}{2}, 1\right] \qquad \text{where} \quad h = \frac{H}{H_A C(T)}$$

Simple scaling factor (independent of angle φ)

$$C(T) = \frac{H_{sw}(T)}{H^0_{sw}} = 1 - \left[\frac{\epsilon_{sw}}{\sigma(T)}\right]^{2/3}$$

with $\sigma = K/(k_B T)$

Same analytical expression as for T=0, but with a **size dependence** through the scaling factor

➡ For a given T, the smaller the particle size, the lower H_{sw}

IRM curves simulation

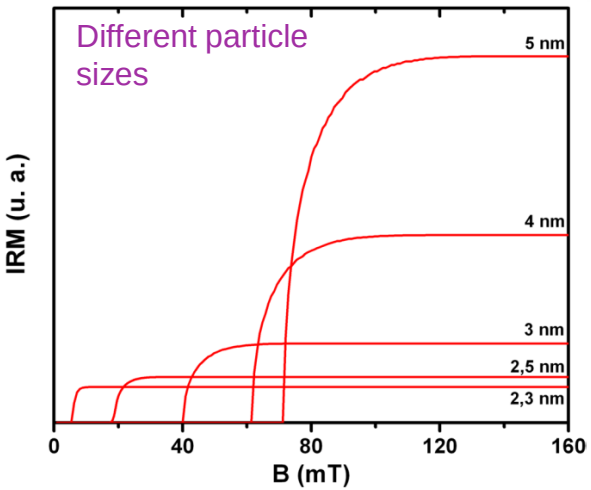

- Easy computation of IRM curves

Extension to the case of a size distribution

$$\mathrm{IRM}(H) = \int_0^{\infty} \mathrm{IRM}(V,H) f(V)\, \mathrm{d}V$$

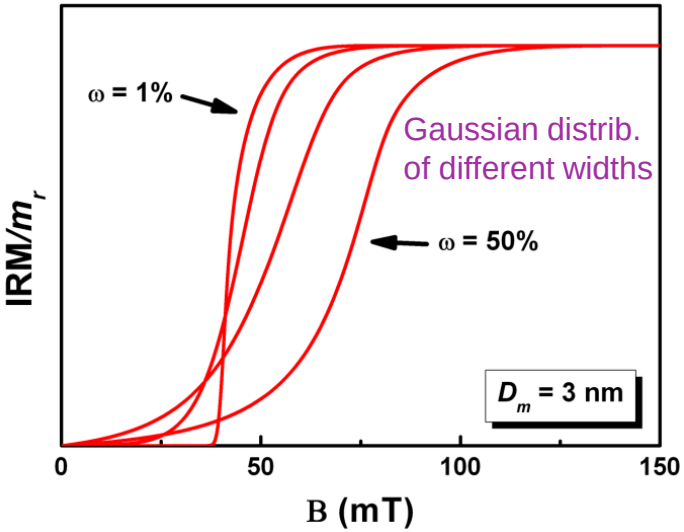

Smoothing due to size distribution → Satisfying approx. (α=3/2, sudden switching…)

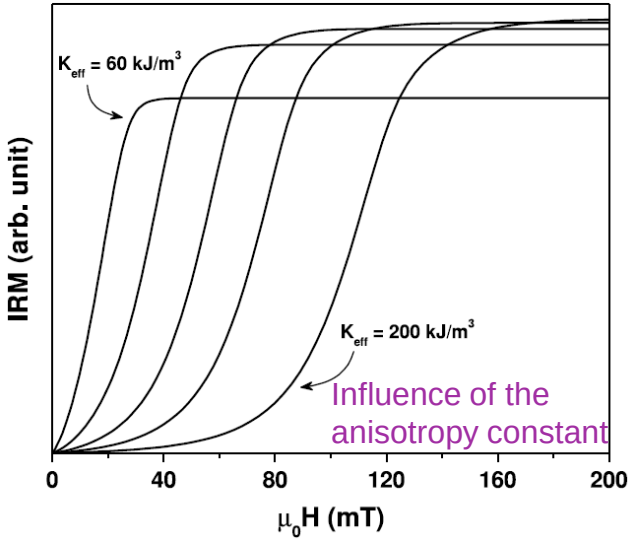

Rationalization of the influence of each parameter

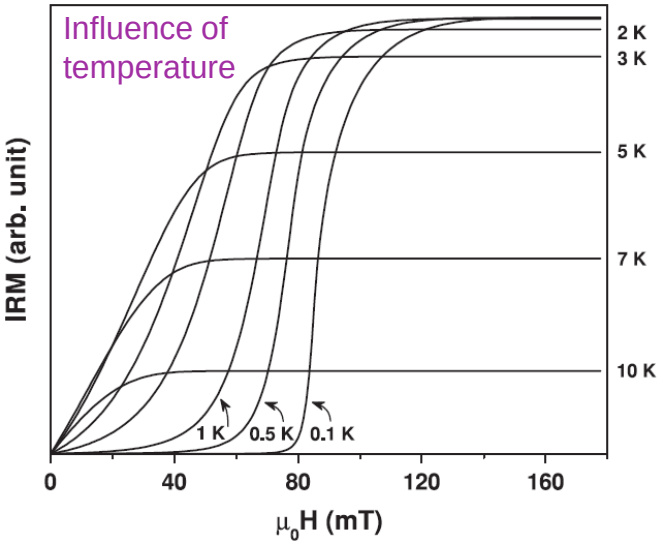

IRM curves simulation and fit

IRM simulation taking into account the influence of

- ✓ Temperature
- ✓ Size distribution
- ✓ K_{eff} distribution
- ✓ Biaxial anisotropy K_2

F. Tournus, J. Magn. Magn. Mater. **375**, 194 (2015).

A. Hillion *et al.*, Phys. Rev. B **88**, 094419 (2013).

Numerical approach:

$$\mathrm{IRM} = 2\iint_{\theta,\varphi}\int_{V_{\min}}^{V_{\mathrm{sw}}^{\theta,\varphi}} M_S V\cos\theta\rho(V)\mathrm{d}V\rho(\theta,\varphi)\mathrm{d}\theta\mathrm{d}\varphi$$

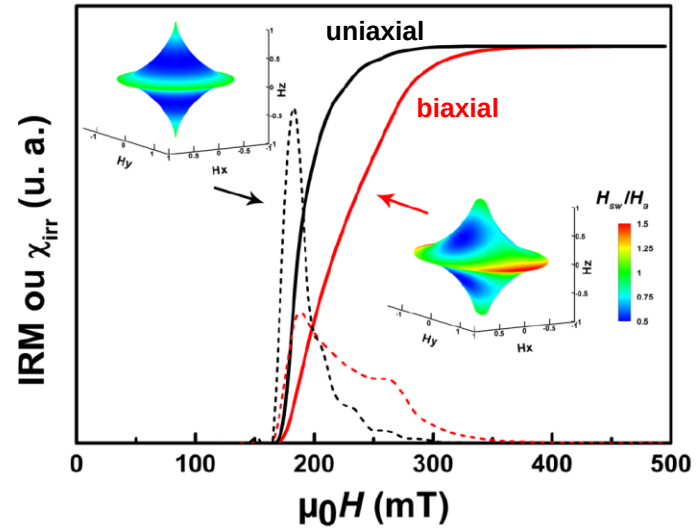

A fit of experimental IRM curves is possible!

Simultaneous fit of different measurements, in order to infer a consistent and accurate set of parameters

3 nm Co nanoparticles diluted in Cu

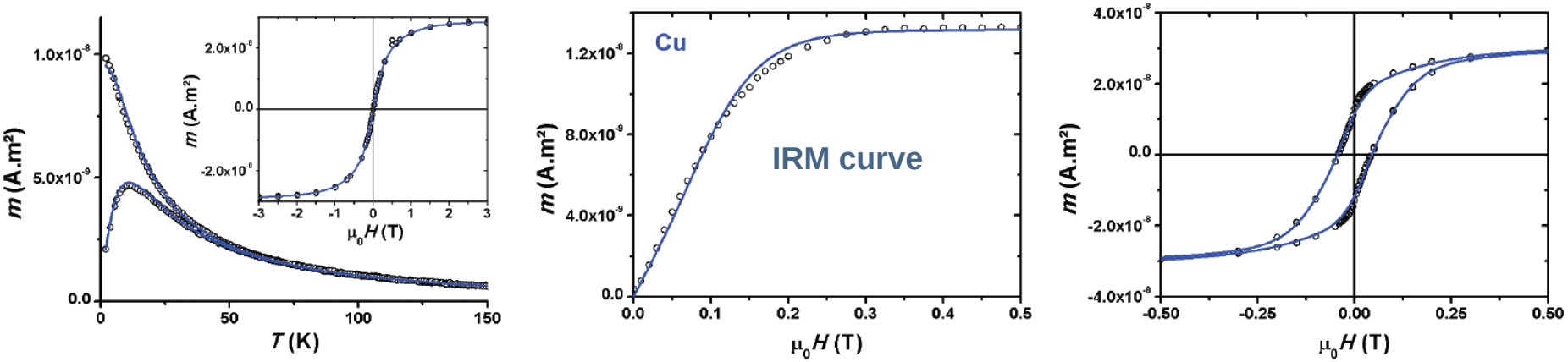

IRM vs. ZFC/FC measurements

Different physical processes → **IRM and ZFC/FC curves are complementary!**

Isothermal Remanent Magnetization (IRM)

IRM(H): the applied field is varied

→ Macrospin switching due to the applied field

Crucial parameter: switching field H_{sw}

Controlled by the **anisotropy field**

$H_A = 2 K_{eff} / (\mu_0 M_S)$

Moderate influence of the size distribution

Sensitive to a biaxial contribution

Zero-Field Cooled/Field Cooled suscept. (ZFC/FC)

ZFC(T): the temperature is varied

→ Thermal switching (relaxation to equilibrium)

Crucial parameter: blocking temperature T_B

Controlled by the **anisotropy energy**

$K = K_{eff} V$

Large influence of the size distribution

Only sensitive to the uniaxial term (minimum energy barrier)

Application to Co nanoparticles

Experimental study

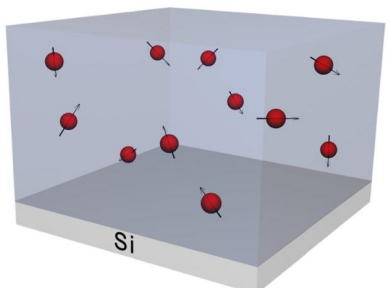

Co nanoparticles around 2.5 nm diameter

- Prepared by low energy cluster beam deposition (laser vaporization and UHV deposition)
- Embedded in an amorphous carbon matrix

No interaction detected ($\Delta m = 0$)

Triple fit: ZFC/FC + m(H) at 300 K → f(D) and K_{eff}

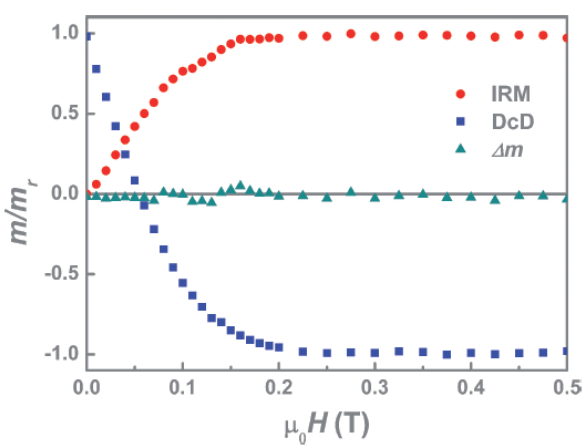

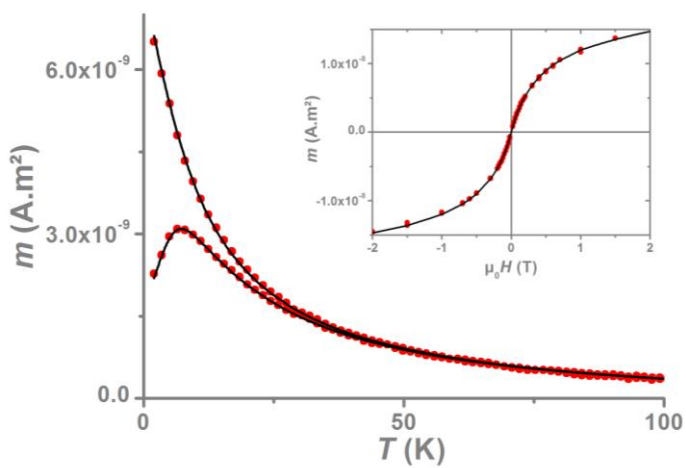

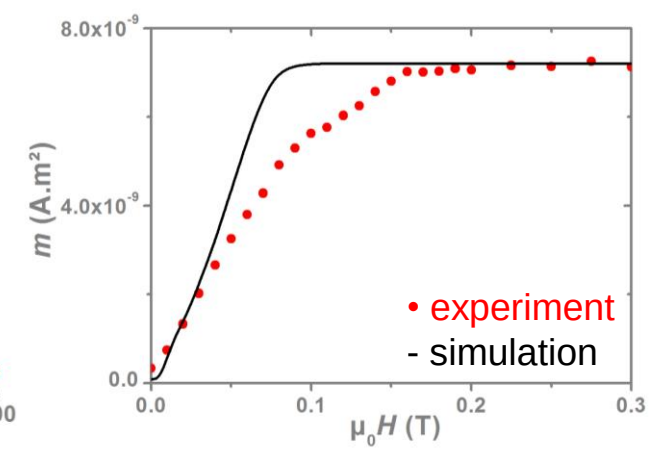

These parameters are then used to simulate the IRM curve

→ **Complete disagreement with the experimental IRM!**

Application to Co nanoparticles

Use of a K_{eff} distribution to fit the IRM

➡ Can reflect the variety of particle shapes

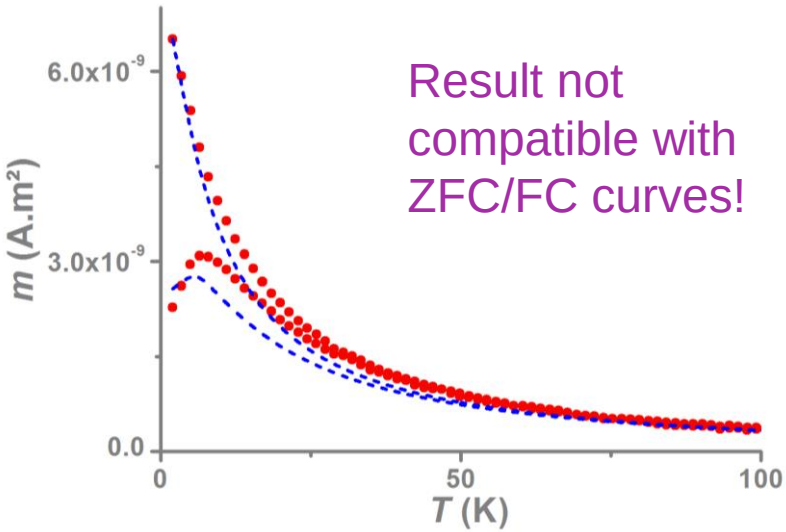

Result not compatible with ZFC/FC curves!

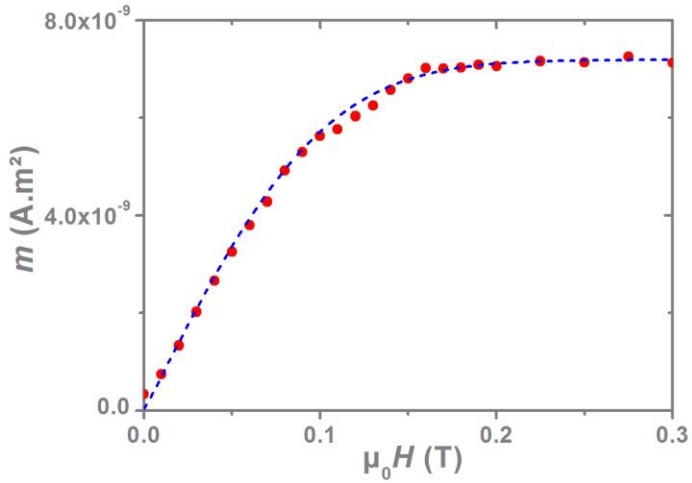

✓ Consistent solution if a **biaxial anisotropy** is used, in addition to a **K_{eff} dispersion**

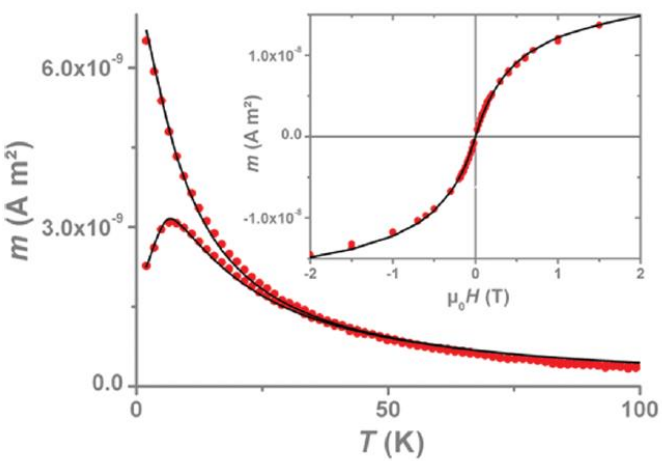

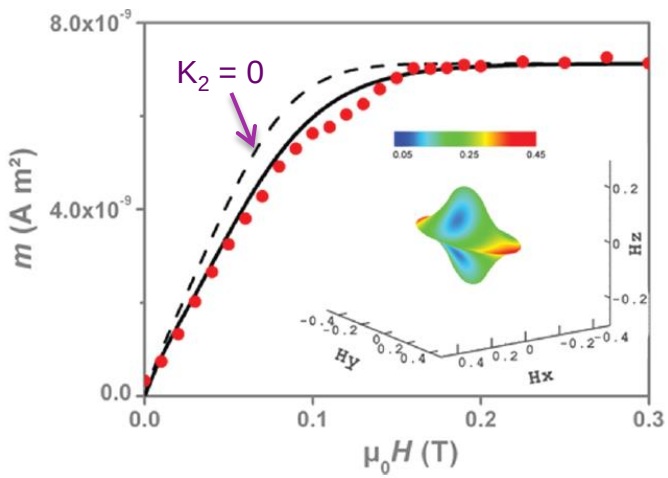

Advanced anisotropy determination

A. Hillion *et al.*, Phys. Rev. B **88**, 094419 (2013).

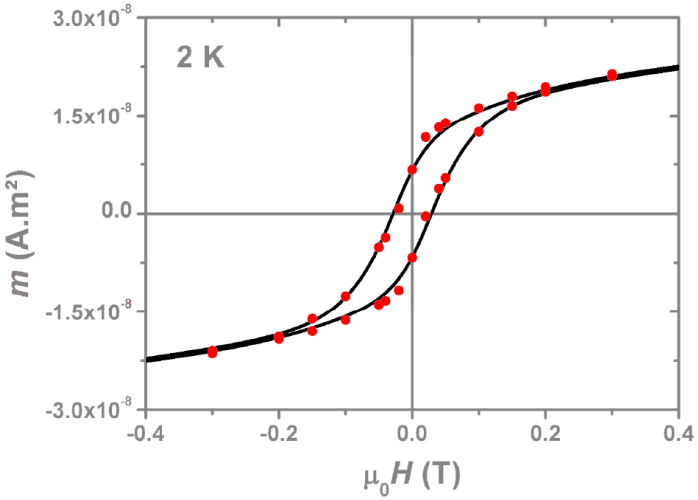

Results validation

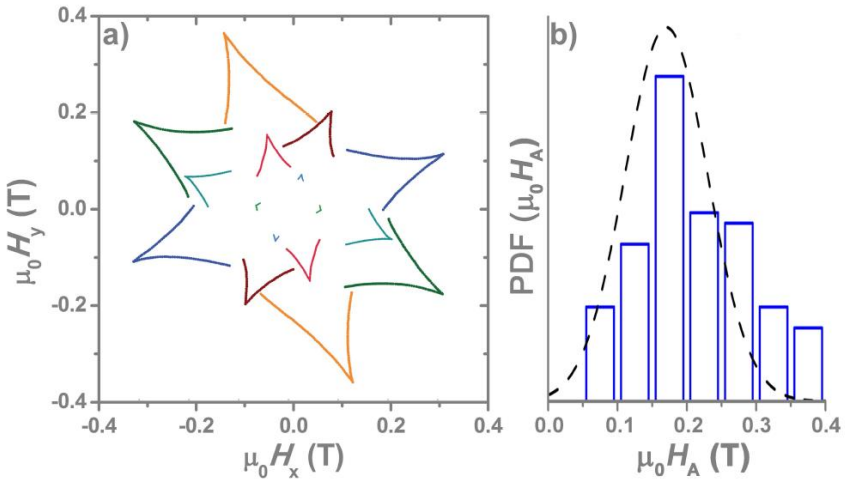

✓ Simulation of the low temperature hysteresis loop

✓ Anisotropy field dispersion, from μ-SQUID measurements on <u>individual particles</u>

Combined fit: exploit the fact that IRM measurements and ZFC/FC are complementary (different types of switching processes)

➡ Advanced characterization of the magnetic anisotropy, from <u>simple measurements on an assembly</u>

IRM/DcD are simple measurements, useful to validate models, and easier to interpret than hysteresis loops

➡ No reason not to do it!

Benefits of IRM analysis, last example

Fe nanoparticles embedded in carbon

→ XMCD indicates a reduced moment per Fe atom

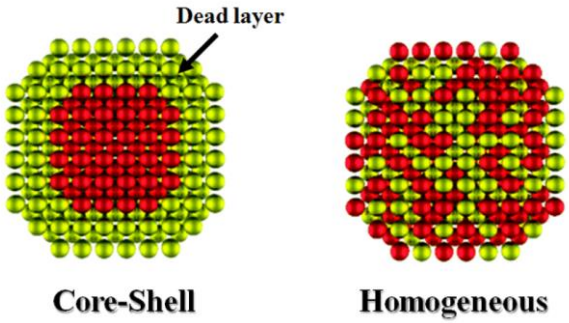

Two hypotheses:

1) Magnetically dead layer, but with core Fe atoms having bulk magnetic moment

2) "Homogeneous disorder", i.e. homogeneous magnetization, reduced compared to bulk Fe

The two possibilities would be compatible with ZFC/FC and superparamagnetic m(H) curves

→ **IRM curve can discriminate the two situations: this is not simply a "dead layer"**

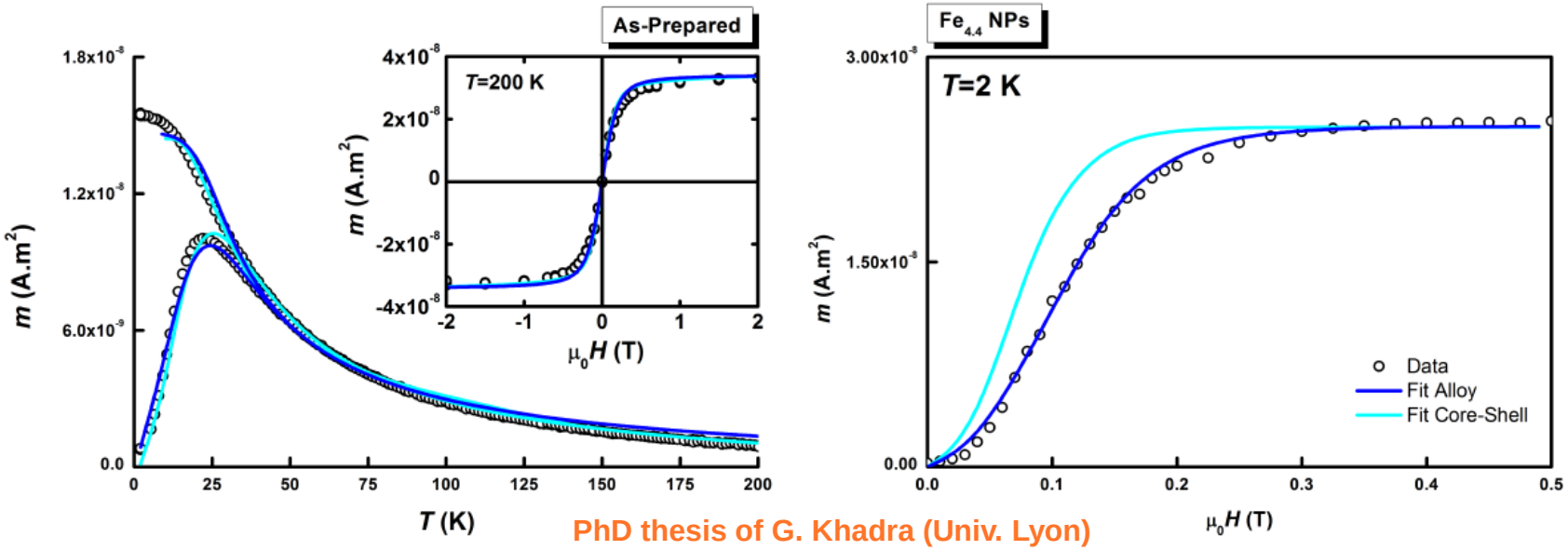

PhD thesis of G. Khadra (Univ. Lyon)

General conclusion

Many size-reduction effects on the magnetic properties

- Model samples of magnetic nanoparticle assemblies

  ➡ Cluster deposition, dilution in a matrix = *macrospin* assembly

- Modelling of various magnetometry measurements is possible

  ➡ Combined fits for an accurate determination of particle size distribution and magnetic anisotropy

  ➡ Magnetic measurements bring *qualitative* and *quantitative* information

- Magnetism is sensitive to the particle structure, environment and electronic configuration…

  ➡ Indirect information and global view of a nanosystem with complementary measurements

- Many perspectives and open questions…

(include the effect of interactions, first-principle magnetic anisotropy calculation, dynamics, etc.)

Acknowledgements

“Magnetic nanostructures” group:

L. Bardotti
V. Dupuis
G. Khadra (PhD)
D. Leroy
O. Loiselet (PhD)
A. Robert (PhD)
A. Tamion
F. Tournus
J. Tuaillon-Combes

N. Blanc (PhD finished in 2009)
A. Hillion (PhD finished in 2012)
S. Oyarzun (PhD finished in 2013)

Engineers, technical support:

C. Albin
O. Boisron

Platforms: PLYRA, CML, CLYM

T. Epicier (MATEIS, INSA Lyon)
K. Sato (IMR, Tohoku University, Japon)
T. J. Konno (IMR, Tohoku University, Japon)

G. M. Pastor (Universität Kassel)
L. E. Díaz-Sánchez (Univ. Autónoma del Estado de México)

A. Y. Ramos (Institut Néel, Grenoble)
H. C. N. Tolentino (Institut Néel, Grenoble)
M. De Santis (Institut Néel, Grenoble)
E. Bonet (Institut Néel, Grenoble)
O. Proux (Obs. Sci. de l'Univers, Grenoble)

A. Rogalev (ESRF synchrotron)
F. Wilhelm (ESRF synchrotron)
P. Ohresser (SOLEIL synchrotron)

M. Hillenkamp (ILM, Lyon)

Networks: